Development of new bioorthogonal strain-promoted alkyne-nitrone cycloaddition methodology for applications in living systems.

Thesis submitted to the

Faculty of Graduate and Postdoctoral Studies

In Partial Fulfilment of the Requirements of the

M.Sc. Degree in Chemistry

uOttawa

In the Ottawa-Carleton Chemistry Institute

Department of Chemistry, University of Ottawa

Candidate

Mariya Chigrinova

Supervisor

Professor John Paul Pezacki

Great is the Truth and mighty above all things;
it endureth and is always strong;
it liveth and conquereth for evermore;
the more thou searchest, the more thou shalt marvel

· *Esdras*

Acknowledgements

I would like to thank Dr John Paul Pezacki. My appreciation for the opportunities he has given me, his belief in my abilities and his ongoing support as a supervisor and mentor is beyond words.

I would like to thank Craig McKay for his guidance and training in the lab, from which I have grown and learned so much, I feel very fortunate to have met and worked with such a passionate chemist. I am also indebted to Jessie Blake for her assistance with the UV-Vis kinetics studies and analysis, which are integral to this project and for which I am extremely thankful. Thank you to my fellow students and colleagues: Mark Legault, Douglas Mackenzie, Matthew Lafreniere, Ashley Hunt and Louis-Philippe B. Beaulieua for taking the time on numerous occasions to chat about chemistry. I also want to thank Malgosia Daroszewska for her incredible support with the mass spectrometry and HPLC equipment and help with analysis of the data; to Don Leak for help with NMR and to Gary Enright and Konstantin A. Udachin for conducting the X-ray crystallography experiments. Finally, I would also like to thank all of the members of Pezacki lab for the good times and fascinating discussions about chemistry and life.

Last but not least, Thank you to my family, without whom I would never be where I am now. Thank you to my parents, who instilled in me the passion for understanding how life and science work, and whose example is a lifelong source of pride and inspiration. Thank you for encouraging and supporting me through the tough times. Thank you to my husband, whose support is beyond measure, for being an absolutely awesome person, my rock and my home. Thank you all.

Abstract

Nitrones are alternatives to azides in rapid strain-promoted 1,3-dipolar cycloadditions with cyclooctynes. To evaluate the differences between nitrones and azides we have performed kinetic studies of strain-promoted alkyne-nitrone cycloaddition (SPANC) reactions of biarylazacyclooctynone (BARAC) with various acyclic and cyclic nitrones. The reactions were conducted under pseudo first-order reaction conditions using UV-visible spectroscopy. The reactivity of the acyclic nitrones was evaluated by varying the stereoelectronic and steric character of substituents at both the α-aryl and nitrogen positions. Cyclic nitrone reactivity was assessed according to the size of the ring and additional steric and strain effects. The obtained second-order rate constants for reactions of BARAC with cyclic nitrones were found to be greater than those for acyclic nitrones. However, all nitrones employed in the kinetic studies herein displayed significantly greater reactivity than azides in the analogous cycloadditions with BARAC. It is of particular note that the five-membered cyclic nitrones showed exceptional reactivity and, if used as rapid alternatives to azides in reactions with BARAC, can increase the reaction rates by up to 50 fold. An attempt to synthesize an allylated BARAC analogue is also described; the rearrangement reaction leading to the unexpected products is reported. The reaction rate for the novel rearrangement under both neutral and acidic conditions was obtained and plausible mechanisms for formation of products are proposed. Based on the results reported herein we anticipate that development of a labelling probe based on BARAC and a five-membered cyclic nitrone would allow for significant decrease of the concentrations of labelling reagents, thereby minimizing reaction time and reagent usage in life sciences applications. Nevertheless, a possible labelling decrease due to side reactions should be given consideration for prolonged labelling.

Table of Contents

List of Abbreviations

ALO	-	aryl-less cyclooctyne
BARAC	-	biarylazacyclooctynone
BCN	-	bicyclononyne
CBz group	-	carboxybenzyl group
CuAAC	-	copper(I)-catalyzed 1,3-dipolar azide-alkyne cycloaddition
DIBAC	-	aza-dibenzocyclooctyne
DIBO	-	dibenzocyclooctynol
DIFO	-	difluororinated cyclooctyne
DIMAC	-	di-methoxy-aza-cyclooctyne
DMPO	-	5,5-Dimethyl-1-Pyrroline-N-Oxide
EWG	-	electron-withdrawing group
HOMO	-	highest occupied molecular orbital
HPLC	-	high-performance liquid chromatography
LC-MS/ESI+	-	liquid chromatography–mass spectrometry/electrospray ionization
LUMO	-	lowest unoccupied molecular orbital
MOFO	-	monofluororinated cyclooctyne
NCEs	-	new chemical entities
NMR	-	nuclear magnetic resonance
NOFO	-	non-fluororinated cyclooctyne
OCT	-	cyclooctyne
ORTEP	-	oak ridge thermal ellipsoid plot
SPAAC	-	Strain-promoted dipolar azide-alkyne cycloaddition
SPANC	-	strain-promoted alkyne-nitrone cycloaddition
SPANOC	-	strain-promoted alkyne-nitrile oxide cycloaddition
TFA	-	trifluoroacetic acid
TLC	-	thin layer chromatography

List of Figures

List of Schemes

List of Tables

Chapter 1 : Bioorthogonal Chemistry

1.1 Introduction

Biological living cells and organisms are highly complex systems, in which numerous chemical entities are present and a multitude of chemical reactions proceed simultaneously. Studying the components and dynamics of such systems poses challenges due to having to account for and eliminate many variables, while controlling and manipulating such systems is even more difficult. The efficiencies of chemical reactions are quite variable, which is generally accepted in the form of reduced yield and rectified by purification and isolation of desired compounds. However, for the applications in living systems the low efficiency of a chemical reaction may be further reduced by cross-reactivity with present functional groups, which will result in too low or no signal at all. Thus any chemical reactions that are used for such applications have to not only to be highly efficient, but also must not participate in any other reactions within the living system being studied.

1.1.1 "Click" chemistry

"Click" chemistry is an umbrella term for a number of organic chemistry reactions that can be used when reliability and selectivity of the outcome is highly desired. The concept of "click" chemistry was first introduced by Sharpless *et al.* in 2001 to describe a set of reactions that can be used to build complex molecules by joining modular "blocks" together both on small and large scales.[1] To be included these reactions had to adhere to a stringent list of criteria: in addition to being modular, two components must react rapidly

with each other, produce very high yields and generate minimal inoffensive by-products. To comply with the above requirements "click" reactions have high thermodynamic driving force, usually greater than 20 kcal mol^{-1}, which sets the reaction on a single reaction trajectory. For example, the prototypical "click" chemistry reaction is the copper(I)-catalyzed 1,3-dipolar azide-alkyne cycloaddition (CuAAC). In CuAAC, which is discussed in more detail further below, azide and alkyne react so rapidly with each other in the presence of copper(I) complex, that the reaction essentially proceeds along a single reaction trajectory to afford high yields of the desired aromatic cycloadduct (Scheme 1.1).

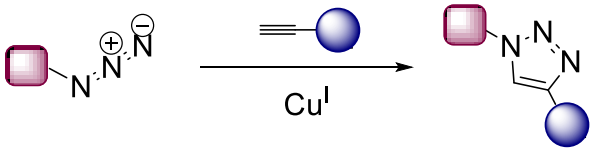

Scheme 1.1. Copper(I)-catalyzed dipolar azide-alkyne cycloaddition (CuAAC).

This mutual exclusiveness of the click reagents renders them virtually unreactive, i.e. orthogonal, with any other functionality present. Since the introduction of the concept, "click" chemistry has found numerous applications in medicinal chemistry, materials science as well as biological applications. The number of publications including "click" chemistry is growing every year as more researchers find the utility applicable to their science. (Figure 1.1)

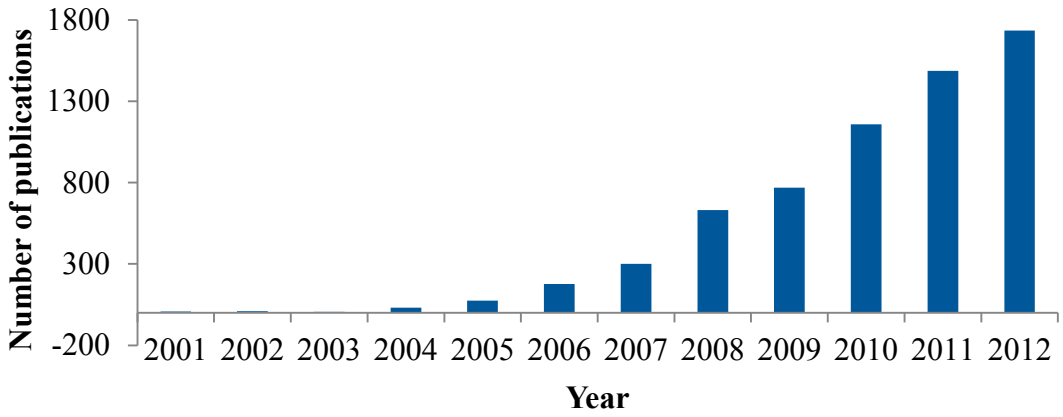

Figure 1.1. Number of publications containing the key words "click chemistry" or "click reaction" from 2001–2012. The literature search was performed via SciFinder Scholar and included journal articles, patents, and reviews.

"Click" chemistry modality allows for new methods for solving synthetic problems or developing methodology for applications. Recently, the materials and pharmaceutical areas have shown acceptance of "click" chemistry philosophy as evident by numerous publications. Reliability and selectivity coupled with multitude of reaction options have helped "click" chemistry popularity to soar.

1.1.2 Medicinal chemistry applications

Lead generation is one of the important steps in drug development. Medicinal chemists employ a wide range of chemical reactions in order to rapidly produce large libraries of new chemical entities (NCEs) for lead identification screening.[2] One of the obvious challenges of this process is synthetic reproducibility. In order for the identified lead compound to be viable for subsequent drug development the synthetic route must be consistent, with reactions occurring in the possible presence of a number of different

functionalities and having the same products and by-products every time. Another challenge is to produce a large number of NCEs as quickly as possible, thus requiring medicinal chemists to use rapid chemical reactions. In the face of these challenges only dependable chemical reactions are employed.[3]

"Click" chemistry was initially introduced to help medicinal chemists quickly and reliably build combinatorial libraries of compounds for drug discovery, essentially making synthesis of large compound libraries more convenient. Rapid high-yielding "click" reactions help address the challenges medicinal chemists face as well as decrease the need for cumbersome purification techniques and expenditures for solvents and materials while providing desired product analogues in a reasonable timeframe. One recent example of the application of "click" chemistry is in its use in fragment-based lead discovery that allowed rapid identification of candidates for protein targets FLT3 and GSK3β kinase.[4]

Natural product analogues present a unique synthetic challenge since fragments need to be connected in the presence of a number of various functional groups.[5] Mutual selectivity of "click" reagents allows for the reaction to proceed without involving functionalities present on other parts of the molecule, making "click" chemistry an invaluable ligation tool in construction of natural product-based libraries since a variety of substituted R groups can be attached to the scaffold of the natural products (Figure 1.2).[6] The ability to efficiently synthesize such a library permits either the study of the influence of substituents on the activity of the scaffold of interest, or discovery of new derivatives which display cytotoxic effect[7] or differential anticancer properties, depending on the linker length,[8] compared to the precursor natural product itself.

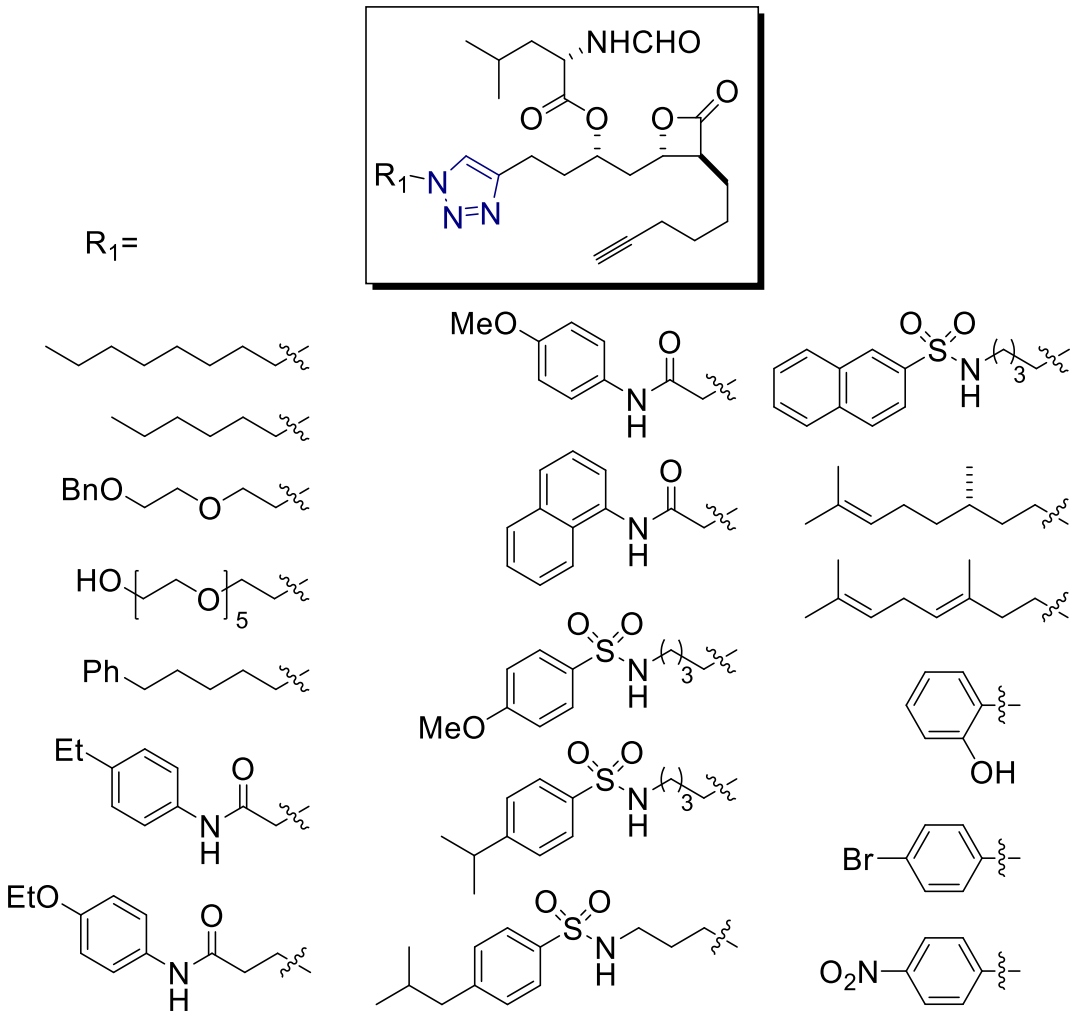

Figure 1.2. Lipstatin analogue library synthesized via "click" chemistry – linkage shown in blue. Figure adapted from the literature.[6]

1.1.3 Materials applications

"Click" chemistry has found diverse applications in materials science for the ability to provide high control over reaction outcome.[9] Since the desired properties of new materials are closely related to their chemical structure, the control over the reactions generating those structures is highly desired. The concept of the "click" reaction has allowed material scientists to design, produce and study the properties of elaborate structures that were previously elusive.[10]

"Click" chemistry became a widely accepted concept in polymer synthesis, post-polymerization modifications and polymer-biomolecule conjugation.[11] CuAAC reaction was used in bioconjugation of Cowpea mosaic virus as the protein target and a fluorescein dye derivative.[12] This study demonstrated the ability to functionalize the viral capsid with multiple handles which are then conjugated to a molecule of choice via "click" chemistry (Figure 1.3). Once functionalized the targets can be tracked allowing further study of the cellular processes of interest.

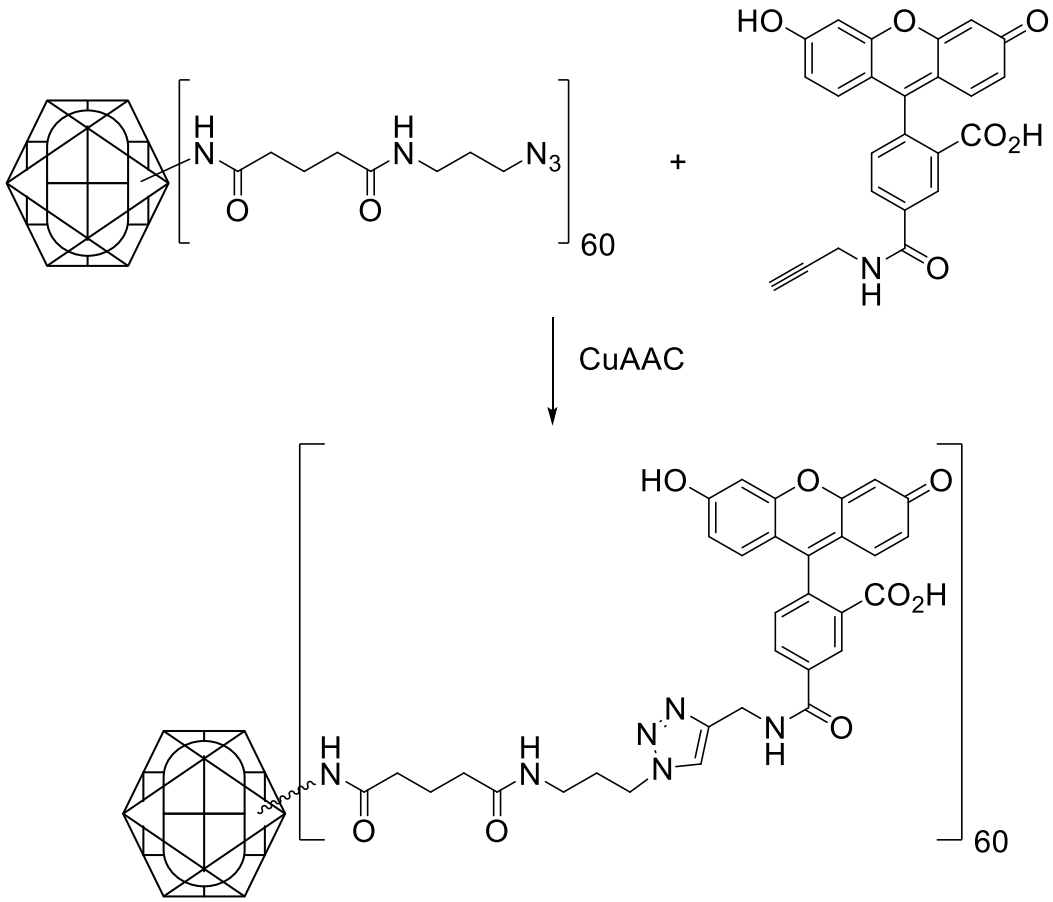

Figure 1.3. Functionalization of viral capsid with fluorescent dye via CuAAC. Figure adapted from literature.[12]

1.1.4 Bioorthogonal chemistry

Biological environments can be both sensitive to and detrimental for the chemical reactions researchers would like to perform in living cells and organisms. Reagents that cross-react with molecules essential for cell survival will alter or destroy the system under study. On the other hand, if the reagent intended for labelling a target reacts with unintended biomolecules, the designed experiment will not yield desirable products. Only chemical reactions that do not interfere with cell biomolecules can be successfully used for labelling. Such reactions are termed bioorthogonal to indicate their inertness towards biological

environments.[13] Therefore, bioorthogonal reactivity is a key requirement for selecting chemical reactions to be used in biological applications. The chemical reactions that are deemed bioorthogonal are transformations that must satisfy stringent criteria: high mutual selectivity, no cross-reactivity with endogenous biological nucleophiles, rapid reaction rates at ambient temperatures and physiological conditions, as well as absence of toxicity to the biological system.[14] "Click" chemistry describes reaction that adhere to most of the above requirements, but only a few reactions satisfy all the above criteria and are often referred to as bioorthogonal "click" reactions that can be performed in the presence of a variety of reactive groups (Figure 1.4) and are used in a plethora of bioconjugation applications.[15]

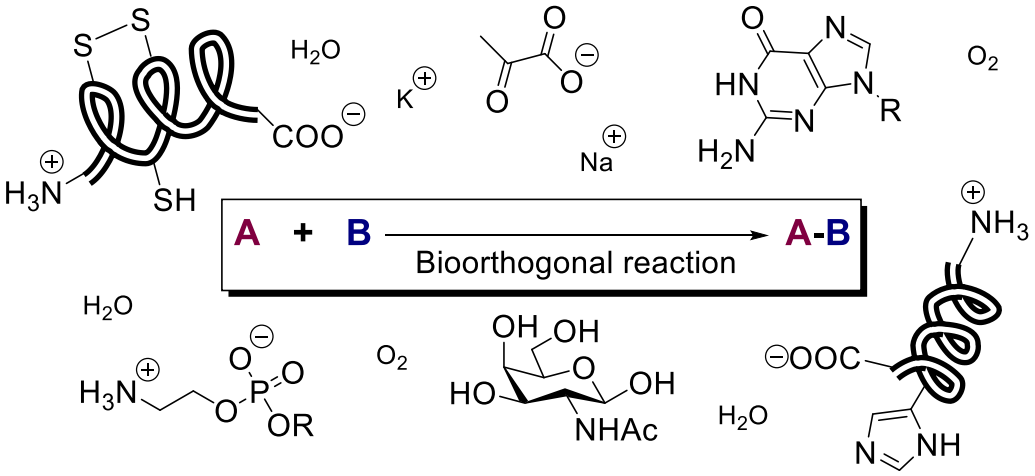

Figure 1.4. Representative bioorthogonal reaction occurring in the presence of multiple reactive functionalities. Figure adapted from the literature.[14]

1.1.5 Copper(I)-catalyzed azide-alkyne cycloaddition

The azide-alkyne 1,3-dipolar cycloaddition, the prototypical "click" chemistry reaction, has become by far the most utilized and popular "click" reaction. Originally described by Huisgen[16], the reaction is modular and affords a stable triazole product.

However, it is too slow to be used in biological applications due to its high activation barrier and therefore prolonged reaction time. In 2002, Sharpless *et al.*[17] and Meldal *et al.*[18] independently showed that copper(I)-catalysis can significantly improve the reaction rate of the azide-alkyne cycloaddition. The fast reaction kinetics, high selectivity and tolerance of a variety of functionalities and reaction conditions allowed this copper(I)-catalyzed 1,3-dipolar azide-alkyne cycloaddition (CuAAC) to become the representative "click" chemistry reaction that it is now.

Many advantages to CuAAC have been unveiled in the recent years, and the reaction is now widely referred to as "click" chemistry and used in broad range of synthetic and biological applications.[19] CuAAC reactions are extensively employed in chemical biology studies; however, the use of the reaction is limited to *in vitro* studies due to the cytotoxicity of the copper catalyst and reliance on delivery of the catalyst to the site of reaction within cells.[20] Ligands utilized in CuAAC are very important both for reactivity and for efficiency of labelling. Short term cell exposure to copper and ligands can be tolerated reasonably well. However, increase in concentration or time of the exposure leads to cell toxicity [21] thus undermining the ability to use the reaction in long-term experiments.

1.1.6 Strain-promoted cycloadditions

In order to extend usage of "click" chemistry to *in vivo* studies there was a need to overcome the detrimental effects of copper catalyst by introducing an alternative means to lower the activation energy of the azide-alkyne cycloaddition. Bertozzi *et al.* developed new methodology for bioconjugation by using ring strain to activate the alkyne for the azide-alkyne cycloadditions.[22] It had been previously shown, that the smallest stable cycloalkyne –

cyclooctyne – reacts rapidly with azides to form a single triazole product.[23] This reactivity is attributed the destabilization of the triple bond due to bond angle distortion. Compared to the ideal acetylene angle of 180º, alkyne incorporated into an eight-membered ring has a bond angle estimated to be ~160º.[24] Such deformation accounts for a significant amount of ring strain energy: at least 18 kcal mol^{-1}, per previous estimations,[25] or up to 19.9 kcal mol^{-1}, per more recent account.[26] This ring strain energy is partially released upon reaction. From a theoretical perspective according to Houk *et al.*, the observed reactivity is in part due to decreased energy requirement for distortion of the azide and alkyne into the transition-state geometry.[24] (Scheme 1.2)

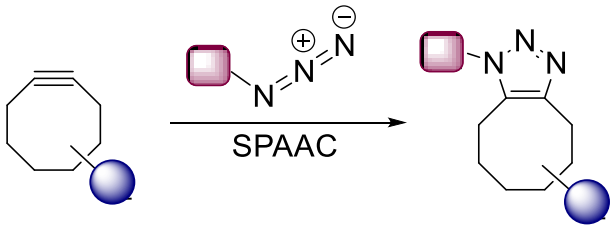

Scheme 1.2. Strain-promoted dipolar azide-alkyne cycloaddition (SPAAC).

The first account of strain-promoted azide-alkyne cycloaddition (SPAAC) was reported by Bertozzi *et al.* on model reactions of functionalized cyclooctyne termed OCT (for cyclooctyne) with organic azides.[22] OCT was found to be stable in water, unreactive to nucleophiles and afforded a mixture of 1,4-substituted triazole regioisomer cycloadducts in reactions with various azides. The second-order rate constant of model cycloaddition with benzyl azide was found to be 1.2×10^{-3} $M^{-1}s^{-1}$.[22,(k_2 revised in 27)] OCT was also successfully applied in a biological labelling experiment, where OCT-biotin derivative was used to detect azides that had been metabolically incorporated into cell-surface glycans. The study showed that OCT-biotin has similar reaction kinetics to that of Staudinger ligation in context if cell-

surface labelling, and displayed no apparent toxicity (Scheme 1.3).[22]

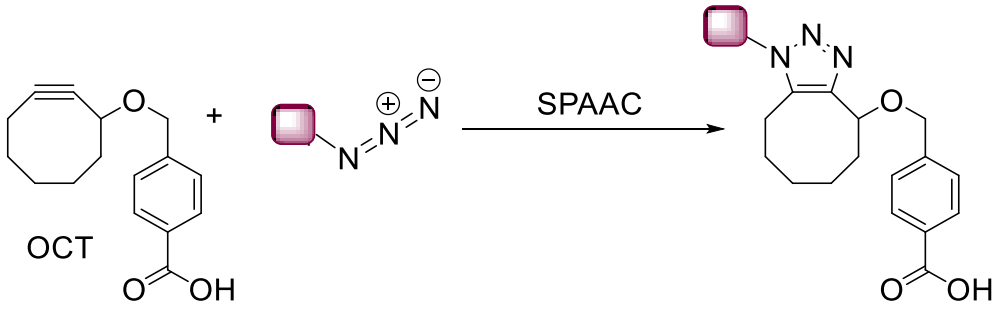

Scheme 1.3. First reported SPAAC reaction with cyclooctyne OCT.

The advent of copper-free "click" chemistry sparked interest in the chemical biology community as a future technique for *in vivo* biological imaging. However, before such application could be widely used, a need for enhanced reaction kinetics and higher sensitivity of SPAAC reagents was apparent. Rate enhancements for bioorthogonal labelling can be achieved either by increasing reagent concentrations or by improving the intrinsic second-order rate constant of the reaction.[14] An increase in concentration of reagents threatens not only with toxicity, but can also cause increased residual fluorescence or non-specific labelling or disturb the dynamics of the system under study. It is clear that the most practical way to improve the reaction kinetics of SPAAC would be to develop novel cyclooctyne reagents that are inherently more reactive with azides.[14] With the goal of improving the kinetics of SPAAC reactions, a number of cycloalkyne derivatives have been synthesized, all attempting to balance optimal reactivity with enhanced stability. (Figure 1.5)

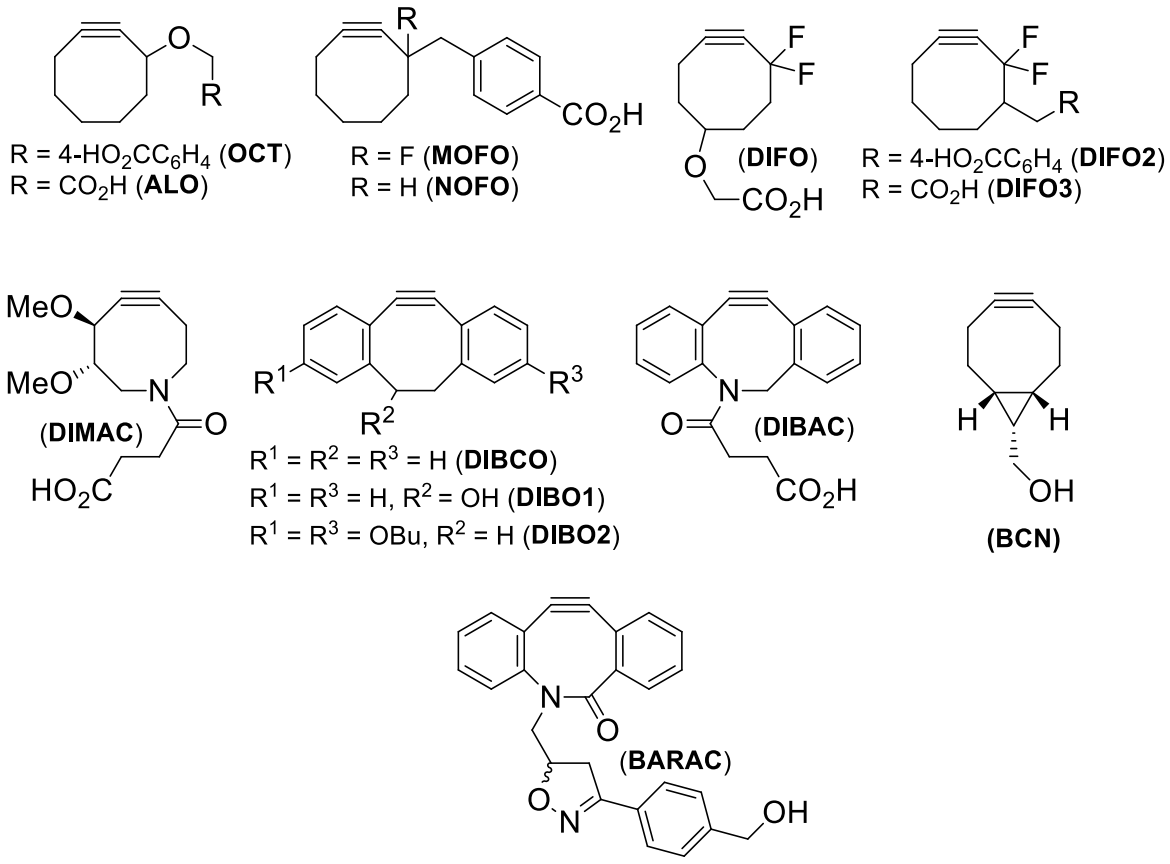

Figure 1.5. Cyclooctynes investigated for SPAAC.

To improve on the reaction rate of OCT, a novel monofluorinated cyclooctyne (MOFO) was synthesized.[28] It was hypothesized that the presence of electron-withdrawing group (EWG) adjacent to the alkyne would increase the reaction kinetics. Indeed, in reaction with benzyl azide, MOFO (k_2 = 4.3 × 10^{-3} $M^{-1}s^{-1}$) was found to be more reactive than OCT (k_2 = 1.2 × 10^{-3} $M^{-1}s^{-1}$ [22,(k_2 revised in 27)]). Through comparing MOFO reactivity to a nonfluorinated analogue (NOFO), Bertozzi *et al.* were able to conclude that the presence of a single fluorine at the propargylic position increased the rate of cycloaddition by ~4-fold.[28] The next step forward was to investigate the effect of a *gem*-difluoro group next to the alkyne moiety, which was accomplished through synthesis of difluororinated cyclooctyne (DIFO)[29], followed by second-generation DIFO2 and DIFO3 (mainly developed for the ease of synthesis).[30] All DIFO (k_2 = 4.2-7.6 × 10^{-2} $M^{-1}s^{-1}$) alkynes had kinetics superior to both OCT and MOFO, reflecting up to 60-fold rate increase.[29,30] In a theoretical study, Houk *et al.* proposed that the rate enhancement of DIFO reagents, compared to unsubstituted cycloalkyne, was due to the increase in interaction of HOMO-LUMO orbital energies during the transition state.[24] The predisposition of the cyclooctyne probes to be hydrophobic posed potential problems for biological applications, was recognized and addressed by Bertozzi *et al.* through synthesis of more hydrophilic cyclooctynes, aryl-less cyclooctyne (ALO)[28] and di-methoxy-aza-cyclooctyne (DIMAC)[31]. Although both ALO and DIMAC were significantly less reactive than DIFO, they may be useful in applications where the lipophilic interactions are sought to be minimized.[14]

Boons *et al.* employed a different approach to activating the alkyne. Instead of using fluoro-activation, fused phenyl rings were introduced on both sides of the alkyne group to increase the ring strain. This strategy was reflected in dibenzocyclooctynol (DIBO) and related analogues (DIBO1 and DIBO2).[32] The second-order rate constants for reactions of

DIBO1 and DIBO2 with benzyl azide (k_2 = 5.7 × 10^{-2} $M^{-1}s^{-1}$ and 7.6 × 10^{-2} $M^{-1}s^{-1}$ respectively) were comparable to that of DIFO.[33] DIBO analogues are especially attractive cyclooctyne derivatives due to their synthetic accessibility. The enhanced stability in DIBO derivatives has been attributed to the ortho-hydrogens on of the phenyl rings protecting the alkyne from nucleophilic attack by water.[32]

One of the more recent cyclooctynes inspired by DIBO derivatives and DIMAC, aza-dibenzocyclooctyne (DIBAC) was developed by Delft *et al.* in 2010 in an attempt to combine the reactivity of DIBO and hydrophilicity of DIMAC.[34] The incorporation of a nitrogen atom into the dibenzocyclooctyne ring not only increased the hydrophilicity of the reagent, it also provided a convenient attachment point for functionalization. The addition of the nitrogen sp^2-like centre to the ring further elevated the ring strain of the alkyne moiety. The second-order rate constant for DIBAC (k_2 = 3.1 × 10^{-1} $M^{-1}s^{-1}$)[34] displayed a 4-fold rate enhancement relative to DIFO. Furthermore, Delft *et al.* developed a novel cyclooctyne – bicyclononyne (BCN), in which the alkyne additional ring strain is derived from fusion of a cyclopropane ring in the backbone of the cyclooctyne as opposed to fused phenyl rings in DIBO. The rate constant for reaction of BCN with benzyl azide (k_2 = 1.9-2.9 × 10^{-1} $M^{-1}s^{-1}$) is comparable to that obtained for analogous reaction with DIBAC and DIFO.[35]

Since the introduction of SPAAC in 2004, the structural features contributing to enhanced reactivity of the cyclooctyne reagents were all combined in the design of the most reactive isolable cyclooctyne – BARAC (biarylazacyclooctynone).[36] The synthesis of BARAC has the advantages of being modular and scalable. The second-order rate constant for the reaction of BARAC with benzyl azide (k_2 = 0.96 $M^{-1}s^{-1}$) [36] is 800-fold greater than that of OCT, 12-fold higher than DIFO and 3-fold higher than DIBAC. BARAC's exceptional reactivity can be attributed to several factors. Similar to DIBO, the fused

dibenzo system enhances the reactivity by increasing ring strain. Further elevation of the ring strain is associated with the presence of the amide linkage as a part of the ring. The electrons of the amide moiety are delocalized between nitrogen and carbonyl giving the C-N bond partial π-character, which causes the C-N bond to be slightly shorter as compared to the C-C bond in an ordinary cyclooctyne. This effectively reduces the size of the ring, which in turn exerts more strain onto the alkyne.[36] Table 1.1 summarizes the second-order kinetic constant data for SPAAC reported to date, and clearly indicates the superiority of the rate of BARAC cycloaddition among the stable cyclooctynes developed so far. The enhanced reactivity and stability of BARAC makes it an optimal choice for further investigation of the strain-promoted cycloadditions.

Table 1.1. Second-order rate constants reported in the recent literature for selected cyclooctynes used in SPAAC.

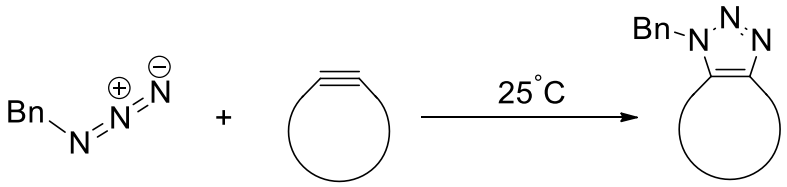

Alkyne [a]	Solvent	k_2 ($M^{-1}s^{-1}$)
OCT	CD_3CN	0.0012 [27]
ALO	CD_3CN	0.0013 [28]
NOFO	CD_3CN	0.0012 [28]
MOFO	CD_3CN	0.0043 [28]
DIFO	CD_3CN	0.076 [29]
DIFO2	CD_3CN	0.042 [30]
DIFO3	CD_3CN	0.052 [30]
DIMAC	CD_3CN	0.003 [31]
DIBCO	C_6D_6	0.062 [37]
DIBO1	CH_3OH	0.057 [33]
DIBO2	CH_3OH	0.076 [33]
DIBAC	CD_3OD	0.31 [34]
BCN	CD_3CN/D_2O (1:2)	0.19-0.29 [35]
BARAC	CD_3CN	0.96 [36]

A product mixture of ~1:1 regioisomers was observed for all reactions. All reactions were performed at 25ºC and atmospheric pressures.[a] The cyclooctyne structures corresponding to the abbreviations are shown in Figure 1.4.

The main incentive to increase the SPAAC reaction rate has been to lower the concentrations of the labelling reagents for bioorthogonal reactions, thereby lowering the risk of potential toxicity, interference with cellular processes and residual fluorescence or non-specific labelling. Until recently, most efforts have focused on increasing the reactivity the cyclooctyne reagent. Their reacting partner, azide, is considered bioorthogonal[17] and is widely used in both CuAAC and SPAAC. However, utilizing more reactive alternatives to azides can greatly enhance the reaction rate leading to the use of lower concentrations of labelling reagents. Nitrones have been used in place of azides as partners in strain-promoted alkyne-nitrone cycloaddition (SPANC) illustrated in Scheme 1.4, for applications such as protein modification.[38,39]

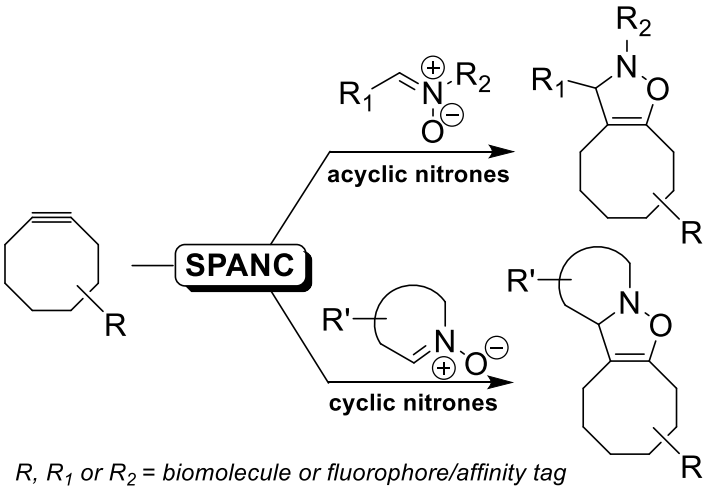

Scheme 1.4. Strain-promoted alkyne-nitrone cycloaddition (SPANC)

Recently, our group has shown that endocyclic nitrones are rapid alternatives to azides in SPANC reactions with dibenzocyclooctyne, proceeding up to 25 times faster than similar reactions of azides.[37] The increased rate was partially due to the added strain in the cyclic nitrone moiety, making the system doubly strain-promoted. Our group has recently expanded on the cyclic nitrone scope and kinetics of doubly-strained SPANC and we have

successfully applied this modular labelling strategy in efficient labelling of cancer cell surface proteins with live-cell imaging applications.[40] In addition to nitrones, other 1,3-dipoles have emerged such as diazo-compounds[41,42] and nitrile oxides[42] for use in strain-promoted cycloadditions with cyclooctynes.

1.2 Outline of work

The purpose of the work described herein was to synthesize BARAC and evaluate its kinetics in SPANC reactions with a series of acyclic and cyclic nitrones. Rate constants were measured under pseudo first-order reaction conditions by UV-visible spectroscopy at ambient temperature in wet acetonitrile and were directly compared to analogous reactions with azides. Synthesis of a simplified analogue of BARAC for kinetic model studies was also attempted; however, the reaction employed was found to proceed via an alternate unexpected pathway. This pathway was explored further, and the novel rearrangement of biarylazacyclooctynones is described herein. It is hoped that the findings of this work will lead to enhanced live cell labelling strategy using strain-promoted BARAC-nitrone cycloadditions. The exceptional reactivity of BARAC with nitrones will allow the use of lower concentrations of labelling reagents with minimal toxicity, cell metabolism interference and residual fluorescence or non-specific labelling.

1.3 References

(1) Kolb, H. C.; Finn, M. G.; Sharpless, K. B. *Angew. Chem. Int. Ed.* **2001**, *40*, 2004.

(2) Roughley, S. D.; Jordan, A. M. *J. Med. Chem.*, *54*, 3451.

(3) Cooper, T. W. J.; Campbell, I. B.; Macdonald, S. J. F. *Angew. Chem. Int. Ed.* **2010**, *49*, 8082.

(4) Irie, T.; Fujii, I.; Sawa, M. *Bioorg. Med. Chem. Lett.*, *22*, 591.

(5) Moorhouse, A. D.; Moses, J. E. *ChemMedChem* **2008**, *3*, 715.

(6) Ngai, M. H.; Yang, P.-Y.; Liu, K.; Shen, Y.; Wenk, M. R.; Yao, S. Q.; Lear, M. J. *Chem. Commun.* **2010**, *46*, 8335.

(7) Petchprayoon, C.; Suwanborirux, K.; Miller, R.; Sakata, T.; Marriott, G. *J. Nat. Prod.* **2005**, *68*, 157.

(8) Zhang, G.; Fang, L.; Zhu, L.; Sun, D.; Wang, P. G. *Bioorg. Med. Chem.* **2006**, *14*, 426.

(9) Lutz, J.-F. *Angew. Chem. Int. Ed.* **2007**, *46*, 1018.

(10) Lahann, J. In *Click Chemistry for Biotechnology and Materials Science*; Lahann, J., Ed.; John Wiley & Sons, Ltd: 2009, p 1.

(11) Lutz, J.-F.; Sumerlin, B. S. In *Click Chemistry for Biotechnology and Materials Science*; Lahann, J., Ed.; John Wiley & Sons, Ltd: 2009, p 69.

(12) Wang, Q.; Chan, T. R.; Hilgraf, R.; Fokin, V. V.; Sharpless, K. B.; Finn, M. G. *J. Am. Chem. Soc.* **2003**, *125*, 3192.

(13) Debets, M. F.; van Hest, J. C. M.; Rutjes, F. P. J. T. *Org. Biomol. Chem.* **2013**, *11*, 6439.

(14) Baskin, J. M., Carolyn R. Bertozzi *Aldrichimica Acta* **2010**, *43*, 15.

(15) Sletten, E. M.; Bertozzi, C. R. *Angew. Chem. Int. Ed.* **2009**, *48*, 6974.

(16) Huisgen, R. *Angew. Chem. Int. Ed.* **1963**, *2*, 565.

(17) Rostovtsev, V. V.; Green, L. G.; Fokin, V. V.; Sharpless, K. B. *Angew. Chem. Int. Ed.* **2002**, *41*, 2596.

(18) Tornøe, C. W.; Christensen, C.; Meldal, M. *J. Org. Chem.* **2002**, *67*, 3057.

(19) Wu, P., Fokin, V. V. *Aldrichimica Acta* **2007**, *40*, 7.

(20) Kennedy, D. C.; Lyn, R. K.; Pezacki, J. P. *J. Am. Chem. Soc.* **2009**, *131*, 2444.

(21) Kennedy, D. C.; McKay, C. S.; Legault, M. C. B.; Danielson, D. C.; Blake, J. A.; Pegoraro, A. F.; Stolow, A.; Mester, Z.; Pezacki, J. P. *J. Am. Chem. Soc.* **2011**, *133*, 17993.

(22) Agard, N. J.; Prescher, J. A.; Bertozzi, C. R. *J. Am. Chem. Soc.* **2004**, *126*, 15046.

(23) Wittig, G.; Krebs, A. *Chem. Ber.* **1961**, *94*, 3260.

(24) Ess, D. H.; Jones, G. O.; Houk, K. N. *Org. Lett.* **2008**, *10*, 1633.

(25) Turner, R. B.; Jarrett, A. D.; Goebel, P.; Mallon, B. J. *J. Am. Chem. Soc.* **1973**, *95*, 790.

(26) Bach, R. D. *J. Am. Chem. Soc.* **2009**, *131*, 5233.

(27) Agard, N. J.; Prescher, J. A.; Bertozzi, C. R. *J. Am. Chem. Soc.* **2005**, *127*, 11196.

(28) Agard, N. J.; Baskin, J. M.; Prescher, J. A.; Lo, A.; Bertozzi, C. R. *ACS Chem. Biol.* **2006**, *1*, 644.

(29) Baskin, J. M.; Prescher, J. A.; Laughlin, S. T.; Agard, N. J.; Chang, P. V.; Miller, I. A.; Lo, A.; Codelli, J. A.; Bertozzi, C. R. *Proc Natl Acad Sci U S A* **2007**, *104*, 16793.

(30) Codelli, J. A.; Baskin, J. M.; Agard, N. J.; Bertozzi, C. R. *J. Am. Chem. Soc.* **2008**, *130*, 11486.

(31) Sletten, E. M.; Bertozzi, C. R. *Org. Lett.* **2008**, *10*, 3097.

(32) Ning, X.; Guo, J.; Wolfert, M. A.; Boons, G.-J. *Angew. Chem. Int. Ed.* **2008**, *47*, 2253.

(33) Poloukhtine, A. A.; Mbua, N. E.; Wolfert, M. A.; Boons, G.-J.; Popik, V. V. *J. Am. Chem. Soc.* **2009**, *131*, 15769.

(34) Debets, M. F.; van Berkel, S. S.; Schoffelen, S.; Rutjes, F. P. J. T.; van Hest, J. C. M.; van Delft, F. L. *Chem. Commun.* **2010**, *46*, 97.

(35) Dommerholt, J.; Schmidt, S.; Temming, R.; Hendriks, L. J.; Rutjes, F. P.; van Hest, J. C.; Lefeber, D. J.; Friedl, P.; van Delft, F. L. *Angew. Chem. Int. Ed.* **2010**, *49*, 9422.

(36) Jewett, J. C.; Sletten, E. M.; Bertozzi, C. R. *J. Am. Chem. Soc.* **2010**, *132*, 3688.

(37) McKay, C. S.; Moran, J.; Pezacki, J. P. *Chem. Commun.* **2010**, *46*, 931.

(38) Ning, X.; Temming, R. P.; Dommerholt, J.; Guo, J.; Ania, D. B.; Debets, M. F.; Wolfert, M. A.; Boons, G.-J.; van Delft, F. L. *Angew. Chem. Int. Ed.* **2010**, *49*, 3065.

(39) Temming, R. P.; Eggermont, L.; van Eldijk, M. B.; van Hest, J. C. M.; van Delft, F. L. *Org. Biomol. Chem.* **2013**, *11*, 2772.

(40) McKay, C. S.; Blake, J. A.; Cheng, J.; Danielson, D. C.; Pezacki, J. P. *Chem. Commun.* **2011**, *47*, 10040.

(41) Moran, J.; McKay, C. S.; Pezacki, J. P. *Can. J. Chem.* **2011**, *89*, 148.

(42) Sanders, B. C.; Friscourt, F.; Ledin, P. A.; Mbua, N. E.; Arumugam, S.; Guo, J.; Boltje, T. J.; Popik, V. V.; Boons, G. J. *J. Am. Chem. Soc.* **2011**, *133*, 949.

Chapter 2 : Strain-Promoted Alkyne-Nitrone Cycloadditions (SPANC) with Biarylazacyclooctynone (BARAC)

2.1 Introduction

Bioorthogonal reactions can be successfully used for site-specific modification of biomolecules in cells and living organisms.[1-4] The criteria for bioorthogonal reactions are very stringent: mutual exclusivity, bio-inertness and lack of toxicity, coupled with rapid reaction rates to ensure product formation at low concentrations required for biological labelling experiments. Only a few of organic chemistry reactions are bioorthogonal and can be used in biological applications.[5]

Several cycloaddition reactions have been shown to exhibit fast kinetics and high selectivity for reacting partner. Cycloadditions between alkynes and 1,3-dipoles have been successfully applied in biological settings, for example, the copper(I)-catalyzed azide-alkyne cycloaddition (CuAAC)[6-9], strain-promoted azide alkyne cycloaddition (SPAAC)[4], strain-promoted alkyne-nitrone cycloaddition (SPANC)[10-12] and strain-promoted alkyne-nitrile oxide cycloaddition (SPANOC)[13,14].

Biocompatibility complications due to copper metal limited the use of CuAAC in living systems. Bertozzi and co-workers developed the copper-free variant, SPAAC, where strain energy in the alkyne moiety drives the rate acceleration. A number of different cyclooctynes have been developed including difluorinated cyclooctyne (DIFO)[15] and derivatives[16], dibenzocyclooctynol (DIBO)[17], tetramethoxy-dibenzocyclooctynol (TMDIBO)[18], aza-dibenzocyclooctyne (DIBAC)[19] biarylazacyclooctynone (BARAC)[20,21]

and bicyclononyne (BCN)[22].

Since the yield of the labelled bioconjugate molecule is proportional to both the concentration of the reagent and the rate constant for the reaction, it follows that the bioorthogonal reactions with large k_2 values are desirable for efficient labelling. The advantage of bioorthogonal coupling reactions with high rates is the relatively short reaction time in biological systems at lower reagent concentrations. Therefore such bioorthogonal labelling reactions can take place efficiently in a wider variety of living systems including live animals where the amounts of reagents required and available may be limited.

Previously, nitrones have been shown to be reactive dipoles in strain-promoted alkyne-nitrone cycloadditions (SPANC)[10-12]. In a recent paper our lab reported the utility of cyclic nitrones in SPANC with dibenzocyclooctyne and 4-dibenzocyclooctynol (DIBO), as well as demonstrated that cyclic nitrones can serve as alternatives to azides with larger k_2 values generally observed with absolute values up to 3.38 M^{-1} s^{-1}.[11] Another finding demonstrated that cyclic nitrones are generally more stable than their acyclic counterparts under aqueous conditions.[10] We also showed that cyclic nitrones could be employed to directly functionalize protein targets *in vitro* as well as on the surface of live human cancer cells.[11]

Recently, a more reactive aza-cyclooctyne, biarylazacyclooctynone (BARAC) was reported.[20] BARAC exhibits greater ring strain than other reported cyclooctynes due to the presence of the highest number of sp^2-hybridized carbon atoms within the cyclooctyne ring. BARAC was tested in SPAAC reactions and was found to react with rate constants significantly larger than those of other cyclooctynes. Since BARAC has never been tested in SPANC reactions with nitrones, we set out to investigate its reactivity towards cyclic and acyclic nitrones (Scheme 2.1).

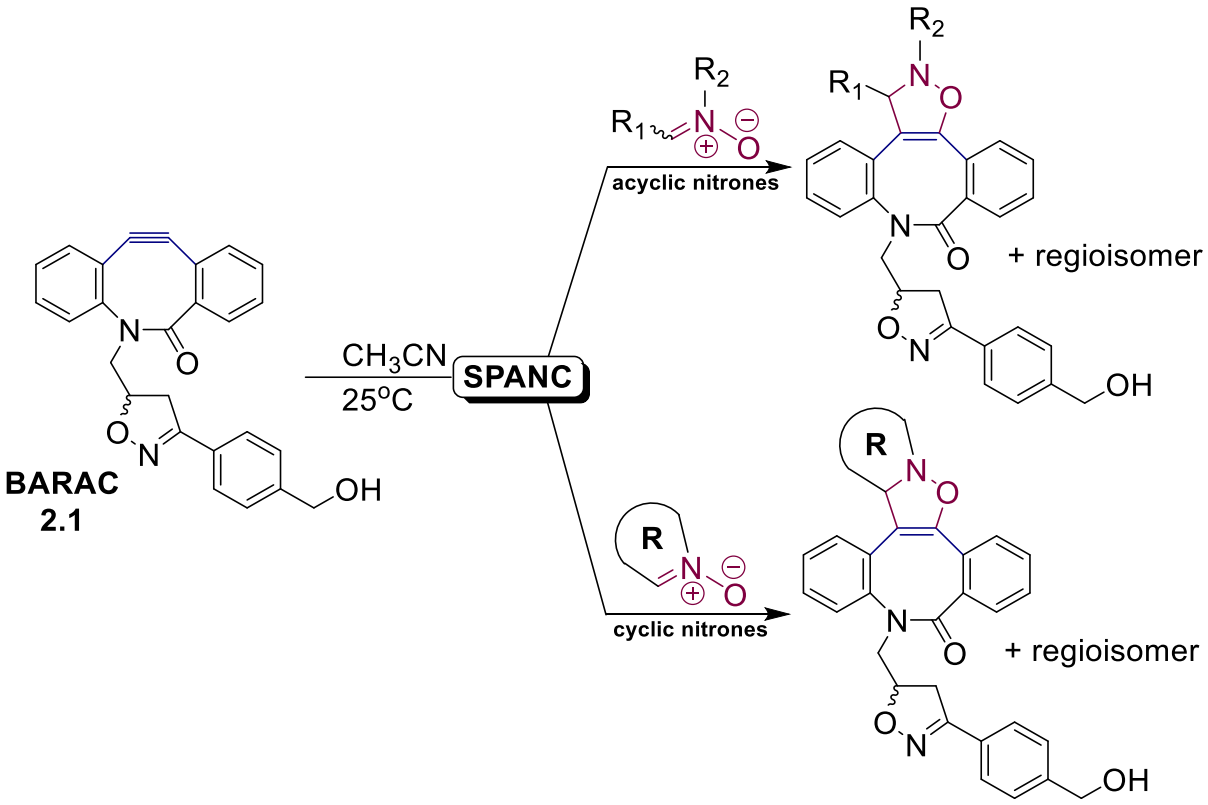

Scheme 2.1. Strain-promoted alkyne-nitrone cycloaddition (SPANC) of BARAC (**2.1**) with various acyclic and cyclic nitrones.

2.2 Hypothesis

The exceptional reactivity of BARAC with azides compared to other cyclooctynes suggests that the cycloaddition reaction of BARAC with nitrones would display even more rapid reaction rates.

2.3 Results and Discussion

Biarylazacyclooctynone (BARAC) **2.1** was synthesized following the reported procedure depicted in Scheme 2.2.[20]

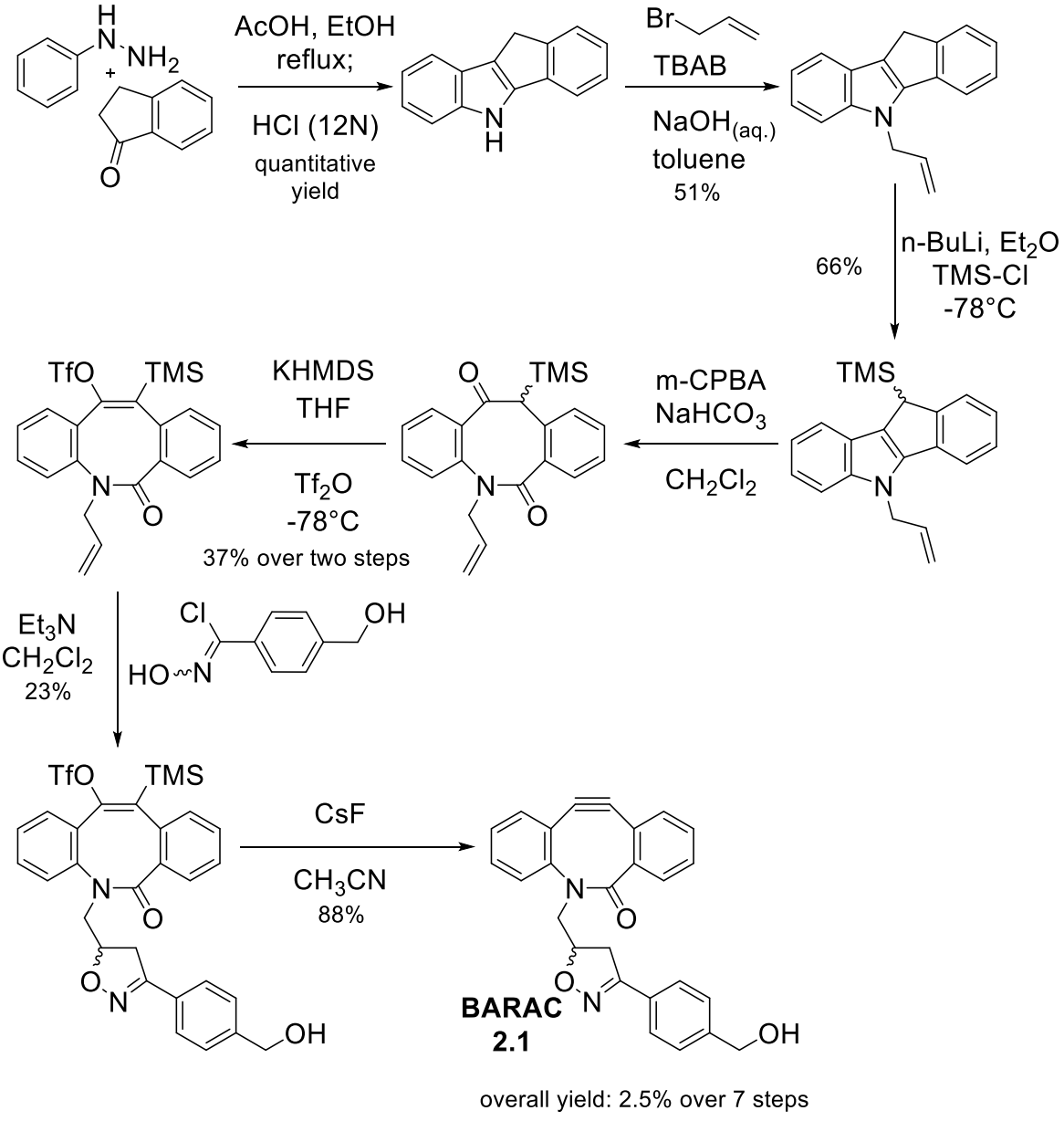

Scheme 2.2. Synthesis of BARAC (**2.1**) for SPANC.

Acyclic nitrones **2.2**, **2.3**, **2.5**, **2.6** and **2.7** were synthesized in good yields following the general procedure, previously reported in literature [23] (Table 2.1). Calcium chloride was employed to drive the condensation reaction towards the products by removing the produced water from the solution.

Table 2.1. General procedure and product yields for synthesized acyclic nitrones.

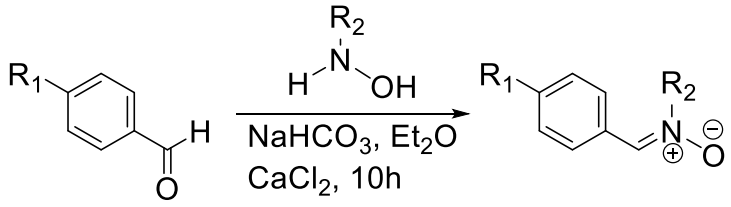

Nitrone	R_1	R_2	Yield
2.2	*p*-$MeOC_6H_4$	Me	>99
2.3	*p*-MeC_6H_4	Me	65
2.5	*p*-ClC_6H_4	Me	87
2.6	*p*-CNC_6H_4	Me	74
2.7	*p*-$NO_2C_6H_4$	Me	65

BARAC (**2.1**)was shown to react quickly and efficiently with azides.[20] To study the efficiency of the analogous reactions of **2.1** with nitrones **2.10-2.13** we measured the percent conversion to products using analytical HPLC. Cyclic nitrones were previously shown to be stable and to work well in SPANC reactions, therefore we expected to observe high percent conversions to products. The reactions were performed between compounds **2.10-2.13** (~1 mM) with **2.1** (~1 mM) in 99.9% MeCN–H_2O at room temperature. HPLC analysis of the reaction mixtures were done using a gradient elution of 10-95% MeCN/H_2O for all experiments. An external standard of **2.1** was used for each reaction. The peak identity was tracked by elution time and characteristic absorption spectra of **2.1**. After 20 min of reaction

we observed high yields of cycloaddition products and greater than 99% conversion (Table 2.4), the results were confirmed by LC-MS/ESI+.Our findings are consistent with the previously reported rapid kinetics of strain-promoted cycloaddition reactions involving **2.1**.

Once the efficiency of the SPANC reaction of BARAC (**2.1**) and nitrones was established, we sought to investigate the kinetics of the reaction. To achieve this we performed kinetic experiments under pseudo first-order reaction conditions utilizing UV-visible absorption spectroscopy and measured the associated second-order rate constants for cycloaddition of **2.1** to each respective nitrone.

2.3.1 Kinetic studies methodology

Prior to each kinetic set, the purity of the starting materials was confirmed using LC-MS. The rate measurements of cycloadditions of BARAC (**2.1**) with various nitrones were performed using UV-visible spectroscopy in aqueous (0.1% water) acetonitrile at 25 ± 0.1 ºC. Reactions were done under pseudo first-order conditions typically with one of the reactants in at least 100 fold excess and were monitored by following the decay of the absorbance at the characteristic wavelengths specified in Table 2.2. Five trials were done for each cycloaddition at the specified wavelength, changing the concentration of the excess reagent by at least 10%.

All reactions were done according to the following general procedure: a calculated amount of stock solution of excess reagent required to achieve the desired final concentration was diluted in a calculated amount of additional acetonitrile in a cuvette, and the solution was thermally equilibrated to 25 ºC. A calculated amount of stock solution of

the reacting partner required to achieve the desired final concentration was rapidly mixed with the thermally equilibrated solution and immediately inserted into the UV-vis spectrophotometer. Absorption was measured at pre-set time intervals of 0.6 to up to 6 seconds at the wavelength chosen. The time taken for the physical manipulations was taken into account automatically. Measurements were stopped once no absorption decrease was observed for a substantial amount of time to give a statistically accurate final absorbance value. Due to the complexity of NMR spectra of the mixture of regio- and diastereomeric products in each reaction, mass spectrometry was used to confirm the formation of products.

Table 2.2. Wavelength for each of the kinetic studies of the SPANC between BARAC (**2.1**) and various nitrones in aqueous (0.1% water) acetonitrile at 25 ± 0.1 ºC using UV-visible spectroscopy

Nitrone	R_1	R_2	λ (nm)
2.2	*p*-$MeOC_6H_4$	Me	302
2.3	*p*-MeC_6H_4	Me	298
2.4	Ph	Me	294
2.5	*p*-ClC_6H_4	Me	300
2.6	*p*-CNC_6H_4	Me	269
2.7	*p*-$NO_2C_6H_4$	Me	307
2.8	Ph	Ph	293
2.9	Ph	Bn	301
2.10	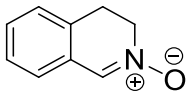		307
2.11	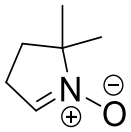		278
2.12	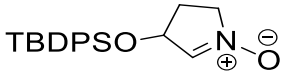		278
2.13	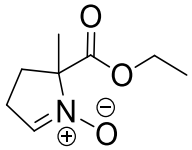		278

The data analysis was identical in all kinetic experiments. The final absorbance (average of at least 15 final recorded values) was subtracted from each measured absorbance value to obtain a relative absorbance, i.e. change in absorbance. Natural logarithms of relative absorbance values were plotted against time (in seconds). Only the linear portion of the regression was used to fit a linear trend line, the negative slope of which represented the observed rate constant (k_{obs}) for the given experiment at the given concentration of the excess reagent. The observed rate constants were then plotted against the corresponding excess reagent concentrations. The slope of the linear trend line fitted to the data points represents the second-order rate constant (k_2) for each of the cycloadditions. Table 2.3 and Figure 2.1 are presented here as examples, the data for each nitrone is attached in the Appendix.

Table 2.3.Observed rate constants for the kinetic studies of cycloadditions of BARAC (**2.1**) with **2.13**, correlated to the various concentrations of **2.13** in aqueous (0.1% water) acetonitrile at 25 ± 0.1ºC.

Nitrone	Structure	Concentration of nitrone (x 10^{-3} M)	k_{obs} (s^{-1})
2.13	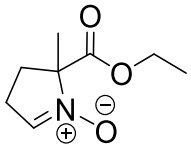	1.0	4.64 x 10^{-2}
		0.8	3.80 x 10^{-2}
		0.7	3.20 x 10^{-2}
		0.6	2.93 x 10^{-2}
		0.5	2.15 x 10^{-2}

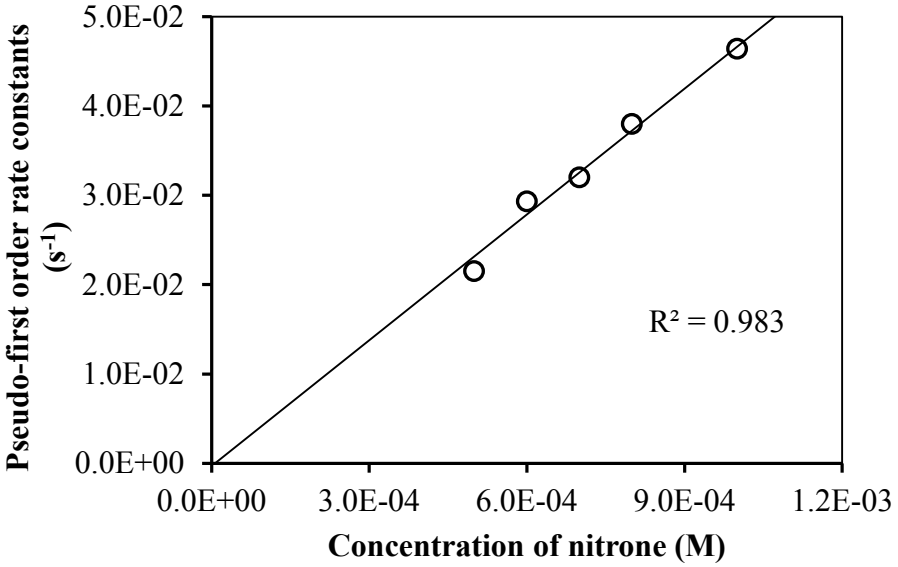

Figure 2.1. Pseudo first-order rate constants of the cycloadditions of **2.13** with BARAC (**2.1**) are plotted against the various concentrations of the nitrone. All reactions were done in aqueous (0.1% water) acetonitrile at 25 ± 0.1ºC

2.3.2 SPANC of BARAC with cyclic nitrones

Based on our previous findings of cyclic nitrones having excellent reaction rates in cycloaddition reactions with cyclooctynes, we measured the second-order rate constants for the cycloaddition of BARAC (**2.1**) with several cyclic nitrones (**2.11**-**2.13**) (Table 2.4). The first measured second-order rate constant of 22.4 M^{-1} s^{-1} belonged to dihydroisoquinoline *N*-oxide, **2.10**. Even though this was the lowest rate constant of all the cyclic nitrones, the value was still higher than most of the rate constants of acyclic nitrones. This can be attributed to the fact that the cyclic nitrones are locked into a rigid conformation and thus are restricted in rotation compared to acyclic nitrones. Cyclic nitrones also benefit from the additional degree of ring strain due to the nitrone moiety incorporated into the ring. This effectively makes the cycloaddition reaction doubly strain-promoted. A higher degree of strain can be inferred by reducing the size of the ring containing the nitrone. Thus the even more strained five-membered pyrroline-*N*-oxides, **2.11**, **2.12** and **2.13**, proceeded with rate constants of 39.2, 41.0 and 46.5 M^{-1} s^{-1}, respectively. This represents a two-fold rate enhancement over the six-membered nitrone, up to 48-fold enhancement over the analogous reaction of benzyl azide and 14-fold faster than previously reported SPANC. Such high rate constants correspond to very fast reaction rates and thus we had to perform the kinetics at very low concentrations that are similar to the concentrations used in biological labelling experiments.[16,17]

Table 2.4. Second-order rate constants and percent conversion of SPANC reactions of BARAC (**2.1**) and cyclic nitrones (**2.11-2.13**).

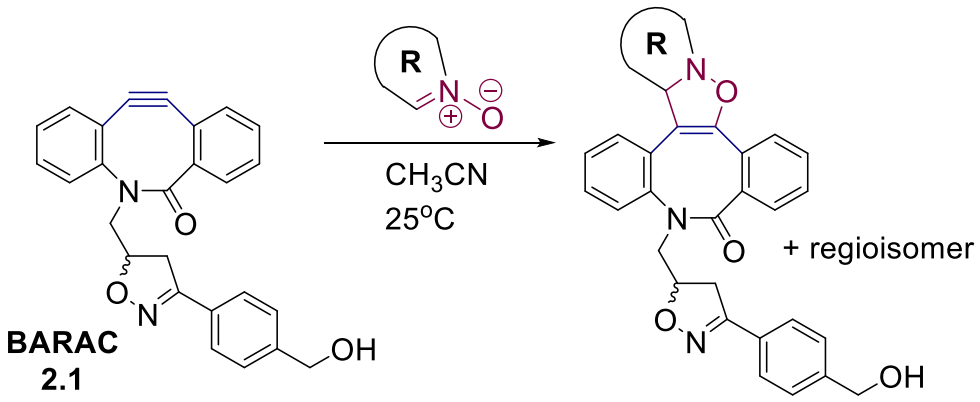

Nitrone	Structure	% Conversion	k_2 (M^{-1} s^{-1})
2.10	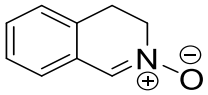	>99	22.4
2.11	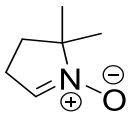	>99	39.2
2.12	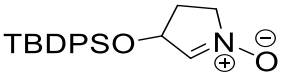	>99	41.0
2.13	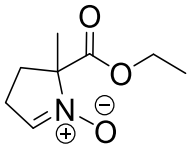	>99	46.5

2.3.3 SPANC of BARAC with acyclic nitrones

To assess the substrate scope and generality of SPANC reactions of BARAC with nitrones, we varied the substituents on the nitrones and measured the corresponding linear free energy relationships. We evaluated a series of acyclic nitrones bearing electron donating and electron withdrawing groups at the para position of the α-aryl substituent. We also changed the substitution at the *N*-position. The nitrone **2.9** bearing an electron withdrawing *N*-phenyl substituent reacted with **2.1** at an exceptionally fast rate (k_2 = 52.8 M^{-1} s^{-1}). Despite the high reaction rate of **2.9** with **2.1**, the resulting cycloadduct is thermally unstable due to the presence of the *N*-phenyl electron withdrawing group. Similar stability issues have been reported in analogous structures that were shown to be prone to thermal rearrangement leading to azomethine ylides.[24,25] In comparison, nitrones **2.8** and **2.4**, having more electron donating methylene or methyl groups at the *N*-positions, demonstrated lower rate constants of 2.76 and 6.77 M^{-1} s^{-1}, respectively (Table 2.5); however, neither reaction product exhibited instability.

Table 2.5. Second-order rate constants of SPANC reactions of BARAC (**2.1**) and acyclic nitrones.

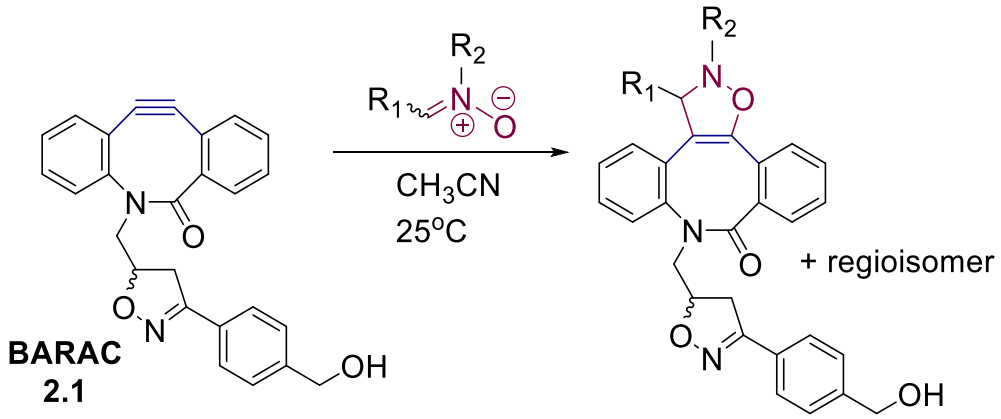

Nitrone	Structure	k_2 (M^{-1} s^{-1})
2.2	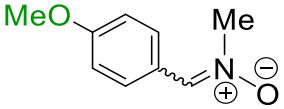	4.87
2.3	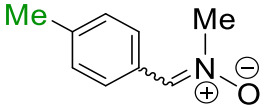	6.65
2.4	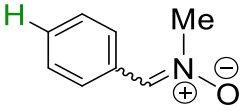	6.77
2.5	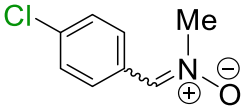	7.86
2.6	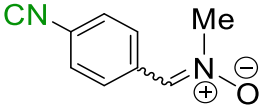	9.23
2.7	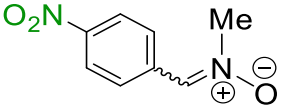	10.1
2.8	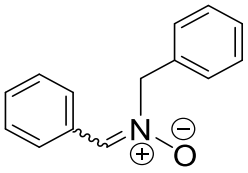	2.76
2.9	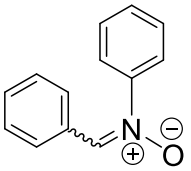	52.8

2.3.4 Structure–reactivity relationships

We chose **2.4** as the core nitrone for our kinetic studies based on its stability and higher reaction rate. In order to investigate the substituent effect on the rate of SPANC we synthesized a series of nitrones varying the group at the *para*-position of the α-aryl substituent. Moderate rate enhancements were observed for acyclic nitrones with the increase of electron withdrawing character of the varying substituent (Table 2.5). This is consistent with the SPANC reaction involving the highest occupied molecular orbital (HOMO) of BARAC and the lowest unoccupied molecular orbital (LUMO) of the nitrone (Scheme 2.3). The electron withdrawing substituent on the α-C of the nitrone lowers the energy of LUMO of the nitrone. This brings HOMO of BARAC and LUMO of the nitrone closer in energy, which in turn allows for a faster reaction of BARAC with more electron deficient nitrones.

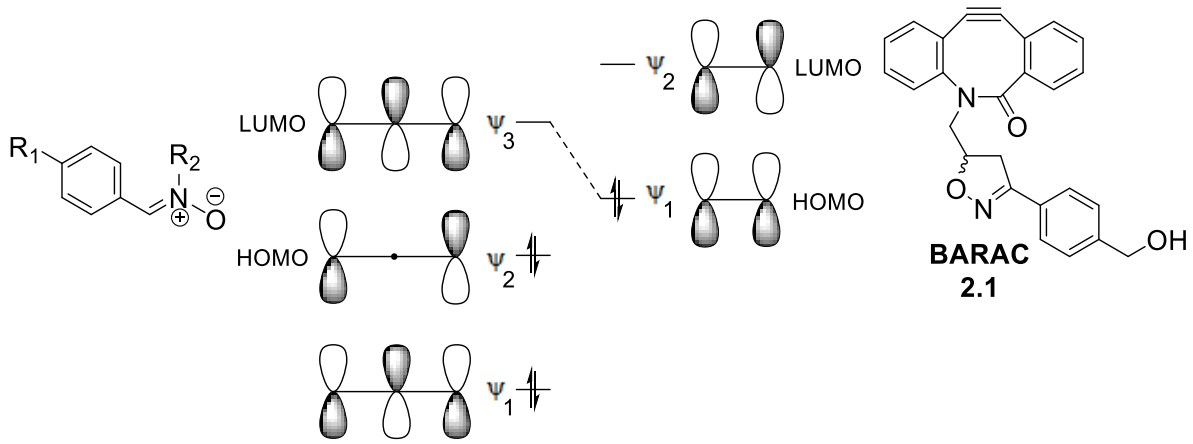

Scheme 2.3. Frontier molecular orbitals diagram for the SPANC reaction between BARAC (**2.1**) and acyclic nitrone.

We produced a Hammett plot based on the kinetic data obtained in order to investigate the substituent effects of acyclic nitrones on the relative rates of SPANC reaction with BARAC (Table 2.6 and Figure 2.2). Due to direct resonance of the para substituents and the nitrone functional group for both electron donating (Scheme 2.4) and electron withdrawing (Scheme 2.5) groups, the best fit for the Hammett plot was produced using σ_P parameters.

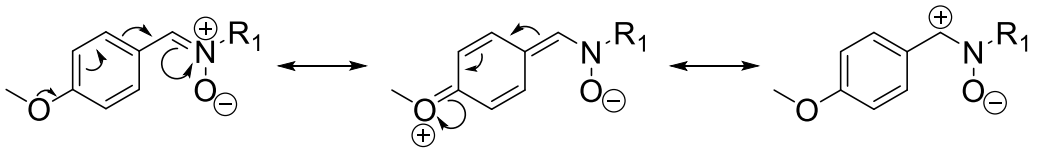

Scheme 2.4. Resonance interactions of acyclic nitrones with electron donating group at the para-position of the α-aryl substituent of the nitrone.

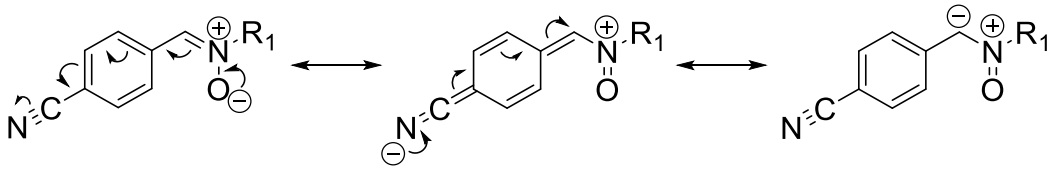

Scheme 2.5. Resonance interactions of acyclic nitrones with electron withdrawing group at the para-position of the α-aryl substituent of the nitrone.

Table 2.6. Kinetic data of SPANC reactions of BARAC (**2.1**) and acyclic nitrones used for the Hammett plot.

Nitrone	σ_P	k_2 ($M^{-1}s^{-1}$)	k_2(2.x)/k_2(2.4)	log(k_2(2.x)/k_2(2.4))
2.2	-0.29	4.87	0.719	-0.143
2.3	-0.17	6.65	0.982	-0.008
2.4	0	6.77	1	0
2.5	0.22	7.86	1.160	0.065
2.6	0.67	9.23	1.364	0.135
2.7	0.77	10.13	1.496	0.175

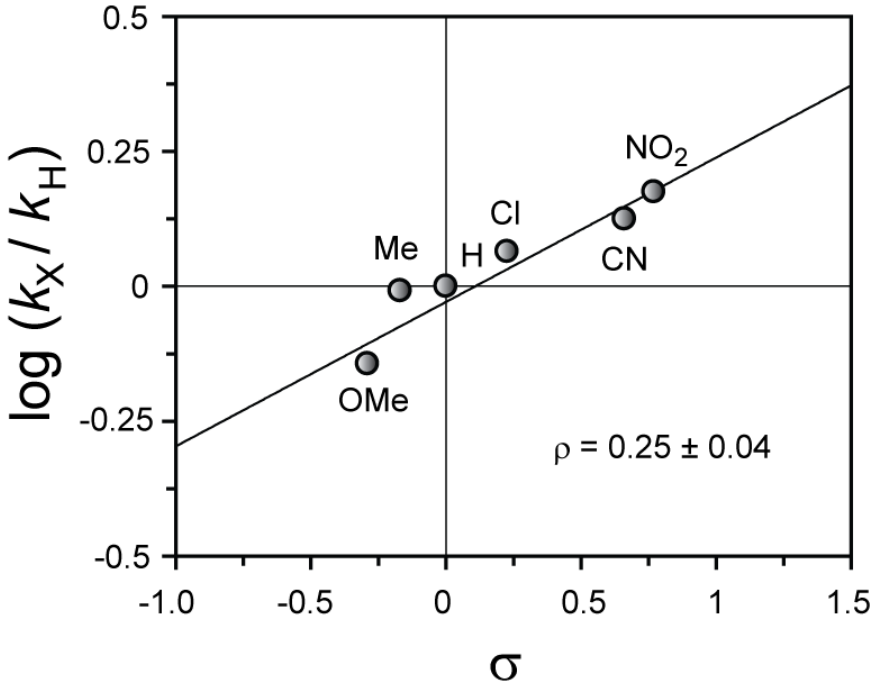

Figure 2.2. Hammett plot obtained from the kinetic data of SPANC reactions of BARAC (**2.1**) and acyclic nitrones. $R^2 = 0.94$

From the plot we extracted the reaction constant, ρ, value of 0.25 ± 0.04 (R^2 = 0.94), which indicates the relative amount of charge build-up on the α-position of the nitrone during the transition state. The small positive value of ρ that we obtained suggests that there is very little to no negative charge build-up during the transition state. This is feasible in two instances: (1) an early transition state or (2) a concerted transition state with no charge build-up.

This ρ value can be compared to that of previously reported analogous reactions of micelle-catalyzed cycloadditions of cyclopentenone with nitrones (Scheme 2.6).[26] These cycloaddition reactions were slow, and the rate constants were obtained based on the ratios of products for reactions in competition. A Hammett plot was obtained based on the kinetic data from a series of nitrones with varying groups at the *para*-position of the α-aryl substituent, and the ρ value of −0.94 was determined.

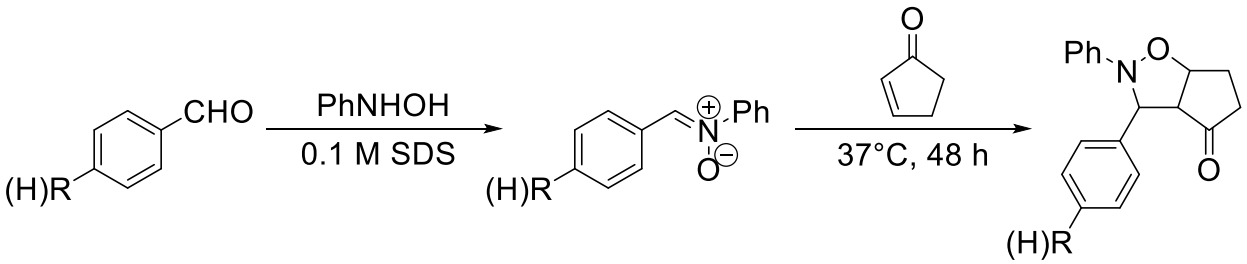

Scheme 2.6. 1,3-dipolar cycloaddition reaction of cyclopentenone with *in situ* generated acyclic nitrones.

The conclusion drawn from this study was that the value of ρ for cyclopentenone-nitrone reaction is consistent with a transition state that has modest positive charge build-up at the α-position of the nitrone during the transition state and is also consistent with a concerted rather than a stepwise mechanism for the micelle-catalyzed cycloaddition.

Cyclopentenone can act as a Michael acceptor, and therefore the transition state may be slightly asynchronous. This draws the possibility of more bond formation between the nitrone oxygen and the β-carbon of the α,β-unsaturated ketone and less bond formation between the nitrone α-carbon and the alkene. In this case there would be a modest positive charge build-up in the transition state that would be stabilized by electron donating substituents.

In comparison to the cyclopentenone-nitrone reaction ρ value, the cycloaddition of BARAC (**2.1**) and acyclic nitrones reaction ρ value has two differences: relatively lower magnitude and a positive sign. The former distinction suggests even less sensitivity to substituent effects, as well as a more synchronous transition state consistent with a concerted mechanism. The latter distinction indicates that the reactions of nitrones with BARAC are slightly accelerated by electron withdrawing substituents at the *para*-position of the α-aryl substituent of the nitrone, which is consistent with more bonding between the nitrone α-carbon and the cyclooctyne and less net positive charge on that α-carbon at the transition state for the reaction relative to the starting materials. The comparison between the two reactions' transition states can be represented by the structures in Figure 2.3, which are consistent with the differences of the slopes of the Hammett plots for these two reactions.

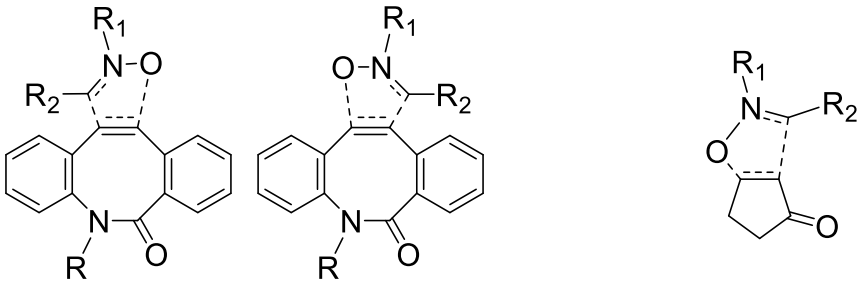

Figure 2.3. Proposed transition states for cycloaddition reactions of substituted nitrones with BARAC (**2.1**) and nitrones with cyclopentenone.

The nitrone addition reactions and their structure–reactivity relationships have been extensively studied.[27-32] In general, such reactions do not have a significant charge build up on the nitrone α-carbon atom in the transition state. The obtained Hammett ρ values range from −1.0 to 0.76. The ρ value reported herein falls in this range and is therefore consistent with previous findings on nitrone reactivity. Recently, Durand *et al.* showed that Hammett σ_P values correlate with nitrone α-H NMR chemical shift values as well as computed nitrone charge density. This suggests that these parameters may also be predictive of reactivity of other nitrones.[33] We also observe a correlation between α-H chemical shift values and the corresponding σ_P constants for the acyclic nitrones **2.2-2.7** tested in this work (Figure 2.4).

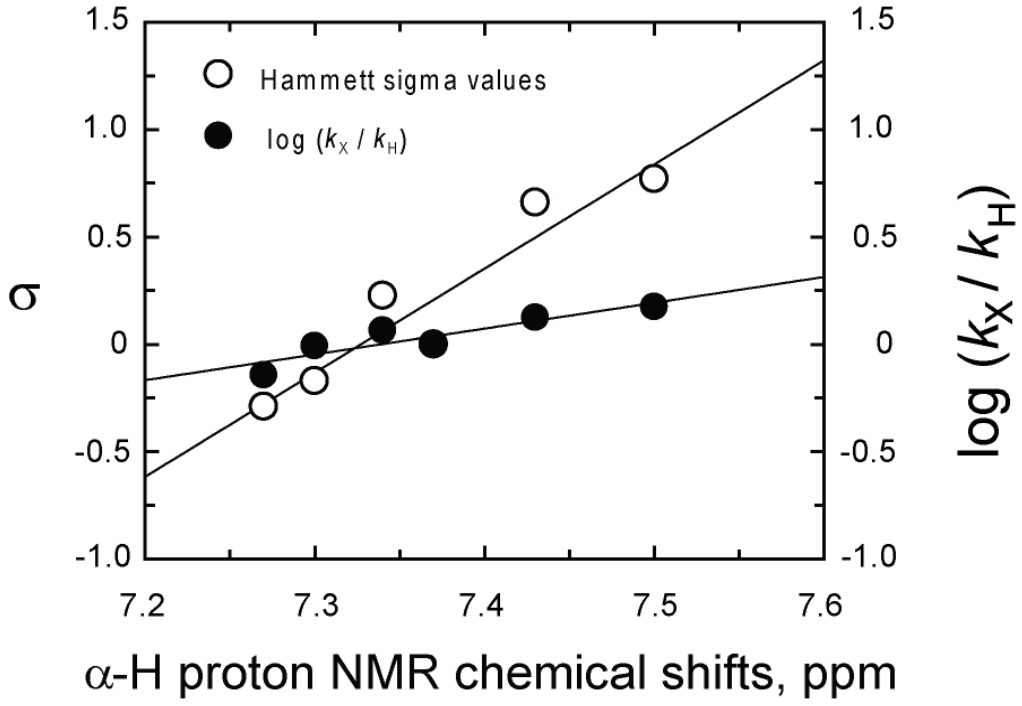

Figure 2.4. Correlation between α-H proton chemical shift values of nitrones and both σ_P constants (R^2 = 0.94), and log(k_X/k_H) (R^2 = 0.95) values for the cycloaddition reactions between nitrones **2.2-2.7** and BARAC (**2.1**).

Among other accepted applications for nitrones is their use as spin traps for free radicals, such as hydroxyl and alkoxyl radicals as well as superoxide radical anions. Therefore, in order for the biological labelling application of SPANC to be fruitful, the reaction rate of SPANC has to be significantly higher than the rates of the competing radical trapping reactions, particularly when the biological systems are under oxidative stress. The rate constants for the spin trapping were determined for DMPO (**2.11**) depending on solvent and range from (2.7–3.6) × 10^9 M^{-1} s^{-1} for HO· and from 1.2 to 310 M^{-1} s^{-1} for $O_2{\cdot}^-$.[34,35] In comparison to these reported values the rate constants for the SPANC of BARAC (**2.1**) with nitrones are within the range of the superoxide spin trapping constants. Furthermore to consider is the fact that the concentrations of these radicals in cells are typically very low and they also can react rapidly with other cellular components. All the above arguments suggest that SPANC labelling should not be hampered by the presence of superoxide. So long as the concentration of BARAC (**2.1**) is significantly higher than the concentration of the free radicals, especially hydroxyl and alkoxyl radicals, the rapid rates of cycloadditions between **2.1** and nitrones are expected to be sufficient to dominate the reactivity of nitrones.

2.4 Summary

We have shown that both acyclic and cyclic nitrones can be utilized as rapid alternatives to azides in strain-promoted cycloadditions with the fastest cyclooctyne developed – BARAC. These SPANC reactions proceed with rate constants up to 46.5 M^{-1} s^{-1}, which corresponds to up to 48-fold enhancement relative to reaction of benzyl azide and a 14-fold enhancement relative to previously reported SPANC. We also found that for acyclic nitrones SPANC reaction is sensitive to substituents on the nitrone nitrogen and

therefore significant rate enhancements can be obtained through change of group of nitrone nitrogen. However, substitution at this position that accelerates the cycloaddition unfortunately also destabilizes the reaction product by weakening the N–O bond.

We concluded based on the near-zero ρ value that the SPANC reaction is not sensitive to substituents on the nitrone α-carbon atom. Even though no rate enhancement can be achieved through substitution at that position, the reaction is tolerant of a broad range of functionalization. Low sensitivity of the reaction to substituent on the nitrone α-carbon allows to utilize SPANC in chemical biology labelling applications via appending a functionalization onto the nitrone α-carbon atom without sacrificing exceptional reactivity. Thus this centre can serve as convenient position for attachment of bio-recognition elements, affinity tags, or labels.

The optimal combination of rate enhancement and reactant and product stabilities is found with cyclic nitrones such as **2.11**-**2.13**. Stability and high reactivity make cyclic nitrones potentially the best dipoles to be used for biological labelling experiments with strained cyclooctynes, since efficient labelling could be achieved at lower concentrations of labelling reagents, with minimal toxicity, cell metabolism interference and residual fluorescence or non-specific labelling.

2.5 Materials and Experimental Methods

Equipment and Reagents

All reagents and solvents were purchased from Sigma-Aldrich, unless otherwise stated, and used without further purification. Deuterated solvents were purchased from Cambridge Isotope laboratories. Thin layer chromatography was performed on Analtech Uniplate® silica gel plates (60 Å F_{254}, layer thickness 250μm). Flash chromatography was performed using silica gel (60 Å, particle size 40–63 μm). LC-MS/MS spectra were obtained using Waters Alliance 2795 liquid chromatograph quipped with Waters 996 PDA diode array detector and connected to Micromass ZQ2000 mass spectrometer equipped with pneumatically assisted electrospray ionization source, operating in both positive and negative mode. Samples were run with gradient elution of acetonitrile/water/0.1% formic acid on the Waters SunFire C18 (2.1 x 100 mm, 3.5 μm) column with flow rate of 0.2 mL/min. Analytical HPLC was performed using Agilent 1100 Series HPLC with auto sampler and SunFire column (4.6 x 100mm, 3.5 μm) with gradient elution of acetonitrile/water at flow rate of 1.0 mL/min. All ^{1}H and ^{13}C NMR spectra were obtained on a Bruker-DRX-400 spectrometer using a frequency of 400 MHz for ^{1}H and 100 MHz for ^{13}C and processed using Bruker TOPSPIN 2.1 software. The following abbreviations were used to designate chemical shift multiplicities: s = singlet, d = doublet, t = triplet, m = multiplet or unresolved, br = broad signal and *J* = coupling constants in Hz. Kinetic experiments were done on a Varian system containing Cary 3 UV-visible Spectrophotometer and Cary Temperature Controller.

Synthesis and characterization of nitrones

General procedure[23] for synthesis of acyclic nitrones **2.2**, **2.3**, **2.5**, **2.6** and **2.7**:

To a stirring solution of *N*-methyl-hydroxylamine (0.3 M, 1.1 equiv.), $NaHCO_3$ (2 equiv.) and $CaCl_2$ (5 equiv.) in Et_2O at 0ºC was added variable aldehyde (0.27 M, 1 equiv.) all at once. The mixture was warmed to room temperature and stirred overnight. The solution was extracted with ethyl acetate. The organic layers were combined, dried over Na_2SO_4, filtered and concentrated under reduced pressure to yield a yellow or colourless oil, which was purified by silica gel column chromatography (100% EtOAc, R_f = 0.25-0.30 for all **2.2**, **2.3**, **2.5**, **2.6**, **2.7**).

***N*-[(4-methoxyphenyl)methylene]-methanamine *N*-oxide (2.2)**

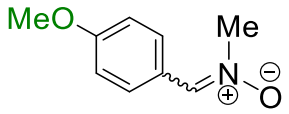

2.2

Synthesized according to the general procedure for preparation of acyclic nitrones. Identity confirmed by MS and NMR. Characterization data previously reported in literature.[36,37] Obtained **2.2** as beige solid in quantitative (108%) yield. **MS** (ESI+) calcd for **2.2** ($C_9H_{11}NO_2$): 166.08 $[M+H]^+$, found 166.2; **^{1}H-NMR** of **2.2** (400 MHz, $CDCl_3$) **δ** 8.07 (d, *J*=8.9 Hz, 2H), 7.16 (s, 1H), 6.76 (d, *J*=8.9 Hz, 2H), 3.65 (s, 6H); **^{13}C-NMR** of **2.2** (100 MHz, $CDCl_3$) **δ** 161.0, 134.9, 130.4, 123.4, 113.8, 55.3, 53.9.

***N*-[(4-methylphenyl)methylene]-methanamine *N*-oxide (2.3)**

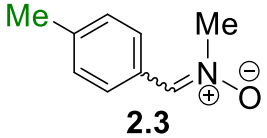

2.3

Synthesized according to the general procedure for preparation of acyclic nitrones. Identity

confirmed by MS and NMR. Characterization data previously reported in literature.[37,38] Obtained **2.3** as white crystals in 65% yield. **MS** (ESI+) calcd for **2.3** ($C_9H_{11}NO$): 150.08 $[M+H]^+$, found 150.1; **^{1}H-NMR** of **2.3** (400 MHz, $CDCl_3$) **δ** 8.10 (d, *J*=8.2 Hz, 2H), 7.33 (s, 1H), 7.21 (d, *J*=8.2 Hz, 2H), 3.86 (s, 3H), 2.37 (s, 3H); **^{13}C-NMR** of **2.3** (100 MHz, $CDCl_3$) **δ** 141.0, 135.4, 129.2, 128.5, 127.8, 54.2, 21.7.

***N*-(phenylmethylene)-methanamine *N*-oxide (2.4)**

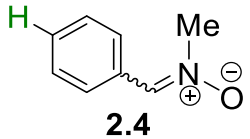

2.4

Obtained from Craig S. McKay.[39] Synthesis and characterization data previously described in literature.[40]

***N*-[(4-clhorophenyl)methylene]-methanamine *N*-oxide (2.5)**

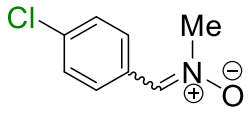

2.5

Synthesized according to the general procedure for preparation of acyclic nitrones. Identity confirmed by MS and NMR. Characterization data previously reported in literature.[36] Obtained **2.5** as white crystals in 87% yield. **MS** (ESI+) calcd for **2.5** (C_8H_8ClNO): 170.03 $[M+H]^+$, found 170.1; **^{1}H-NMR** of **2.5** (400 MHz, $CDCl_3$) **δ** 8.16 (d, *J*=8.7 Hz, 2H), 7.40 (d, *J*=8.7 Hz, 2H), 7.34 (s, 1H), 3.87 (s, 3H); **^{13}C-NMR** of **2.5** (100 MHz, $CDCl_3$) **δ** 135.9, 134.1, 129.6, 128.9, 128.8, 54.5.

***N*-[(4-cyanophenyl)methylene]-methanamine *N*-oxide (2.6)**

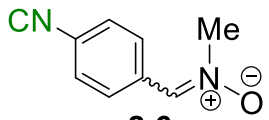

2.6

Synthesized according to the general procedure for preparation of acyclic nitrones. Identity confirmed by MS and NMR. Characterization data previously reported in literature.[38] Obtained **2.6** as white crystals in 74% yield. **MS** (ESI+) calcd for **2.6** ($C_9H_8N_2O$): 161.06 $[M+H]^+$, found 161.1; **^{1}H-NMR** of **2.6** (400 MHz, $CDCl_3$) **δ** 8.28 (d, *J*=8.4 Hz, 2H), 7.66 (d, *J*=8.3 Hz, 2H), 7.45 (s, 1H), 3.90 (s, 3H); **^{13}C-NMR** of **2.6** (100 MHz, $CDCl_3$) **δ** 134.3, 133.5, 132.2, 128.3, 118.5, 113.0, 55.0.

***N*-[(4-nitrophenyl)methylene]-methanamine *N*-oxide (2.7)**

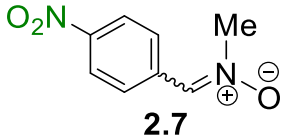

2.7

Synthesized according to the general procedure for preparation of acyclic nitrones. Identity confirmed by MS and NMR. Characterization data previously reported in literature.[36,38] Obtained **2.7** as yellow crystals in 65% yield. **MS** (ESI+) calcd for **2.7** ($C_8H_8N_2O_3$): 181.05 $[M+H]^+$, found 181.1; **^{1}H-NMR** of **2.7** (400 MHz, $CDCl_3$) **δ** 8.39 (d, *J*=9.0 Hz, 2H), 8.26 (d, *J*=9.0 Hz, 2H), 7.52 (s, 1H), 3.95 (s, 3H); **^{13}C-NMR** of **2.7** (100 MHz, $CDCl_3$) **δ** 147.8, 136.0, 133.1, 128.6, 123.8, 55.2.

***N*-(phenylmethylene)-phenylamine *N*-oxide (2.8)**

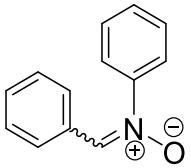

2.8

Obtained from Craig S. McKay.[39] Synthesis and characterization data previously described in literature.[40]

_N_-(phenylmethylene)-benzylamine _N_-oxide (2.9)

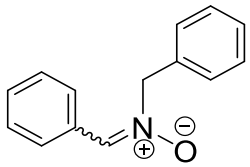

2.9

Obtained from Craig S. McKay.[39] Synthesis and characterization data previously described in literature.[40]

3,4-dihydroisoquinoline 2-oxide (2.10)

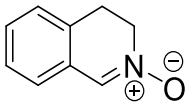

2.10

Synthesized according to the procedure previously reported in literature[41] and purified by silica gel column chromatography (CH_2Cl_2:CH_3OH / 95:5, R_f = 0.3). Identity confirmed by MS and NMR. Characterization data previously reported in literature.[42,43] Obtained **2.10** light yellow solid in 86% yield. **MS** (ESI+) calcd for **2.10** (C_9H_9NO): 148.07 $[M+H]^+$, found 148.0; **^{1}H-NMR** (400 MHz, $CDCl_3$) δ 7.61 (s, 1H), 7.14 (m, 2H), 7.08 (dd, *J*=5.8, 3.0 Hz, 1H), 6.98 (dd, *J*=6.2, 2.6 Hz, 1H), 3.96 (t, *J*=7.8, 7.8 Hz, 2H), 3.04 (t, *J*=7.8, 7.8 Hz, 2H). **^{13}C-NMR** (100 MHz, $CDCl_3$) δ 133.9, 130.0, 129.3, 128.3, 127.5, 127.2, 125.3, 57.9, 27.6.

5,5-Dimethyl-1-pyrroline _N_-oxide (2.11)

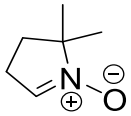

2.11

Nitrone **2.11** was purchased from Sigma-Aldrich.

3-*tert*-Butyldiphenylsilyloxy-1-pyrroline *N*-oxide (2.12)

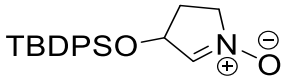

2.12

Obtained from Craig S. McKay.[39] Synthesis and characterization data previously described in literature.[40,41]

5-Ethoxycarbonyl-5-methyl-1-pyrroline *N*-oxide (2.13)

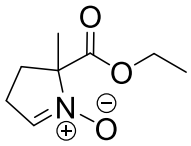

2.13

Synthesized according to the procedure previously reported in literature[44] and purified by silica gel column chromatography (Hx:EtOH / 4:6, R_f = 0.4). Identity confirmed by MS and NMR. Characterization data previously reported in literature.[44,45] Obtained **2.13** light yellow solid in 92% yield. **MS** (ESI+) calcd for **2.13** ($C_8H_{13}NO_3$): 172.09 $[M+H]^+$, found 172.3; **^{1}H-NMR** (400 MHz, $CDCl_3$) δ 7.28 (s, 1H), 4.24 (m, 2H), 2.80 (m, 2H), 2.60 (ddd, *J*=5.7, 7.2, 13.1 Hz, 1H), 2.27 (td, *J*=8.1, 8.1, 13.5 Hz, 1H), 1.67 (s, 3H), 1.29 (t, *J*=7.1, 7.1 Hz, 3H). **^{13}C-NMR** (100 MHz, $CDCl_3$) δ 169.7, 141.4, 79.3, 62.1, 31.8, 26.0, 19.7, 12.9.

Kinetic studies procedure

*This procedure outlines the general method of kinetic trial while indicating the parameters specific to the nitrone **2.13**. All kinetic studies were performed following the general method outlined, varying the concentrations and wavelength correspondingly. For monitoring wavelength specific to each nitrone, please see Table 2.2 on page 28.*

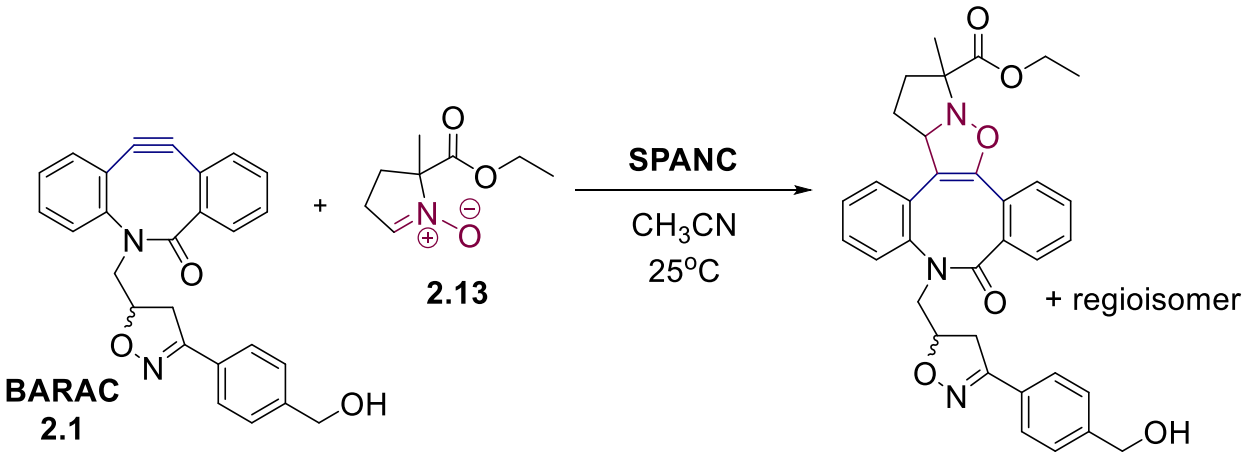

Stock solutions were prepared using volumetric flasks for BARAC **2.1** (23.8 mg in 15 mL of MeCN, 3.9 mM stock) and nitrone **2.13** (21.8 mg in 100 mL of MeCN, 1.3 mM stock). Care was taken to ensure flasks were properly closed when not in use as to minimize the evaporation and alteration of the concentrations of the starting materials. Before preparation of each solution UV-vis cuvettes (path length of 1 cm, total volume of 3 mL) were rinsed three times with MeCN and rinsings were discarded. Prior to each placement into the UV-vis spectrophotometer the cuvettes were wiped with Kimwipes to remove any residue on the outer surface. All reactions were performed at 25 ± 0.1 ºC.

In order to choose the wavelength for the kinetic trials, a series of full spectra (200 nm to 600 nm) was obtained. This series included a spectrum of:

- Solvent only as baseline
- Each of the starting materials at 0.065 mM
    - BARAC (**2.1**): 0.065 mM = 0.065 mM*3 mL/3.9 mM = 50 uL (mixed with 2950 of MeCN)

    - Nitrone **2.13**: 0.065 mM = 0.065 mM*3 mL/1.3 mM= 150 uL (mixed with 2850 of MeCN)

- Mixture of 2800 uL of MeCN with 50 uL of stock of BARAC (**2.1**) and 150 uL of stock of nitrone **2.13** (for final concentration of ~0.065 mM each)
    - Full spectrum scans of the above mixture to follow the reaction over several minutes. Once no more change in spectrum was observed these overlaid spectra were used to choose the wavelength to perform the kinetic studies. For nitrone **2.13** the wavelength of 278 nm was chosen.

New BARAC (**2.1**) stock of 0.39 mM was made for the kinetics from original stock. A blank of only MeCN solvent for the series was made in cuvette 1. In cuvette 2 the appropriate amount indicated in Table 2.7 of MeCN was added first, followed by the corresponding volume of nitrone stock. Cuvette 2 was closed and shaken, The UV-vis spectrophotometer was blanked with wiped clean cuvette 1. Once ready to add the BARAC, the machine was put on countdown in order to take time for manipulation and mixing into account. BARAC was added swiftly, the cuvette was shaken and placed into the spectrophotometer, the lid was closed and the kinetic was started. For each kinetic trial data was collected for approximately 2-3 minutes at 0.1 s intervals until a consistent plateau was reached. Data was saved as .csv file and a new run was set up and started. Kinetic trials with the highest correlation coefficients were used for the final plot of observed rate constants vs concentrations of the excess reagent to find the second-order rate constant.

Table 2.7. Reagent data for kinetic trial of SPANC reaction of BARAC (**2.1**) with nitrone **2.13**. Amounts (in uL) mixed and resulting concentrations are indicated along with the correlation coefficients of the data.

Run # Cycle 0.01	**Volume of BARAC stock (0.39 mM) in uL**	**Volume of MeCN in uL**	**Volume of 2.13 stock (1.3 mM) in uL**	**[BARAC] (mM) in uL**	**[2.13] (mM) in uL**	**R^2**
3 rerun	77	615	2308	0.01	1	0.868
6	77	1077	1846	0.01	0.8	0.908
5	11.6 (2.575 mM stock)	1373.4	1615	0.01	0.7	0.986
7 rerun	77	1538	1385	0.01	0.6	0.922
8	77	1769	1154	0.01	0.5	0.917

2.6 References

(1) Prescher, J. A.; Bertozzi, C. R. *Nat. Chem. Biol.* **2005**, *1*, 13.

(2) Boyce, M.; Bertozzi, C. R. *Nat. Meth.* **2011**, *8*, 638.

(3) Sletten, E. M.; Bertozzi, C. R. *Angew. Chem. Int. Ed.* **2009**, *48*, 6974.

(4) Sletten, E. M.; Bertozzi, C. R. *Acc. Chem. Res.* **2011**, *44*, 666.

(5) Lim, R. K. V.; Lin, Q. *Chem. Commun.* **2010**, *46*, 1589.

(6) Soriano del Amo, D.; Wang, W.; Jiang, H.; Besanceney, C.; Yan, A. C.; Levy, M.; Liu, Y.; Marlow, F. L.; Wu, P. *J. Am. Chem. Soc.* **2010**, *132*, 16893.

(7) Dehnert, K. W.; Beahm, B. J.; Huynh, T. T.; Baskin, J. M.; Laughlin, S. T.; Wang, W.; Wu, P.; Amacher, S. L.; Bertozzi, C. R. *ACS Chem. Biol.* **2011**, *6*, 547.

(8) Kennedy, D. C.; McKay, C. S.; Legault, M. C. B.; Danielson, D. C.; Blake, J. A.; Pegoraro, A. F.; Stolow, A.; Mester, Z.; Pezacki, J. P. *J. Am. Chem. Soc.* **2011**, *133*, 17993.

(9) Hong, V.; Steinmetz, N. F.; Manchester, M.; Finn, M. G. *Bioconjugate Chem.* **2010**, *21*, 1912.

(10) McKay, C. S.; Moran, J.; Pezacki, J. P. *Chem. Commun.* **2010**, *46*, 931.

(11) McKay, C. S.; Blake, J. A.; Cheng, J.; Danielson, D. C.; Pezacki, J. P. *Chem. Commun.* **2011**, *47*, 10040.

(12) Ning, X.; Temming, R. P.; Dommerholt, J.; Guo, J.; Ania, D. B.; Debets, M. F.; Wolfert, M. A.; Boons, G.-J.; van Delft, F. L. *Angew. Chem. Int. Ed.* **2010**, *49*, 3065.

(13) Singh, I.; Heaney, F. *Chem. Commun.* **2011**, *47*, 2706.

(14) Sanders, B. C.; Friscourt, F.; Ledin, P. A.; Mbua, N. E.; Arumugam, S.; Guo, J.; Boltje, T. J.; Popik, V. V.; Boons, G. J. *J. Am. Chem. Soc.* **2011**, *133*, 949.

(15) Baskin, J. M.; Prescher, J. A.; Laughlin, S. T.; Agard, N. J.; Chang, P. V.; Miller, I. A.; Lo, A.; Codelli, J. A.; Bertozzi, C. R. *Proc Natl Acad Sci U S A* **2007**, *104*, 16793.

(16) Codelli, J. A.; Baskin, J. M.; Agard, N. J.; Bertozzi, C. R. *J. Am. Chem. Soc.* **2008**, *130*, 11486.

(17) Ning, X.; Guo, J.; Wolfert, M. A.; Boons, G.-J. *Angew. Chem. Int. Ed.* **2008**, *47*, 2253.

(18) Stockmann, H.; Neves, A. A.; Stairs, S.; Ireland-Zecchini, H.; Brindle, K. M.; Leeper, F. J. *Chem. Sci.* **2011**, *2*, 932.

(19) Debets, M. F.; van Berkel, S. S.; Schoffelen, S.; Rutjes, F. P. J. T.; van Hest, J. C. M.; van Delft, F. L. *Chem. Commun.* **2010**, *46*, 97.

(20) Jewett, J. C.; Sletten, E. M.; Bertozzi, C. R. *J. Am. Chem. Soc.* **2010**, *132*, 3688.

(21) Jewett, J. C.; Bertozzi, C. R. *Org. Lett.* **2011**, *13*, 5937.

(22) Dommerholt, J.; Schmidt, S.; Temming, R.; Hendriks, L. J.; Rutjes, F. P.; van Hest, J. C.; Lefeber, D. J.; Friedl, P.; van Delft, F. L. *Angew. Chem. Int. Ed.* **2010**, *49*, 9422.

(23) DeShong, P.; Leginus, J. M. *J. Org. Chem.* **1984**, *49*, 3421.

(24) Baldwin, J. E.; Pudussery, R. G.; Qureshi, A. K.; Sklarz, B. *J. Am. Chem. Soc.* **1968**, *90*, 5325.

(25) Liguori, A.; Ottana, R.; Romeo, G.; Sindona, G.; Uccella, N. *Tetrahedron* **1988**, *44*, 1255.

(26) Lorello, G. R.; Legault, M. C. B.; Rakic, B.; Bisgaard, K.; Pezacki, J. P. *Bioorg. Chem.* **2008**, *36*, 105.

(27) Abe, Y.; Seno, S.-y.; Sakakibara, K.; Hirota, M. *J. Chem. Soc., Perkin Trans. 2* **1991**, *2*, 897.

(28) Janzen, E. G.; Evans, C. A.; Nishi, Y. *J. Am. Chem. Soc.* **1972**, *94*, 8236.

(29) Janzen, E. G.; Evans, C. A. *J. Am. Chem. Soc.* **1973**, *95*, 8205.

(30) Schmid, P.; Ingold, K. U. *J. Am. Chem. Soc.* **1978**, *100*, 2493.

(31) Sueishi, Y.; Yoshioka, C.; Olea-Azar, C.; Reinke, L. A.; Kotake, Y. *Bull. Chem. Soc. Jpn.* **2002**, *75*, 2043.

(32) Sueishi, Y.; Yoshioka, D.; Yoshioka, C.; Yamamoto, S.; Kotake, Y. *Org. Biomol. Chem.* **2006**, *004*, 896.

(33) Durand, G.; Choteau, F.; Pucci, B.; Villamena, F. A. *J. Phys. Chem. A* **2008**, *112*, 12498.

(34) Villamena, F. A.; Xia, S.; Merle, J. K.; Lauricella, R.; Tuccio, B.; Hadad, C. M.; Zweier, J. L. *J. Am. Chem. Soc.* **2007**, *129*, 8177.

(35) Rosen, G. M.; Britigan, B. E.; Halpern, H. J.; Pou, S., Oxford Univeristy Press: New York.

(36) Tyrrell, E.; Allen, J.; Jones, K.; Beauchet, R. *Synthesis* **2005**, *2005*, 2393.

(37) Tsuge, O.; Sone, K.; Urano, S.; Matsuda, K. *J. Org. Chem.* **1982**, *47*, 5171.

(38) Colacino, E.; Nun, P.; Colacino, F. M.; Martinez, J.; Lamaty, F. *Tetrahedron* **2008**, *64*, 5569.

(39) McKay, C. S. *PhD Thesis* **2012**, University of Ottawa.

(40) Evans, D. A.; Song, H.-J.; Fandrick, K. R. *Org. Lett.* **2006**, *8*, 3351.

(41) Gella, C.; Ferrer, E.; Alibes, R.; Busque, F.; de March, P.; Figueredo, M.; Font, J. *J. Org. Chem.* **2009**, *74*, 6365.

(42) Murahashi, S.-I.; Mitsui, H.; Shiota, T.; Tsuda, T.; Watanabe, S. *J. Org. Chem.* **1990**, *55*, 1736.

(43) Shono, T.; Matsumura, Y.; Inoue, K. *J. Org. Chem.* **1986**, *51*, 549.

(44) Tsai, P.; Ichikawa, K.; Mailer, C.; Pou, S.; Halpern, H. J.; Robinson, B. H.; Nielsen, R.; Rosen, G. M. *J. Org. Chem.* **2003**, *68*, 7811.

(45) Olive, G.; Mercier, A.; Moigne, F. L.; Rockenbauer, A.; Tordo, P. *Free Radical Bio. Med.* **2000**, *28*, 403.

Chapter 3 : Novel Rearrangement of Biarylazacyclooctynones

3.1 Introduction

Biomolecules that are not accessible to labelling *via* conventional genetic encoding methods can be tracked using bioorthogonal reactions.[1-4] The most widely used bioorthogonal reactions are azide-based, such as Staudinger ligations with triaryl phosphines,[5,6] Cu(I)-catalysed azide-alkyne cycloaddition (CuAAC),[7,8] and strain-promoted azide-alkyne cycloaddition (SPAAC)[9]. SPAAC has been confirmed to be biocompatible,[10] and its rate has undergone an extensive improvement, mainly through modifying the strained cyclooctyne.[11-16] An important benefit to optimization of cyclooctyne reactivity for *in vivo* applications was the improvement in the hydrophilicity and pharmacokinetics within living organisms. This was achieved by embedding an additional nitrogen atom within the cyclooctyne ring in an effort to improve upon solubility as well as the reaction rate due to further ring contraction. This modification is found in di-methoxy-aza-cyclooctyne (DIMAC)[17], aza-dibenzocyclooctyne (DIBAC or ADIBO)[18,19] and biarylazacyclooctynone (BARAC)[20,21].

The efforts to improve the kinetics of the bioorthogonal reactions have been driven by the necessity of the labelling to be sufficiently fast. However, faster reactivity can allow for reduced selectivity and lead to inefficient labelling due to side reactions. One such side reaction was observed by van Delft *et al.* when attempting to synthesize DIBAC (Scheme 3.1).[18] The authors hypothesized that the indole product was formed via 5-endo-dig cyclisation in order to relieve ring strain during Cbz-group removal.

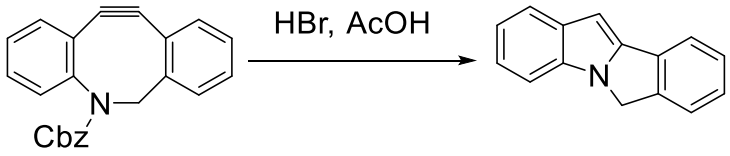

Scheme 3.1. DIBAC cyclization reaction observed by van Delft *et al*.

A recent study conducted in mice evaluated the strained alkyne probes to assess the utility of Cu-free "click" reaction in living organisms. The authors reported low reactivity for the DIFO and DIBO, which limits potential use *in vivo* pre-targeting applications at low concentrations.[22] These results were attributed to serum interactions and possible albumin interactions with the cyclooctyne part of the probes, which interfere with the cycloaddition. In addition, the low bioavailability of the probes studies further complicates their use in labelling applications. The authors expressed hope that newly developed cyclooctynes, such as BARAC, may have higher reactivity and hydrophilicity to allow effective bioorthogonal chemistry in living organisms at low concentrations.

3.2 Hypothesis

Biarylazacyclooctynones undergo addition and rearrangement reactions that could potentially impede the biological labelling tagging.

3.3 Results and Discussion

3.3.1 Initial observations of rearrangement

The initial purpose of the synthesis of **3.2** was to afford an accessible derivative analogous to BARAC (**3.6** same as **2.1**) for kinetic studies of SPANC with nitrones. **3.2** has a simple allyl side chain on the nitrogen as opposed to more complex isoxazoline derived side chain on **3.6**. We expected that having an allyl linker and essentially removing the additional stereocentre from the starting material would simplify the characterization of products of kinetic reactions. We synthesized known intermediate **3.1** according to a reported procedure[20] and attempted to synthesize **3.2** by stirring **3.1** (0.01M, 1 equiv.) with excess of CsF (6 equiv.) in MeCN for 45 min (Scheme 3.2). The mixture was then filtered to remove excess CsF. The filtrate was evaporated under reduced pressure and the crude oil was stored at -20 ºC overnight. The crude was purified by silica gel column chromatography to yield two products, **3.3** and **3.4**, in a 9:1 ratio respectively: **3.3** as white solid in 90% yield (R_f = 0.16, Hx:EtOAc/1:1) and **3.4** as light yellow solid in 2.7% yield (R_f = 0.6, Hx:EtOAc/8:2). Both products were characterized by NMR and MS. **3.4** was deemed to be the desired alkyne product based on NMR and MS data, which was consistent with the expected values. However, after several failed attempts at obtaining cycloaddition products of **3.4** with nitrones, we decided to characterize **3.4** further. X-ray crystallography of both **3.3** and **3.4** confirmed that we did not synthesize **3.2** and, instead, obtained products **3.3** and **3.4** depicted in Scheme 3.2 and Figure 3.1.

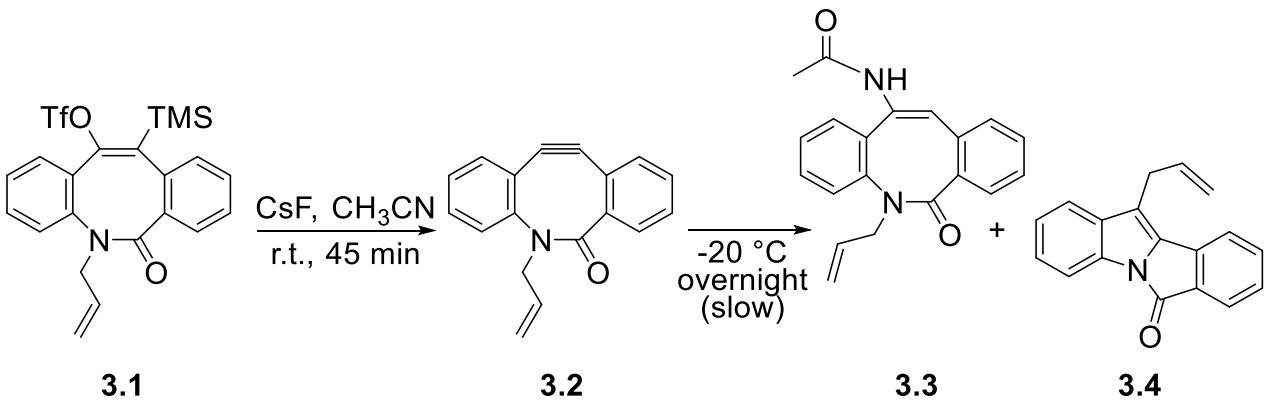

Scheme 3.2. Synthesis of **3.2** and first observation of its decomposition into products **3.3** and **3.4**.

We proceeded with the synthesis of BARAC (**3.6** same as **2.1**) with a full isoxazoline linker for use in the kinetic studies of SPANC with series of nitrones. The results of these studies are discussed in detail in Chapter 2. However, concurrently, we decided to explore this novel reactivity of biarylazacyclooctynones through studying the rearrangement reaction of **3.2**. We rationalized that the *N*-alkyl amide by-product **3.3** was formed through a Ritter reaction,[23] first by protonation of the alkyne, followed by electrophilic addition with solvent MeCN, and subsequent hydrolysis of the nitrilium ion by water present. Observations of a product analogous to **3.4** have been mentioned by van Delft *et al.* during the synthesis of DIBAC.[18] In that case the authors believed that the indole was formed via 5-endo-dig cyclisation in order to relieve ring strain during Cbz-group removal.[18]

3.3.2 Reversibility studies and optimized synthesis of 3.2

We confirmed that **3.2** is obtained from **3.1** by conducting the elimination reaction in the presence of a trap: nitrone **2.7**. To a mixture of **3.1** (0.14 M, 1 equiv.), **2.7** (1 equiv.) and CsF (6 equiv.) was added CH_3CN all at once. The solution was stirred vigorously for 5

hours and the solvent was removed. The crude oil was purified by silica gel column chromatography (Hx:EtOAc/6:4, R_f = 0.3) to yield a light yellow oil in 46% yield (Scheme 3.3).

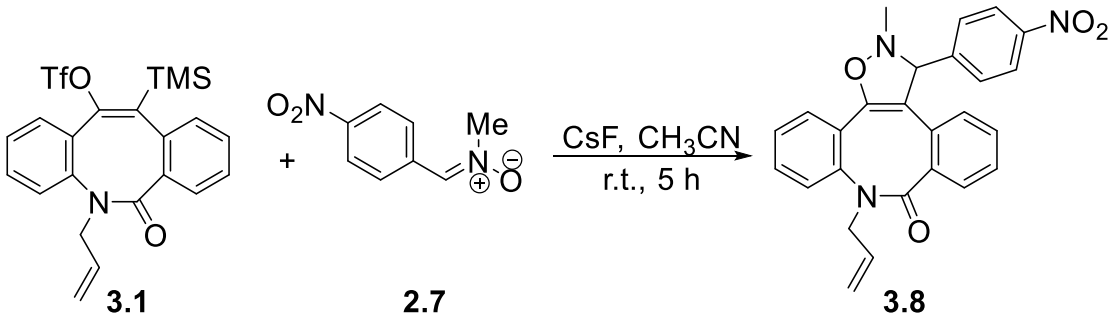

Scheme 3.3. Elimination reaction of **3.1** in the presence of nitrone **2.7** confirming the formation of **3.2**.

Encouraged by these observations we sought to determine if the rearrangement of **3.1** to **3.4** was reversible. To this end we heated **3.4** (0.027 M, 1 equiv.) in deuterated acetonitrile in the presence of benzyl azide (1.2 equiv.) as a trap to 78 °C for 1 hour and monitored the reaction mixture by NMR. However, no change of the starting materials was observed (Scheme 3.4).

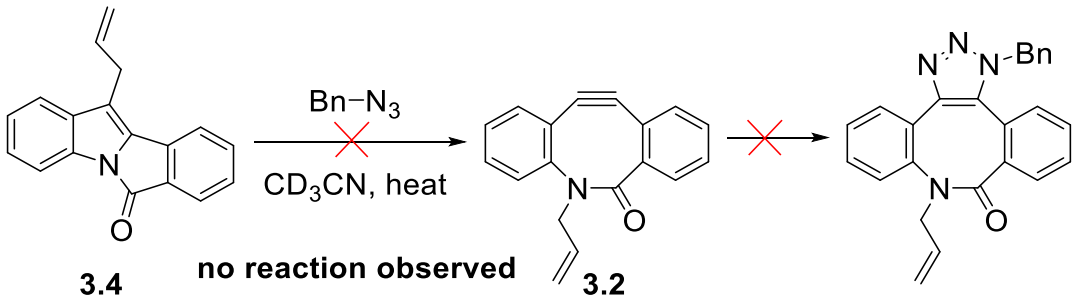

Scheme 3.4. Attempt at reversing the rearrangement and trapping **3.2** with benzyl azide.

Next, to determine if CsF had a role in the reverse reaction, we added CsF (1 equiv.) to

the solution of **3.4** (0.027 M, 1 equiv.) in deuterated acetonitrile. The solution was stirred at r.t. for several days with no change observed by TLC or LC-MS. The mixture was transferred to an NMR tube and heated to 78 ºC for 1 hour. No reaction was observed (Scheme 3.5).

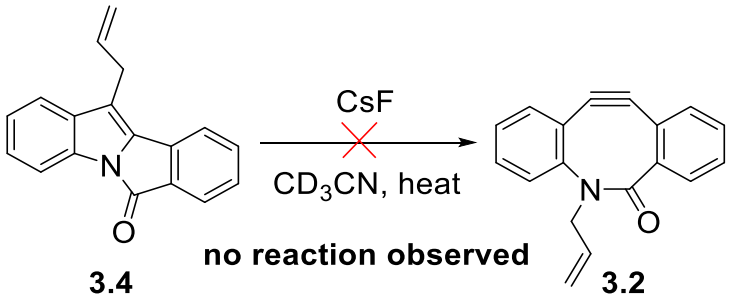

Scheme 3.5. Attempt at reversing the rearrangement in the presence of CsF.

Lastly, heating **3.4** (0.027 M, 1 equiv.) to 78 °C for 1 hour in the presence of CsF (1 equiv.) and TMS-Cl (1 equiv.) in deuterated acetonitrile resulted in no reaction as well (Scheme 3.6). The above results led us to the conclusion that **3.4** product is formed irreversibly from the rearrangement of cyclooctyne **3.2**.

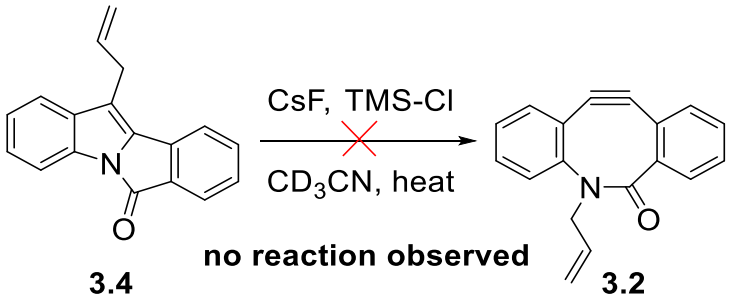

Scheme 3.6. Attempt at reversing the rearrangement in the presence of CsF and TMS-Cl.

After repeated attempts to obtain pure **3.2** in good yield we optimized the procedure for its synthesis. To a mixture of **3.1** (0.2 M, 1 equiv.) and CsF (6 equiv.) was added CH_3CN all at once. The solution was stirred vigorously for 1.5 h, and the solvent was removed. The resultant crude oil was immediately purified by silica gel column chromatography (Hx:EtOAc/9:1, R_f = 0.28). The SiO_2 was neutralised with 96:4/Hx:Et_3N prior to purification of **3.2**. Gratifyingly **3.2** compound was obtained as a light yellow in 74% yield and was characterized in neutralized deuterated chloroform and stored under argon at -80 ºC (Scheme 3.7).

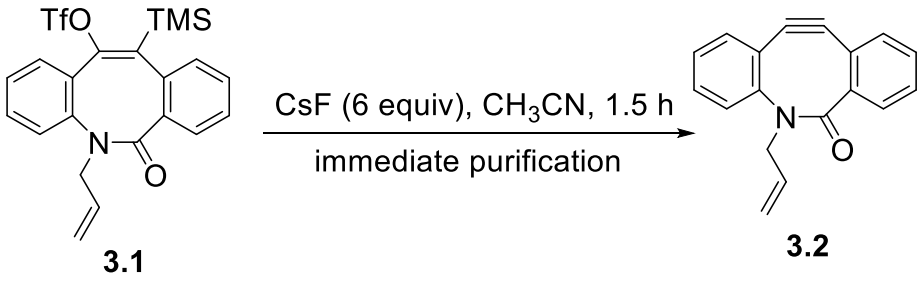

3.1 **3.2**

Scheme 3.7. Synthesis of **3.2**

3.3.3 Kinetic studies of the rearrangement under neutral conditions

To characterize the reaction we measured the kinetics of the rearrangement of **3.2** utilizing ^{1}H NMR. In order to avoid the competing nucleophilic addition of solvent we performed the kinetic experiments in deuterated chloroform rather than acetonitrile. Also, to avoid acid interference, both the chloroform used for azeotroping as well as solvent for kinetic studies were carefully neutralized before usage by filtering through a short plug of solid sodium bicarbonate. The NMR tube was heat sealed and kept in a water bath at 25 ºC. Caution was also taken as to not expose the reaction to light. A ^{1}H NMR spectrum was taken daily for 9 days until **3.2** had disappeared completely. The stacked ^{1}H NMR spectra in Scheme 3.8 illustrate the progression of rearrangement of **3.2** to only two products: **3.4** and **3.5** in a ratio of 1.3:1. Once the reaction was complete, the solvent was evaporated under reduced pressure and crude was purified by silica gel column chromatography (Hx:EtOAc/8:2, R_f (**3.4**) = 0.6, R_f (**3.5**) = 0.3) to yield **3.4** as light yellow solid in 53% yield and **3.5** as red solid in 41% yield. The formation of **3.5** was also confirmed by the X-ray crystallography (Figure 3.1).

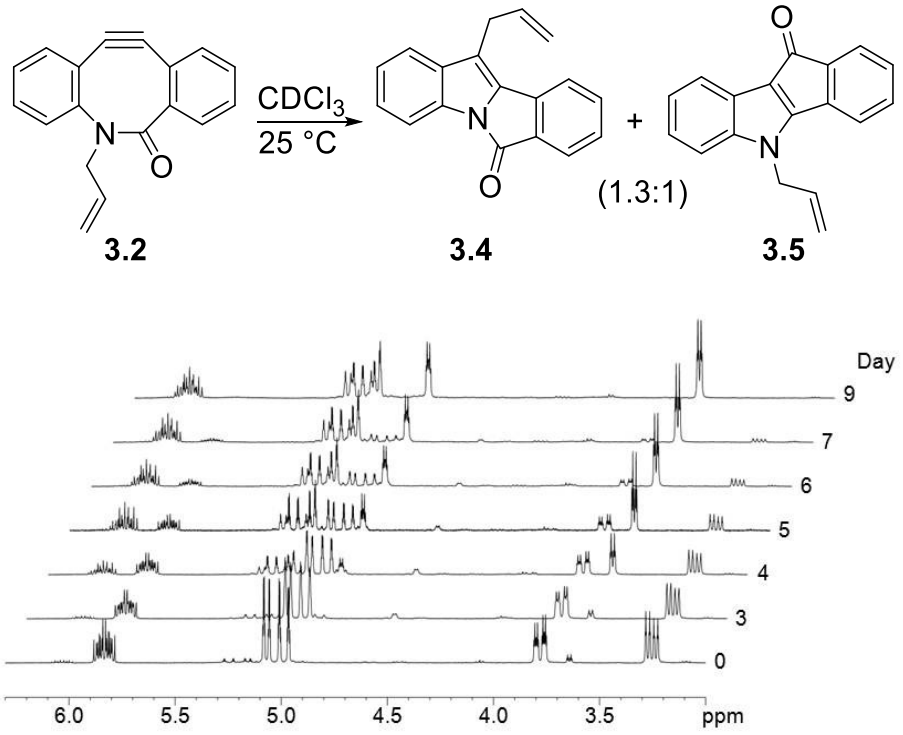

Scheme 3.8. Overlay of ^{1}H NMR spectra showing time-dependent rearrangement of **3.2** over time in $CDCl_3$ at 25 ± 0.1 °C.

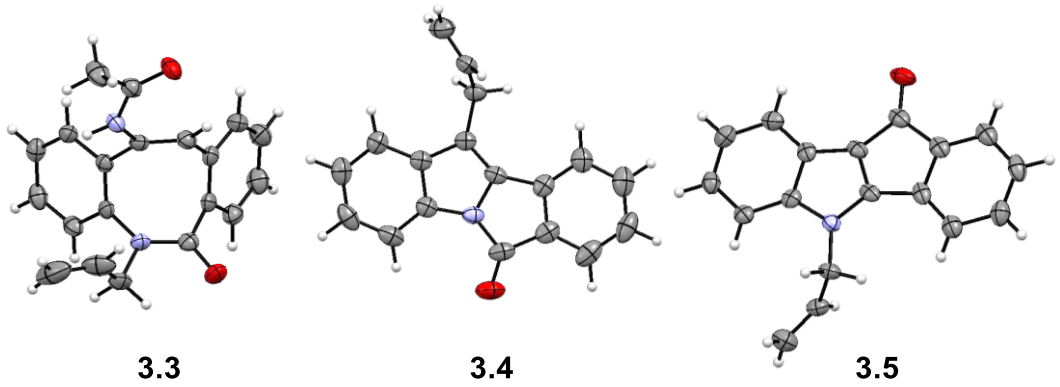

Figure 3.1. ORTEP diagrams of **3.3**, **3.4** and **3.5** with thermal ellipsoids.

In order to determine the rate constant for the rearrangement we processed the kinetic data in the following way. The intensity of a characteristic peak of **3.2** was calibrated to 100%. The same peak in all spectra in the kinetic trial was integrated using the initial calibration. Natural logarithms of intensity values were plotted against time (in seconds). The data spanning over 5 half-lives of the reaction fitted a linear trend line, the negative slope of which represented the rate constant for the given experiment. This data analysis was identical for all kinetic experiments.

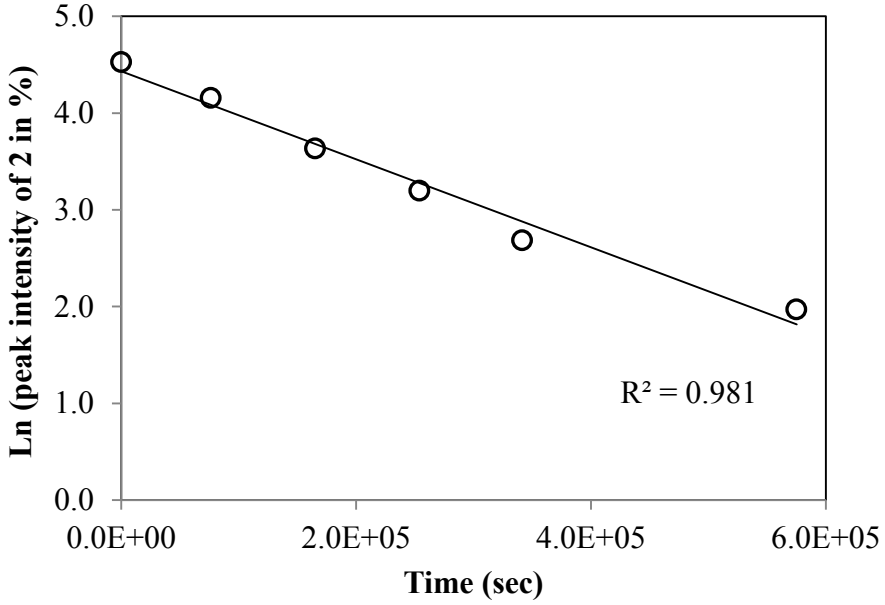

Figure 3.2. Plot of Ln ([**3.2**]) vs. time for the rearrangement reaction under neutral conditions as monitored for a period of over 9 days by ^{1}H NMR in $CDCl_3$ at 25 ± 0.1 ºC.

We found the unimolecular rate constant for the rearrangement reaction under neutral conditions to be 4.54 x 10^{-6} s^{-1} (Figure 3.2). Even though k_{rear} was found to be of relatively low value, the half-life derived from the constant corresponded to ~42 hrs. The slow rate of the rearrangement reaction means that it is not likely to interfere with the intended strain-promoted click chemistry labelling reactions, since the SPAAC and SPANC reactions have

significantly faster rates. However, it can play a role in interfering with labelling using azacyclooctynones for bioorthogonal reactions, especially in cases where reagents must be incubated in living systems over extended periods of time.[24,25]

We also found that the rearrangement of biarylazacyclooctynones is not exclusive to analogues bearing the allyl side chain such as **3.2**. BARAC (**3.6** same as **2.1**) was also observed to undergo the rearrangement to an analogous product **3.7**, the structure of which was elucidated by X-ray crystallography (Scheme 3.9). BARAC (**3.6** same as **2.1**) was dissolved in CD_3CN and stored at -20 ºC. Over time the solution turned from yellow to orange-red and a single red crystal was obtained. Interestingly, the rearrangement of **3.6** occurred over a significantly longer period of time compared to **3.2**. This difference can be attributed to the fact that the 4,5-didehydro-oxazole linker found in **3.6** is a poor leaving group compared to an allyl linker in **3.2**. We roughly estimated the half-life of **3.6** to be approximately 5 days in $CDCl_3$.

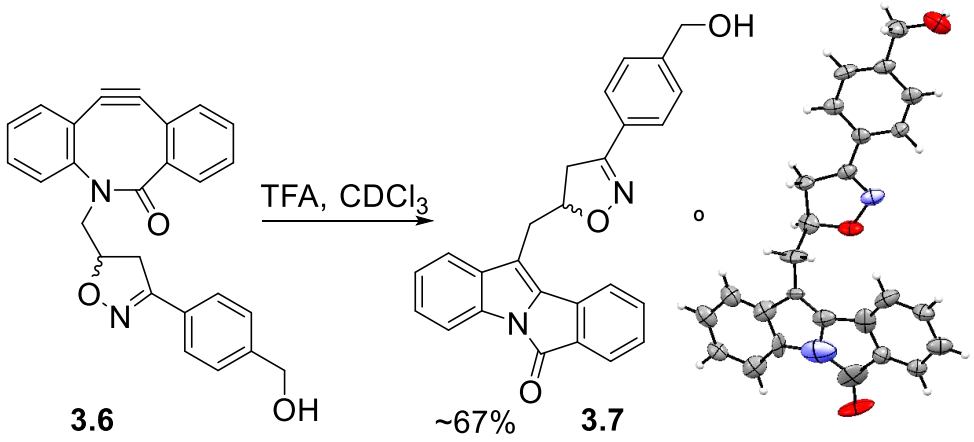

Scheme 3.9. Rearrangement of **3.6** to **3.7** with the ORTEP diagram of **3.7**.

We hypothesized that this novel rearrangement will be accelerated in the presence of

acid. While the proton transfers with heteroatoms are diffusion controlled and are therefore generally fast[26], the proton transfers to carbon are slower, with only a few exceptions.[27] We expected that the protonation of the amide would accelerate the addition of water to the alkyne leading to product **3.5**, while protonation of the alkyne would likely accelerate the 5-endo-dig transannular cyclization resulting in product **3.4**. The plausible mechanisms for the formation of **3.4** and **3.5** are discussed in a following section.

3.3.4 Kinetic studies of the rearrangement under acid catalysis

To measure the acid catalysis of the rearrangement we subjected **3.2** to varying concentrations of TFA in $CDCl_3$ and monitored reaction by ^1H NMR at 25 ± 0.1 ºC. Precautions were taken to not introduce acid into the starting material **3.2**. Analogous to kinetic studies under neutral conditions, non-deuterated chloroform for azeotroping and deuterated chloroform used as solvent in all reactions were carefully neutralised by filtering through a short plug of solid sodium bicarbonate. Fresh batch of neutralised solvent was used for each reaction. A ^1H-spectra was taken of each sample without acid for assuring purity of starting material. A calculated amount of stock solution of TFA required to achieve the desired final concentration was added to the solution of **3.2** in NMR-tube. A ^1H-spectra was taken periodically over several hours until complete disappearance of the starting material. All reaction were performed at 25 ± 0.1 ºC using the NMR spectrometer built-in temperature control system. Kinetic data for each reaction was processed as previously described for the neutral conditions (Figure 3.3).

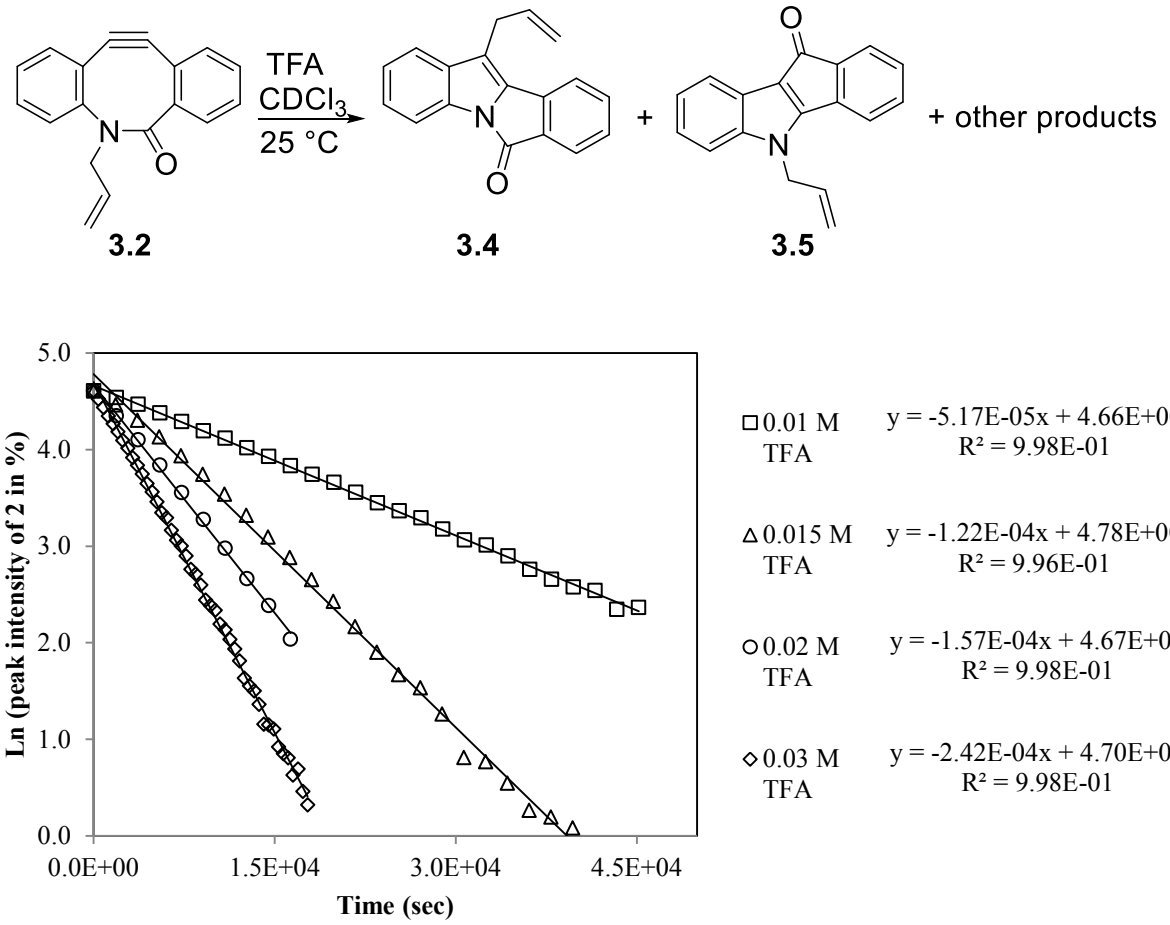

Figure 3.3. Plot of Ln ([**3.2**]) vs. time for the rearrangement reactions under acidic conditions as monitored for several hours by ^{1}H NMR in $CDCl_3$ at 25 ± 0.1 ºC.

The determined rate constants were then plotted against the corresponding TFA concentrations. The slope of the linear trend line fitted to the data points represents the k_{cat} for the rearrangement reaction under acid catalysis. The rate acceleration correlating to the increase in the concentration of TFA (0-0.3 M) suggests that the rearrangement is, indeed, acid catalysed with a k_{H+} value of 8.18 x 10^{-3} $M^{-1}s^{-1}$ (Figure 3.4). BARAC (**3.6** same as **2.1**) also undergoes comparable acid catalysed rearrangement.

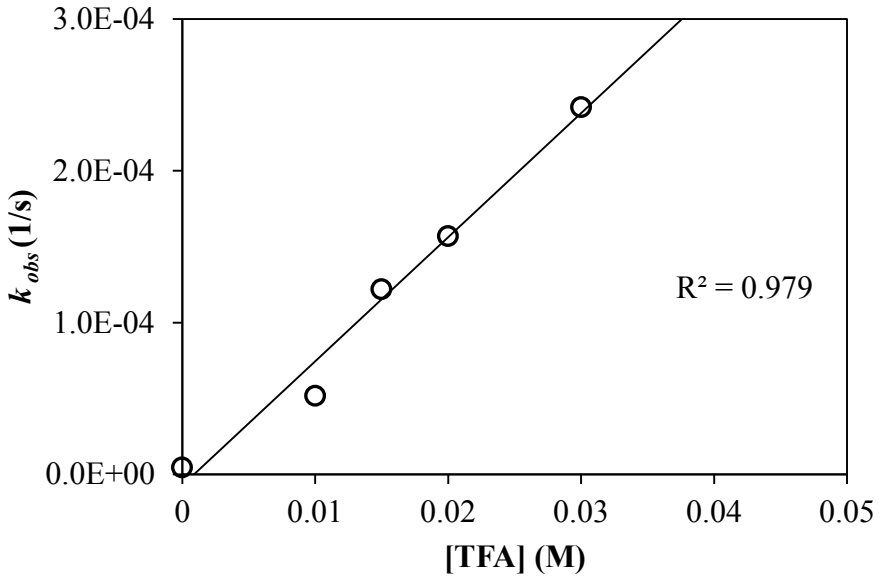

Figure 3.4. Rate constants for the kinetic studies of rearrangement of **3.2** correlated to the various concentrations of TFA in $CDCl_3$ at 25 ± 0.1 ºC

3.3.5 Proposed mechanisms of formation of products

The results of our investigation of the rearrangement of **3.2** support our proposed mechanisms of the formation of products. Since the alkyne of **3.2** is highly strained, it can easily react with various nucleophiles present. A computational study of the MM2 energy-minimised geometry of **3.2** using ChemBio3D Ultra shows orbital overlap between the nitrogen lone pair and the alkyne π* molecular orbital (Figure 3.5). This supports the proposition that **3.4** is the product of transannular 5-endo-dig cyclisation of the endocyclic amide nitrogen in a cyclization/aza-Claisen rearrangement sequence (Scheme 3.10).

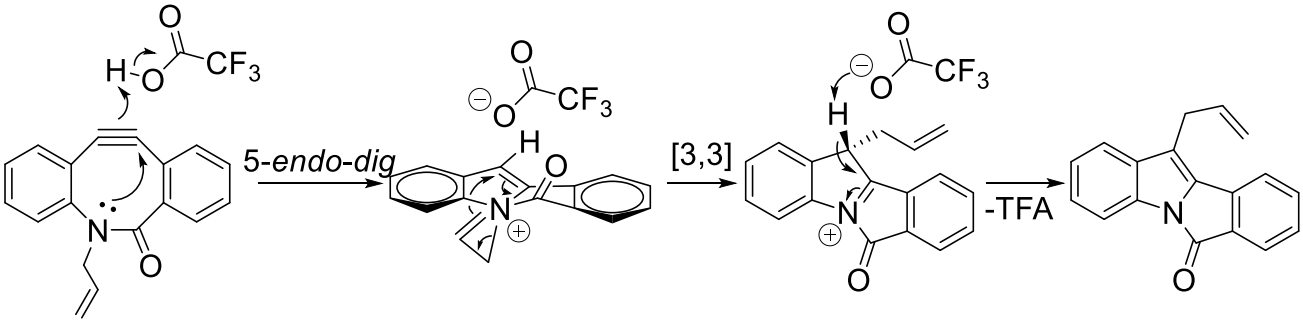

Scheme 3.10. Plausible mechanism for the formation of **3.4** under TFA catalysis.

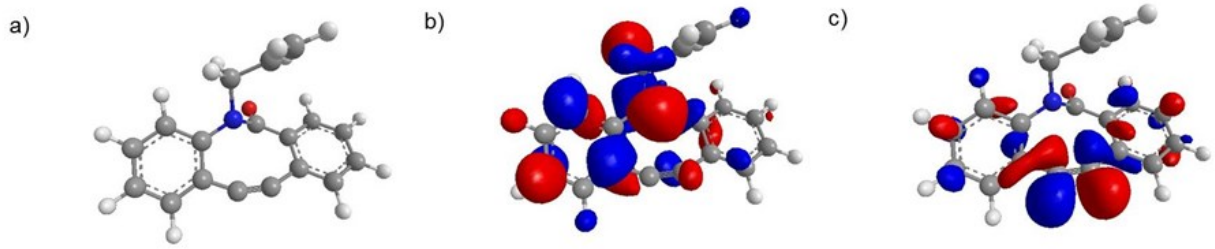

Figure 3.5. a) MM2 energy-minimised force field results for **3.2** determined using ChemBio3D Ultra. b) HOMO extended Hückel molecular model calculation results. c) LUMO extended Hückel molecular model calculation results

Our suggested mechanism is further corroborated by a previous account of a Brønsted acid-catalysis of the 5-endo-dig cyclisation of propargylglycine derivatives to synthesize the corresponding pyrroles.[28,29] In addition, the aza-Claisen rearrangement of a quaternary *N*-allyl enammonium salt at room temperature has been reported.[30,31] We presume that **3.5** was formed from reaction of the strained alkyne with residual H_2O in the presence of TFA (Scheme 3.11).

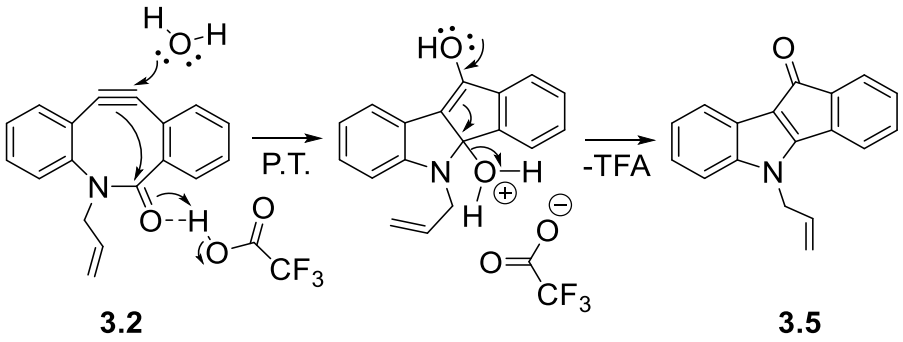

Scheme 3.11. Plausible mechanism for the formation of **3.5** under TFA catalysis.

At this time, we have yet to investigate whether the rearrangement happens under specific or general acid catalysis. However, further studies, for example with deuterated acid or at constant or varying pH of reaction, would provide insight into the type of acid catalysis observed.

Cyclooctynes have been reported to react with some of the cellular nucleophiles such as glutathione[32,33] or undergo spontaneous homotrimerisation.[34] While BARAC was designed for rapid strain-promoted 1,3-dipolar cycloadditions in living systems, it is important to remember that increased reactivity may impart reduced bioorthogonality.

3.4 Summary

We discovered and investigated a novel rearrangement of biarylazacyclooctynone derivatives, which together with various addition reactions could limit their practical utility as bioorthogonal reporters. We showed that this novel rearrangement is accelerated in the presence of acid and found that BARAC containing the 4,5-didehydro-oxazole side chain (**3.6** same as **2.1**) also undergoes analogous rearrangement, albeit over a prolonged period of

time than **3.2**. This difference in the rates has allowed us to theorize that the linker group has profound effects on the rate of the rearrangement. In turn we can conclude that BARAC analogues containing linkers that can become good leaving groups will likely rearrange at a faster rate compared to whose with poorer leaving groups. Thus the rearrangement can be minimized through utilizing side chains consisting of poor leaving groups, for example, primary alkyl groups or exocyclic amide.[18,20,21]

This novel rearrangement combined with the addition reactions of biarylazacyclooctynones are of particular relevance to biological labelling applications utilizing strain-promoted click chemistry. It is possible that at low concentrations of labelling reagents rearrangement may lower the efficiency of the tagging by competing with the cycloaddition reaction. Therefore, it is important to minimize the rearrangement while keeping the desired cycloaddition fast. Also, the use of BARAC analogues should be avoided in conditions where acid catalysis is possible.

3.5 Future directions

Following our findings of superior kinetics of strain-promoted cycloadditions of BARAC with nitrones, we envision the use of this strategy for efficient and rapid labelling of biomolecules within living cells. To achieve this, we will affix the cyclic nitrone *via* C-N or C-C coupling reactions to a biomolecule or metabolic precursor of choice, e.g. protein, nucleotide or amino acid. Following the metabolic incorporation into the target being studied, the nitrone modified biomolecule will undergo a rapid doubly-strained SPANC with BARAC conjugated to a fluorophore or affinity tag for detection of labelling events. The high reaction rate of the cycloaddition of BARAC and five-membered nitrones reported herein will allow specific labelling at low concentrations to visualize RNA or proteins inside living cells. We anticipate efficient labelling with very low residual fluorescence or non-specific labelling.

To further study the rearrangement reactions in biarylcyclooctynones, we envision widening the background study beyond BARAC to assess whether other cyclooctynes can undergo similar rearrangement reactions. We are also interested in pursuing tuning possibilities to try and favor one product or the other as well as minimizing the rearrangement in general. We anticipate studies to determine whether the rearrangement happens under specific or general acid catalysis as well as exploring the limitations of labelling *via* similar mechanisms.

3.6 Materials and Experimental Methods

Equipment and Reagents

Solvents, reagents and equipment utilized are described in Chapter 2, Section 2.5.

X-ray crystallography was performed at the National Research Council of Canada facilities. The X-ray experiments and data analysis was done by Gary Enright and Konstantin A. Udachin. The kinetic experiments were performed on Bruker-DRX-400 NMR spectrometer.

X-ray Data Collection and Structure Solution for Compounds 3.3, 3.4, 3.5 and 3.7

Single crystal X-ray diffraction data were measured on a Bruker Apex 2 Kuppa diffractometer at 100 K, using graphite monochromatized Mo K_α radiation (λ = 0.71073 Å). The unit cell was determined from randomly selected reflections obtained using the Bruker Apex2 automatic search, center, index, and least squares routines. Integration was carried out using the program SAINT, and an absorption correction was performed using SADABS.[35] The crystal structures were solved by direct methods and the structure was refined by full-matrix least-squares routines using the SHELXTL program suite.[36] All atoms were refined anisotropically. Hydrogen atoms were placed in calculated positions and allowed to ride on the parent atoms. Structure was refined as a twin with twin matrix 1 0 0 0 -1 0 -1 0 -1 and BASF parameter 0.26104.

Preparation of reagents

The nitrone **2.7** was prepared according to the procedure described in Chapter 2. Intermediate **3.1** and BARAC (**3.6** same as **2.1**) were prepared according to literature procedures described and referenced in Chapter 2.

Synthesis of 11,12-didehydro-5-allyl-dibenz[*b*,*f*]azocin-6(*5H*)-one (3.2)

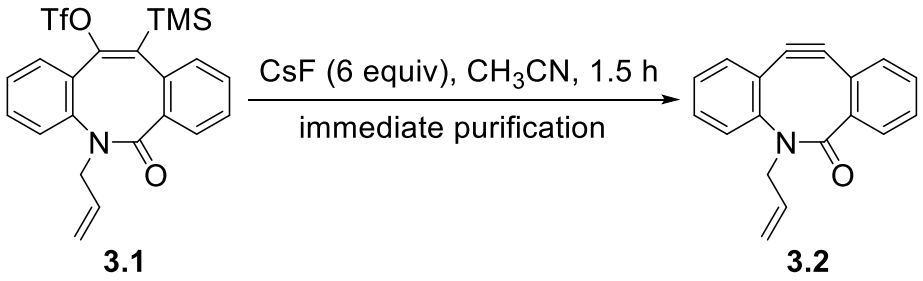

3.1 **3.2**

To a mixture of **3.1** (0.2 M, 1 equiv.) and CsF (6 equiv.) was added CH_3CN all at once. The solution was stirred vigorously for 1.5 h, and the solvent was removed under reduced pressure. The resultant crude oil was immediately purified by silica gel column chromatography (Hx:EtOAc/9:1, $R_f = 0.28$). The SiO_2 was neutralised with 96:4/Hx:Et_3N prior to purification. **3.2** was obtained as a light yellow oil (59.3 mg, 0.23 mmol, 74%), characterized in neutralized deuterated chloroform and was stored under argon at -80 ºC. **MS** (ESI+) calcd for **3.2** ($C_{18}H_{13}NO$): 260.10 $[M+H]^+$, found 260.1; **^{1}H-NMR** of **3.2** (400 MHz, $CDCl_3$): **δ** 7.59 (dd, *J*=6.8, 1.9 Hz, 1H), 7.54 (dd, *J*=6.4, 2.8 Hz, 1H), 7.4-7.5 (m, 4H), 7.34-7.39 (m, 2H), 5.83 (dddd, *J*=17.1, 10.2, 7.2, 5.0 Hz, 1H), 5.07 (ddd, *J*=10.2, 2.5, 1.25 Hz, 1H), 4.99 (ddd, *J*=17.0, 2.9, 1.4 Hz, 1H), 3.78 (tdd, *J*=15.2, 4.9, 1.6 Hz, 1H), 3.26 (tdd, *J*=15.4, 7.2, 1.0 Hz, 1H); **^{13}C-NMR** of **3.2** (100 MHz, $CDCl_3$): **δ** 176.7, 155.1, 149.2, 133.9, 130.6, 129.5, 129.3, 128.7, 128.1, 127.5, 126.4, 126.0, 122.6, 122.4, 118.2, 109.8, 109.4, 54.7.

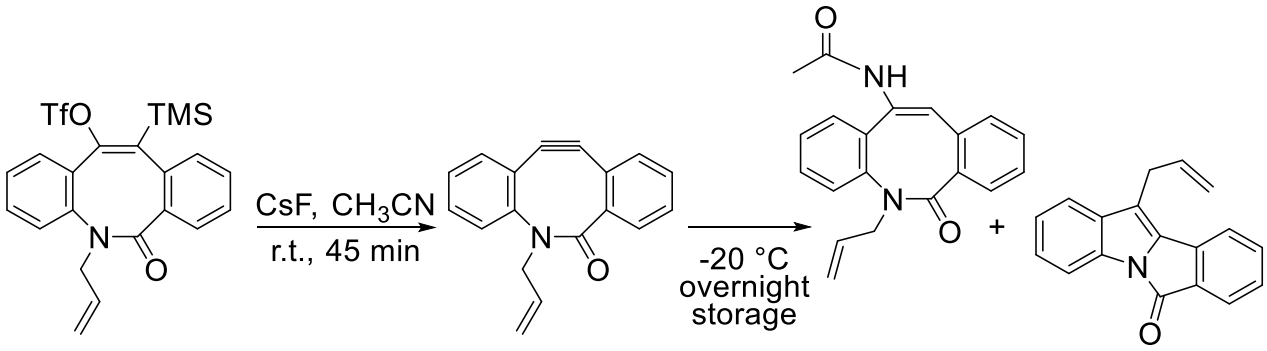

3.1 **3.2** **3.3** **3.4**

3.1 (0.01M, 1 equiv.) was stirred with excess of CsF (6 equiv.) in MeCN for 45 min. The mixture was then filtered to remove excess CsF. The filtrate was concentrated under reduced pressure and the crude oil was stored at -20 ºC overnight. The crude was purified by silica gel column chromatography to yield two products, **3.3** and **3.4**, in a 9:1 ratio respectively: **3.3** as white solid in 90% yield (R_f = 0.16, Hx:EtOAc/1:1) and **3.4** as light yellow solid in 2.7% yield (R_f = 0.6, Hx:EtOAc/8:2).

(E)-N-(5-allyl-6-oxo-5,6-dihydrodibenzo[b,f]azocin-12-yl)acetamide (3.3)

HR-MS calcd for **3.3** ($C_{20}H_{18}N_2O_2Na^+$): 341.12479 $[M+Na]^+$, found 341.12605; **^{1}H-NMR** of **3.3** (400 MHz, $CDCl_3$). **δ** 7.54 (br s, 1H), 7.31 (dd, *J*=7.2, 1.5 Hz, 1H), 7.1-7.25 (m, 6H), 7.02 (dd, *J*=7.1, 1.1 Hz, 1H), 6.90 (br s, 1H), 5.95 (tdd, *J* =17.0, 10.4, 6.4 Hz, 1H), 5.12 (m, 2H), 4.80 (dd, *J*=14.7, 5.7 Hz, 1H), 4.14 (dd, *J*=14.8, 7.0 Hz, 1H), 2.07 (s, 3H); **^{13}C-NMR** of **3.3** (100 MHz, $CDCl_3$): **δ** 170.7, 168.4, 141.3, 137.0, 135.4, 133.9, 133.4, 129.6, 128.7, 128.4, 127.9, 127.9, 127.8, 127.1, 126.9, 117.9, 116.8, 100.0, 52.6, 24.5.

11-allyl-6*H*-isoindolo[2,1-*a*]indol-6-one (3.4)

MS (ESI+) calcd for **3.4** ($C_{18}H_{13}NO$): 260.10 $[M+H]^+$, found 260.1; **^{1}H-NMR** of **3.4** (400 MHz, $CDCl_3$): **δ** 7.89 (d, *J*=8.0 Hz, 1H), 7.77 (d, *J*=7.6 Hz, 1H), 7.51 (m, 2H), 7.42 (d, *J*=7.8 Hz, 1H), 7.30 (m, 2H), 7.15 (m, 1H), 6.03 (tdd, *J*=16.2, 10.1, 6.1 Hz, 1H), 5.20 (ddd,

J=13.6, 11.5, 1.6 Hz, 2H), 3.63 (td, *J*=6.1, 1.6 Hz, 2H). **^{13}C-NMR** of **3.4** (100 MHz, $CDCl_3$): **δ** 162.4, 135.1, 135.0, 134.8, 134.5, 134.0, 133.7, 133.6, 133.6, 128.3, 26.6, 125.4, 123.7, 121.6, 120.6, 117.3, 116.7, 113.4, 28.9.

Rearrangement of 3.2 under neutral conditions

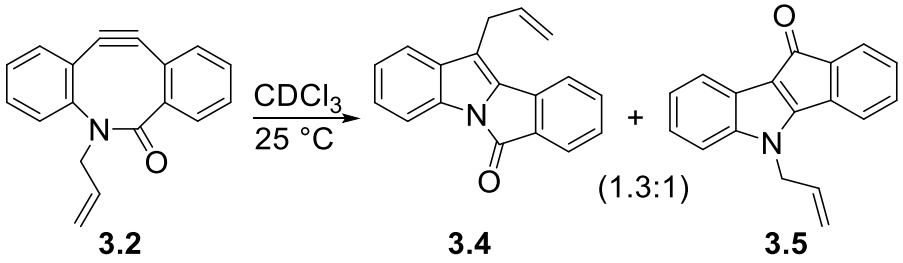

3.2 **3.4** **3.5**

Both the chloroform used for azeotroping as well as solvent were neutralized before usage by filtering through a short plug of solid sodium bicarbonate. Freshly synthesized **3.2** (76.4 mg, 0.16 mmol) was dissolved in neutralized $CDCl_3$ and transferred into an NMR tube. The NMR tube was heat sealed and kept in a water bath at 25 ºC. Caution was also taken as to not expose the reaction to light. A ^{1}H NMR spectrum was taken daily for 9 days until **3.2** had disappeared completely. Once the reaction was complete, the solvent was removed under reduced pressure and the crude was purified by silica gel column chromatography (Hx:EtOAc/8:2, R_f (**3.4**) = 0.6, R_f (**3.5**) = 0.3) to yield **3.4** (10.7 mg, 0.041 mmol) as light yellow solid in 53% yield and **3.5** (8.2 mg, 0.0312 mmol) as red solid in 41% yield. **5-allylindeno[1,2-*b*]indol-10(5*H*)-one (3.5) MS** (ESI+) calcd for **3.4** ($C_{18}H_{13}NO$): 260.10 $[M+H]^+$, found 260.1; **^{1}H-NMR** of **3.5** (400 MHz, $CDCl_3$): **δ** 7.81 (ddd, *J*=8.0, 1.3, 0.7 Hz, 1H), 7.46 (ddd, *J*=7.0, 1.4, 0.6 Hz, 1H), 7.15-7.25 (m, 4H), 7.11 (ddd, *J*=7.1, 1.1, 0.6 Hz, 1H), 6.06 (tdd, *J*=17.1, 10.2, 4.8 Hz, 1H), 5.29 (dtd, *J*=10.5, 1.8, 0.5 Hz, 1H), 5.16 (dtd, *J*=17.1, 1.8, 0.4 Hz, 1H), 4.92 (td, *J*=4.7, 1.8 Hz, 2H); **^{13}C-NMR** of **3.5** (100 MHz, $CDCl_3$): **δ** 185.1, 158.6, 142.4, 141.2, 134.7, 132.0, 131.5, 129.7, 123.6, 123.3, 123.2, 123.0, 120.9, 118.6, 118.0, 115.4, 110.8, 47.4.

Synthesis of 9-allyl-2-methyl-3-(4-nitrophenyl)-2,3-dihydrodibenzo[*b,f*]isoxazolo[5,4-*d*]azocin-8(9*H*)-one (3.8)

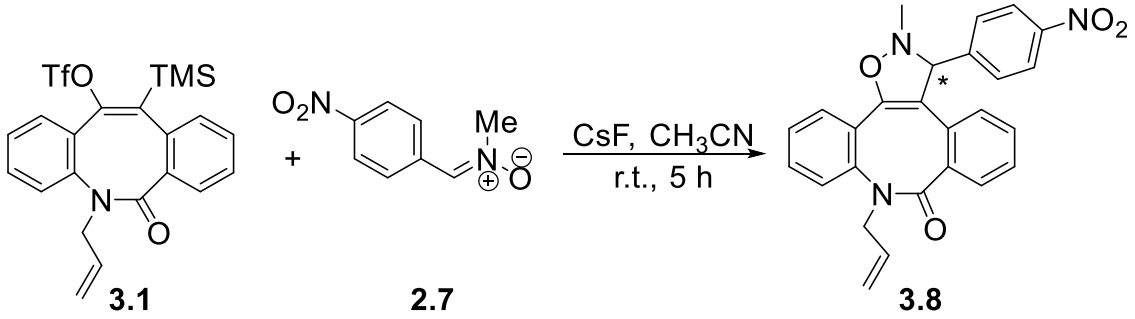

To a mixture of **3.1** (0.14 M, 1 equiv.), **2.7** (1 equiv.) and CsF (6 equiv.) was added CH_3CN all at once. The solution was stirred vigorously for 5 hours and the solvent was removed under reduced pressure. The crude oil was purified by silica gel column chromatography (Hx:EtOAc/6:4, $R_f = 0.3$) to yield a light yellow oil in 46% yield that represented a mixture of enantiomers and diastereomers. **HR-MS** calcd for **3.8** radical cation ($C_{26}H_{20}N_3O_4^+$): 438.14874 $[M-H]^+$, found 438.14483; The NMR is complex due to presence of all of the isomers of **3.8**. ^1H and ^{13}C spectra are provided in the appendix.

Synthesis of 11-((3-(4-(hydroxymethyl)phenyl)-4,5-dihydroisoxazol-5-yl)methyl)-6*H*-isoindolo[2,1-*a*]indol-6-one (3.7):

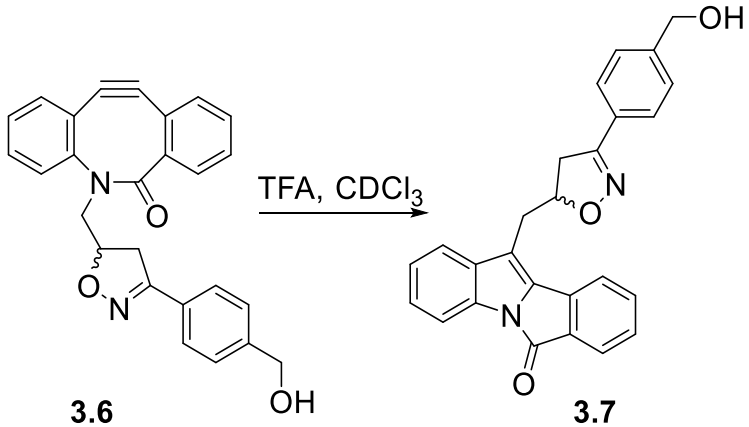

A kinetic experiment with **3.6** following the kinetic studies procedure of rearrangement of **3.2** under acidic conditions (with [TFA] =0.03M, in $CDCl_3$) was performed to yield **3.7** as red solid. A mixture of isomers of **3.7** was observed by LC-MS with estimated yield of

~67%. **HR-MS** calcd for **3.7** ($C_{26}H_{20}N_2O_3Na^+$): 431.13626 $[M+Na]^+$, found 431.13661; **^{1}H-NMR** of **3.7** (400 MHz, $CDCl_3$): **δ** 7.77 (m, 1H), 7.64 (m, 1H), 7.59 (m, 3H), 7.51 (m, 1H), 7.43 (m, 3H), 7.37 (m, 4H), 7.31 (m, 3H), 7.22 (m, 3H), 7.18 (m, 3H), 7.14 (m, 2H), 5.28-5.40 (m, 1H), 5.22 (qd, *J*=10.6, 6.3, 6.2, 6.2 Hz, 1H), 4.74 (m, 4H), 4.47 (ddd, *J*=20.6, 15.0, 6.0 Hz, 2H), 4.09 (t, *J*=6.7, 6.7 Hz, 1H), 3.47 (dd, *J*=16.8, 10.3 Hz, 1.5H), 3.24 (dd, *J*=16.9, 6.3 Hz, 1.5H), 2.78 (s, 1H), 2.07 (s, 2H); **^{13}C-NMR** of **3.7** (100 MHz, $CDCl_3$) **δ** 186.3, 159.6, 159.3, 158.9, 158.5, 158.1, 156.8, 156.6, 156.2, 143.0, 142.6, 141.0, 135.8, 134.5, 132.5, 131.0, 130.1, 129.7, 129.6, 128.9, 128.8, 128.2, 128.0, 127.8, 127.8, 127.4, 127.2, 127.1, 127.0, 126.9, 126.8, 126.3, 124.3, 123.8, 123.0, 122.3, 121.1, 121.0, 120.3, 119.1, 119.1, 118.9, 116.1, 115.5, 113.2, 110.8, 110.4, 109.7, 78.9, 78.7, 68.7, 64.9, 64.7, 60.9, 47.8, 47.8, 38.1, 37.9, 30.5, 29.5, 21.1, 21.1, 19.1, 17.3, 14.1, 13.9, 13.7.

Kinetic studies procedure of rearrangement of 3.2 under acidic conditions

This procedure outlines the general method of kinetic trial while indicating the parameters specific to the TFA concentration of 0.01 M. All kinetic studies were performed following the general method outlined, varying the concentration of TFA.

Non-deuterated chloroform for azeotroping and deuterated chloroform used as solvent in all reactions were carefully neutralized by filtering through a short plug of solid sodium bicarbonate. Fresh batch of neutralized solvent was used for each reaction. Stock solutions were prepared in separate vials for **3.2** (22.8 mg in 585 uL of neutral CDCl3, 0.15 mM stock) and TFA (184 uL in 816 uL of neutral $CDCl_3$, 2.4 mM stock). Care was taken to ensure flasks were properly closed when not in use as to minimize the evaporation and alteration of the concentrations of the starting materials. The stock solutions were used the same day they were made.

The reaction was performed at 25 ± 0.1 ºC with total volume of 800 uL and final concentrations of **3.2** at 0.03 M and TFA at 0.01 M. To achieve this, 160 uL of stock solution of **3.2** was added to 637 uL of neutral $CDCl_3$ in NMR tube. The tube was inverted to ensure proper mixing. A ^{1}H-spectra was taken without acid for assuring purity of starting material and 33 uL of TFA was added to the NMR tube. The tube was inverted a few times and promptly placed back into NMR spectrometer. A ^{1}H-spectra was taken at to serve as a baseline reading for the kinetic algorithm. The kinetic was started collecting 32 scans every 30 minutes for 24 times. The products were confirmed by LC-MS. Kinetic data for each reaction was processed as previously described for the neutral conditions (page 64).

3.7 References

(1) Jewett, J. C.; Bertozzi, C. R. *Chem. Soc. Rev.* **2010**, *39*, 1272.

(2) Lim, R. K. V.; Lin, Q. *Chem. Commun.* **2010**, *46*, 1589.

(3) Prescher, J. A.; Bertozzi, C. R. *Nat. Chem. Biol.* **2005**, *1*, 13.

(4) Sletten, E. M.; Bertozzi, C. R. *Angew. Chem. Int. Ed.* **2009**, *48*, 6974.

(5) Saxon, E.; Bertozzi, C. R. *Science* **2000**, *287*, 2007.

(6) Prescher, J. A.; Dube, D. H.; Bertozzi, C. R. *Nature* **2004**, *430*, 873.

(7) Soriano del Amo, D.; Wang, W.; Jiang, H.; Besanceney, C.; Yan, A. C.; Levy, M.; Liu, Y.; Marlow, F. L.; Wu, P. *J. Am. Chem. Soc.* **2010**, *132*, 16893.

(8) Kennedy, D. C.; McKay, C. S.; Legault, M. C. B.; Danielson, D. C.; Blake, J. A.; Pegoraro, A. F.; Stolow, A.; Mester, Z.; Pezacki, J. P. *J. Am. Chem. Soc.* **2011**, *133*, 17993.

(9) Sletten, E. M.; Bertozzi, C. R. *Acc. Chem. Res.* **2011**, *44*, 666.

(10) Agard, N. J.; Baskin, J. M.; Prescher, J. A.; Lo, A.; Bertozzi, C. R. *ACS Chem. Biol.* **2006**, *1*, 644.

(11) Baskin, J. M.; Prescher, J. A.; Laughlin, S. T.; Agard, N. J.; Chang, P. V.; Miller, I. A.; Lo, A.; Codelli, J. A.; Bertozzi, C. R. *Proc Natl Acad Sci U S A* **2007**, *104*, 16793.

(12) Codelli, J. A.; Baskin, J. M.; Agard, N. J.; Bertozzi, C. R. *J. Am. Chem. Soc.* **2008**, *130*, 11486.

(13) Ning, X.; Guo, J.; Wolfert, M. A.; Boons, G.-J. *Angew. Chem. Int. Ed.* **2008**, *47*, 2253.

(14) Dommerholt, J.; Schmidt, S.; Temming, R.; Hendriks, L. J.; Rutjes, F. P.; van Hest, J. C.; Lefeber, D. J.; Friedl, P.; van Delft, F. L. *Angew. Chem. Int. Ed.* **2010**, *49*, 9422.

(15) Mbua, N. E.; Guo, J.; Wolfert, M. A.; Steet, R.; Boons, G.-J. *ChemBioChem* **2011**, *12*, 1912.

(16) de Almeida, G.; Sletten, E. M.; Nakamura, H.; Palaniappan, K. K.; Bertozzi, C. R. *Angew. Chem. Int. Ed.* **2012**, *51*, 2443.

(17) Sletten, E. M.; Bertozzi, C. R. *Org. Lett.* **2008**, *10*, 3097.

(18) Debets, M. F.; van Berkel, S. S.; Schoffelen, S.; Rutjes, F. P. J. T.; van Hest,

J. C. M.; van Delft, F. L. *Chem. Commun.* **2010**, *46*, 97.

(19) Kuzmin, A.; Poloukhtine, A.; Wolfert, M. A.; Popik, V. V. *Bioconjugate Chem.* **2010**, *21*, 2076.

(20) Jewett, J. C.; Sletten, E. M.; Bertozzi, C. R. *J. Am. Chem. Soc.* **2010**, *132*, 3688.

(21) Jewett, J. C.; Bertozzi, C. R. *Org. Lett.* **2011**, *13*, 5937.

(22) van den Bosch, S. M.; Rossin, R.; Verkerk, P. R.; ten Hoeve, W.; Janssen, H. M.; Lub, J.; Robillard, M. S. *Nucl. Med. Biol.* **2013**, *40*, 415.

(23) Ritter, J. J.; Minieri, P. P. *J. Am. Chem. Soc.* **1948**, *70*, 4045.

(24) Plass, T.; Milles, S.; Koehler, C.; Schultz, C.; Lemke, E. A. *Angew. Chem. Int. Ed.* **2011**, *50*, 3878.

(25) Plass, T.; Milles, S.; Koehler, C.; Szymański, J.; Mueller, R.; Wießler, M.; Schultz, C.; Lemke, E. A. *Angew. Chem. Int. Ed.* **2012**, *51*, 4166.

(26) Kresge, A. J. *Acc. Chem. Res.* **1975**, *8*, 354.

(27) Pezacki, J. P. *Can. J. Chem.* **1999**, *77*, 1230.

(28) Knight, D. W.; Sharland, C. M. *Synlett* **2003**, *2003*, 2258.

(29) Gilmore, K.; Alabugin, I. V. *Chem. Rev.* **2011**, *111*, 6513.

(30) McComsey, D. F.; Maryanoff, B. E. *J. Org. Chem.* **2000**, *65*, 4938.

(31) Nubbemeyer, U. In *Natural Products Synthesis II*; Mulzer, J., Ed.; Springer Berlin Heidelberg: 2005; Vol. 244, p 149.

(32) Beatty, K. E.; Fisk, J. D.; Smart, B. P.; Lu, Y. Y.; Szychowski, J.; Hangauer, M. J.; Baskin, J. M.; Bertozzi, C. R.; Tirrell, D. A. *ChemBioChem* **2010**, *11*, 2092.

(33) Chang, P. V.; Prescher, J. A.; Sletten, E. M.; Baskin, J. M.; Miller, I. A.; Agard, N. J.; Lo, A.; Bertozzi, C. R. *Proc. Natl. Acad. Sci. U.S.A.* **2010**, *107*, 1821.

(34) Sletten, E. M.; Nakamura, H.; Jewett, J. C.; Bertozzi, C. R. *J. Am. Chem. Soc.* **2010**, *132*, 11799.

(35) Sheldrick, G. M. *SADABS Version 2.03, University of Gottingen, Germany* **2002**.

(36) Sheldrick, G. M. *SHELXTL, Version 6.10; Bruker AXS Inc., Madison, Wisconsin, USA* **2000**.

Appendix

A. Kinetic data for cycloaddition reactions of BARAC and nitrones

Table A.1. Observed rate constants for the kinetic studies of cycloadditions of BARAC (**2.1**) with **2.10** correlated to the various concentrations of **2.10** in aqueous (0.1% water) acetonitrile at 25 ± 0.1ºC.

Nitrone	Structure	Concentration of nitrone (x 10^{-3} M)	k_{obs} (s^{-1})
2.10	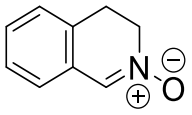	0.125	2.64 x 10^{-3}
		0.10	2.36 x 10^{-3}
		0.08	1.90 x 10^{-3}
		0.06	1.32 x 10^{-3}
		0.04	8.93 x 10^{-4}

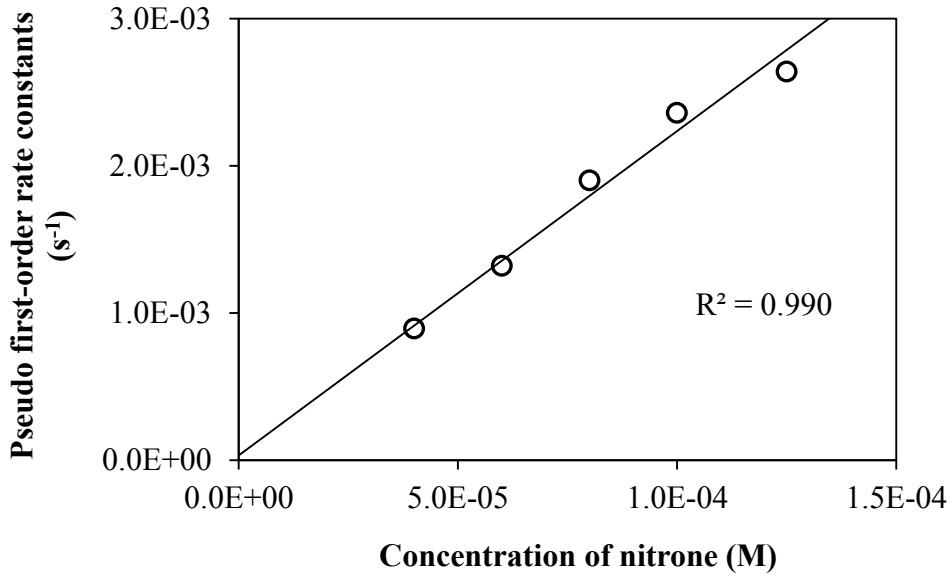

Figure A.1. Pseudo first-order rate constants of the cycloadditions of **2.10** with BARAC (**2.1**) plotted against the various concentrations of the nitrone. The slope represents the second-order rate constant and equals to 22.4 $M^{-1}s^{-1}$ All reactions were done in aqueous (0.1% water) acetonitrile at 25 ± 0.1ºC.

Table A.2. Observed rate constants for the kinetic studies of cycloadditions of BARAC (**2.1**) with **2.11** correlated to the various concentrations of **2.11** in aqueous (0.1% water) acetonitrile at 25 ± 0.1ºC.

Nitrone	Structure	Concentration of nitrone (x 10^{-3} M)	k_{obs} (s^{-1})
2.11	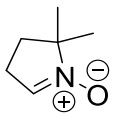	1.1	4.38 x 10^{-2}
		1.0	3.92 x 10^{-2}
		0.9	3.61 x 10^{-2}
		0.8	2.95 x 10^{-2}

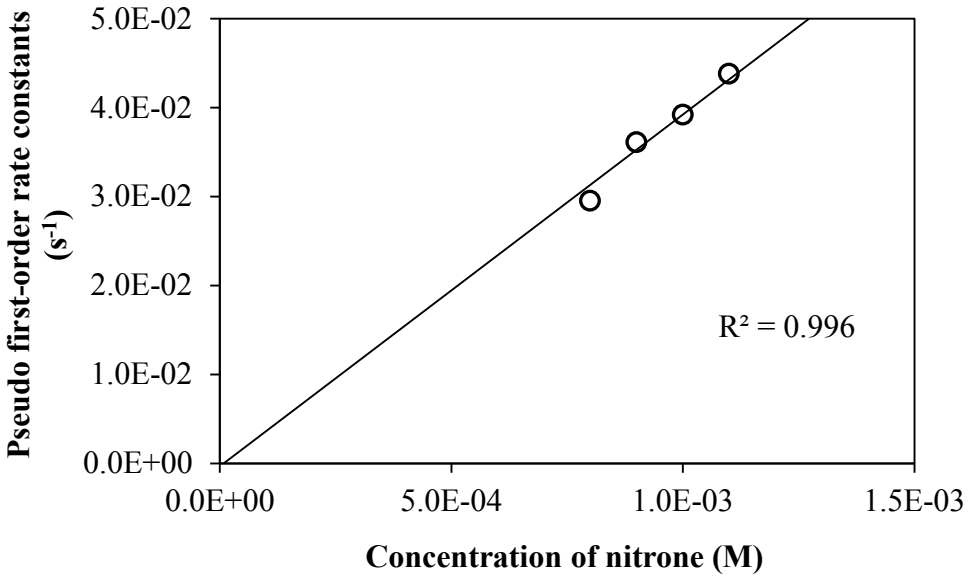

Figure A.2. Pseudo first-order rate constants of the cycloadditions of **2.11** with BARAC (**2.1**) plotted against the various concentrations of the nitrone. The slope represents the second-order rate constant and equals to 39.2 $M^{-1}s^{-1}$ All reactions were done in aqueous (0.1% water) acetonitrile at 25 ± 0.1ºC

Table A.3. Observed rate constants for the kinetic studies of cycloadditions of BARAC (**2.1**) with **2.12** correlated to the various concentrations of **2.12** in aqueous (0.1% water) acetonitrile at 25 ± 0.1ºC.

Nitrone	Structure	Concentration of nitrone (x 10^{-3} M)	k_{obs} (s^{-1})
2.12	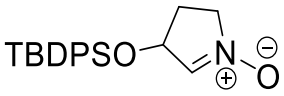	0.8	3.16 x 10^{-2}
		0.7	2.81 x 10^{-2}
		0.6	2.55 x 10^{-2}
		0.5	2.09 x 10^{-2}
		0.4	1.74 x 10^{-2}
		0.3	1.29 x 10^{-2}

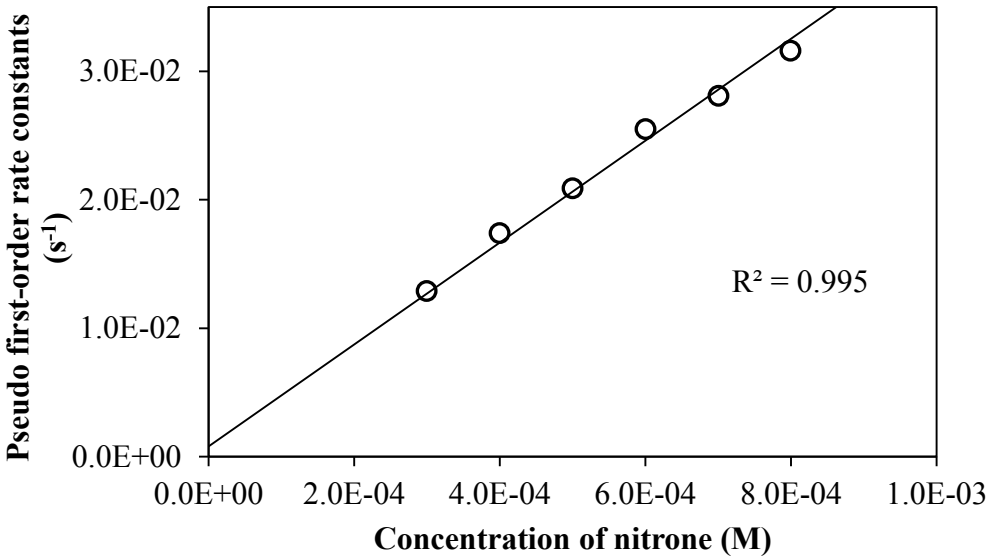

Figure A.3. Pseudo first-order rate constants of the cycloadditions of **2.12** with BARAC (**2.1**) plotted against the various concentrations of the nitrone. The slope represents the second-order rate constant and equals to 41.0 $M^{-1}s^{-1}$ All reactions were done in aqueous (0.1% water) acetonitrile at 25 ± 0.1ºC

Table A.4. Observed rate constants for the kinetic studies of cycloadditions of BARAC (**2.1**) with **2.2** correlated to the various concentrations of **2.2** in aqueous (0.1% water) acetonitrile at 25 ± 0.1ºC.

Nitrone	Structure	Concentration of nitrone (x 10^{-3} M)	k_{obs} (s^{-1})
2.2	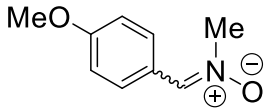	0.12	6.08 x 10^{-4}
		0.10	4.63 x 10^{-4}
		0.08	3.98 x 10^{-4}
		0.06	2.81 x 10^{-4}
		0.04	1.81 x 10^{-4}

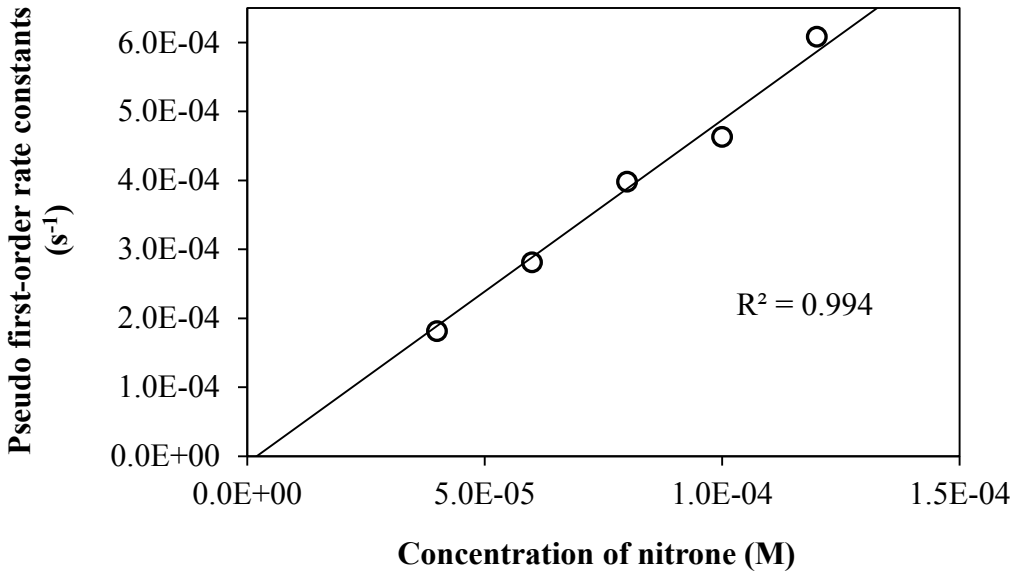

Figure A.4. Pseudo first-order rate constants of the cycloadditions of **2.2** with BARAC (**2.1**) plotted against the various concentrations of the nitrone. The slope represents the second-order rate constant and equals to 4.87 $M^{-1}s^{-1}$ All reactions were done in aqueous (0.1% water) acetonitrile at 25 ± 0.1ºC

Table A.5. Observed rate constants for the kinetic studies of cycloadditions of BARAC (**2.1**) with **2.3** correlated to the various concentrations of **2.3** in aqueous (0.1% water) acetonitrile at 25 ± 0.1ºC.

Nitrone	Structure	Concentration of nitrone (x 10^{-3} M)	k_{obs} (s^{-1})
2.3	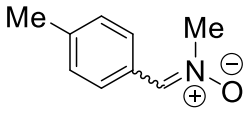	0.12	8.14 x 10^{-4}
		0.10	6.34 x 10^{-4}
		0.08	5.27 x 10^{-4}
		0.06	4.30 x 10^{-4}
		0.04	2.59 x 10^{-4}

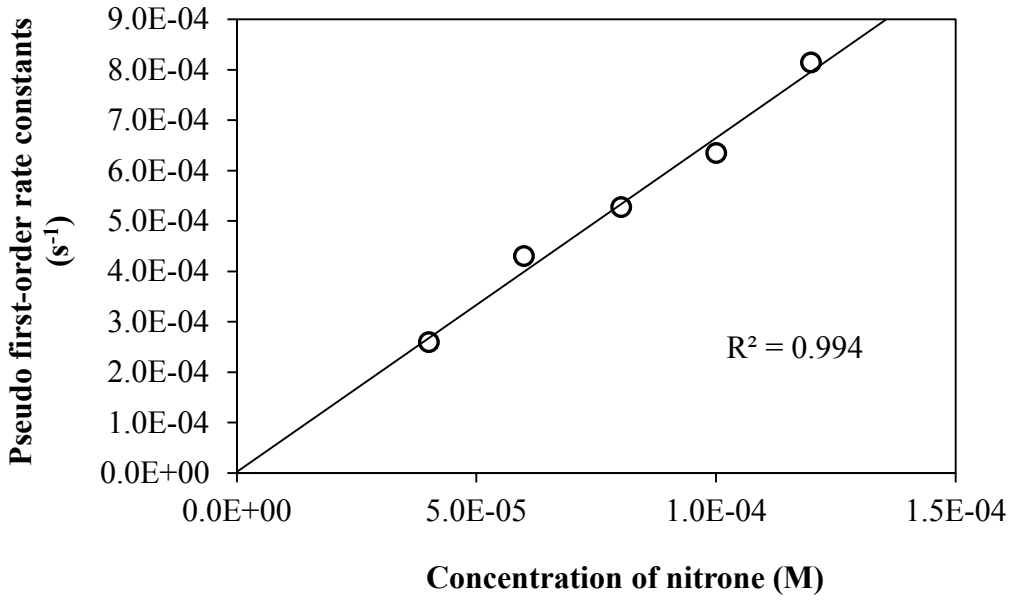

Figure A.5. Pseudo first-order rate constants of the cycloadditions of **2.3** with BARAC (**2.1**) plotted against the various concentrations of the nitrone. The slope represents the second-order rate constant and equals to 6.65 $M^{-1}s^{-1}$ All reactions were done in aqueous (0.1% water) acetonitrile at 25 ± 0.1ºC

Table A.6. Observed rate constants for the kinetic studies of cycloadditions of BARAC (**2.1**) with **2.4** correlated to the various concentrations of **2.4** in aqueous (0.1% water) acetonitrile at 25 ± 0.1ºC.

Nitrone	Structure	Concentration of nitrone (x 10^{-3} M)	k_{obs} (s^{-1})
2.4	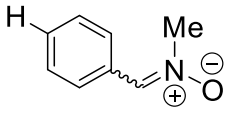	0.14	9.73 x 10^{-4}
		0.12	8.08 x 10^{-4}
		0.10	6.75 x 10^{-4}
		0.08	5.34 x 10^{-4}
		0.06	3.70 x 10^{-4}

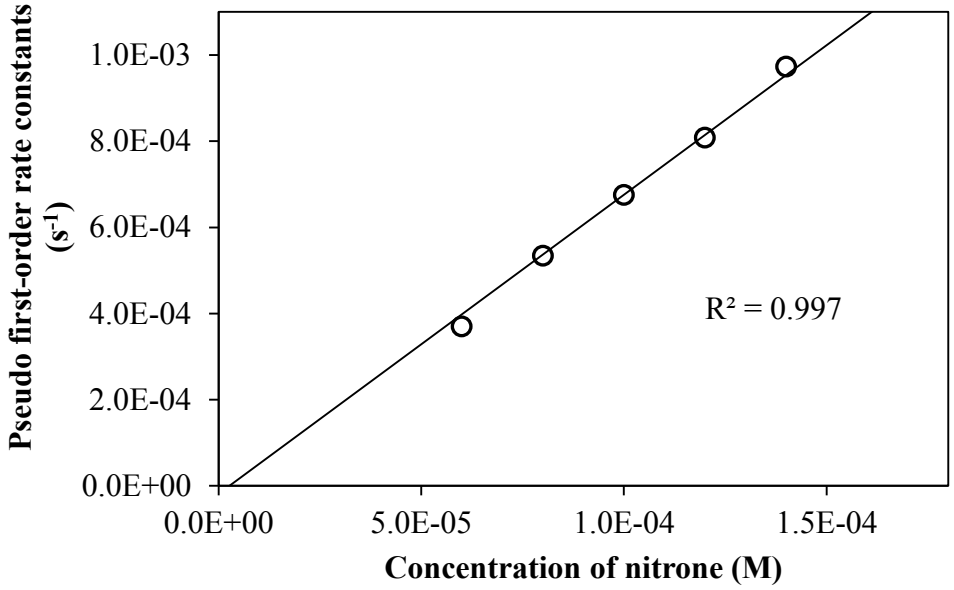

Figure A.6. Pseudo first-order rate constants of the cycloadditions of **2.4** with BARAC (**2.1**) plotted against the various concentrations of the nitrone. The slope represents the second-order rate constant and equals to 6.77 $M^{-1}s^{-1}$ All reactions were done in aqueous (0.1% water) acetonitrile at 25 ± 0.1ºC

Table A.7. Observed rate constants for the kinetic studies of cycloadditions of BARAC (**2.1**) with **2.5** correlated to the various concentrations of **2.5** in aqueous (0.1% water) acetonitrile at 25 ± 0.1ºC.

Nitrone	Structure	Concentration of nitrone (x 10^{-3} M)	k_{obs} (s^{-1})
2.5	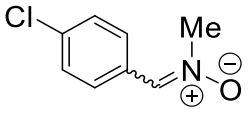	0.14	1.07 x 10^{-3}
		0.12	9.49 x 10^{-4}
		0.10	8.29 x 10^{-4}
		0.08	6.07 x 10^{-4}
		0.06	4.88 x 10^{-4}

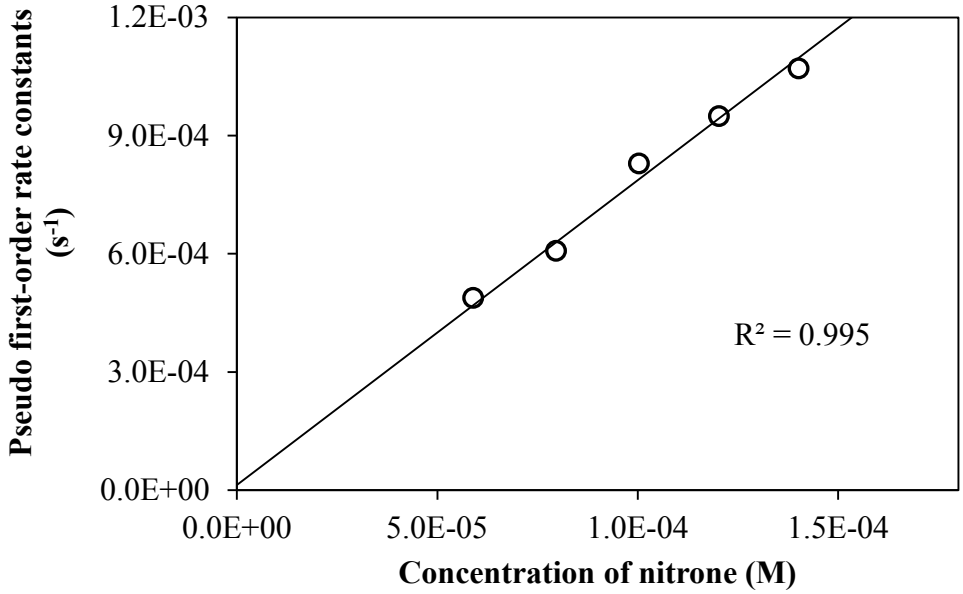

Figure A.7. Pseudo first-order rate constants of the cycloadditions of **2.5** with BARAC (**2.1**) plotted against the various concentrations of the nitrone. The slope represents the second-order rate constant and equals to 7.86 $M^{-1}s^{-1}$ All reactions were done in aqueous (0.1% water) acetonitrile at 25 ± 0.1ºC

Table A.8. Observed rate constants for the kinetic studies of cycloadditions of BARAC (**2.1**) with **2.6** correlated to the various concentrations of **2.6** in aqueous (0.1% water) acetonitrile at 25 ± 0.1ºC.

Nitrone	Structure	Concentration of nitrone (x 10^{-3} M)	k_{obs} (s^{-1})
2.6	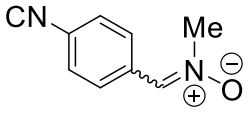	0.55	5.25 x 10^{-3}
		0.48	4.32 x 10^{-3}
		0.40	3.54 x 10^{-3}
		0.32	2.99 x 10^{-3}
		0.24	2.25 x 10^{-3}

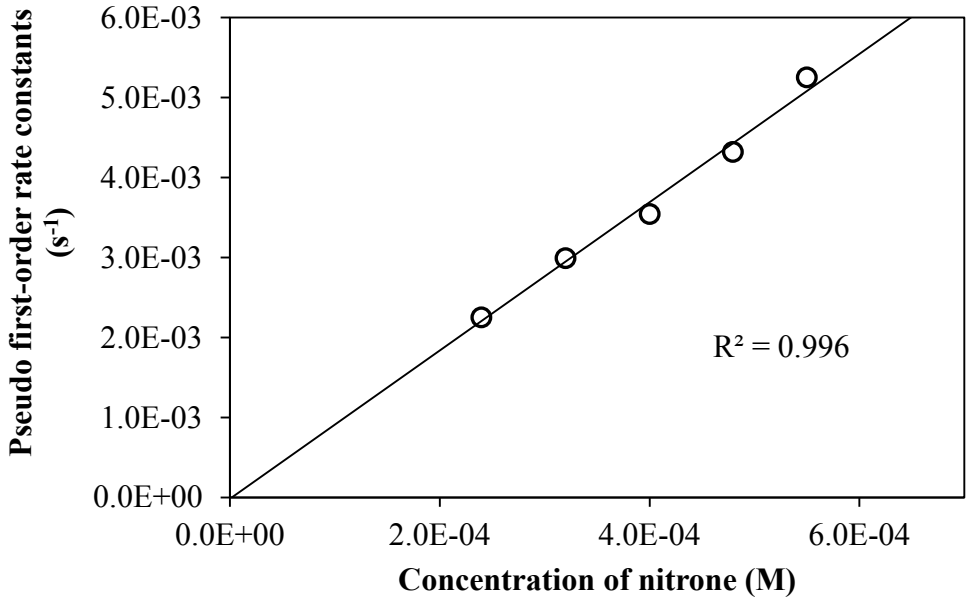

Figure A.8. Pseudo first-order rate constants of the cycloadditions of **2.6** with BARAC (**2.1**) plotted against the various concentrations of the nitrone. The slope represents the second-order rate constant and equals to 9.23 $M^{-1}s^{-1}$ All reactions were done in aqueous (0.1% water) acetonitrile at 25 ± 0.1ºC

Table A.9. Observed rate constants for the kinetic studies of cycloadditions of BARAC (**2.1**) with **2.7** correlated to the various concentrations of **2.7** in aqueous (0.1% water) acetonitrile at 25 ± 0.1ºC.

Nitrone	Structure	Concentration of nitrone (x 10^{-3} M)	k_{obs} (s^{-1})
2.7	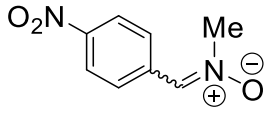	0.70	7.00 x 10^{-3}
		0.60	6.19 x 10^{-3}
		0.50	5.01 x 10^{-3}
		0.40	4.10 x 10^{-3}
		0.30	3.04 x 10^{-3}

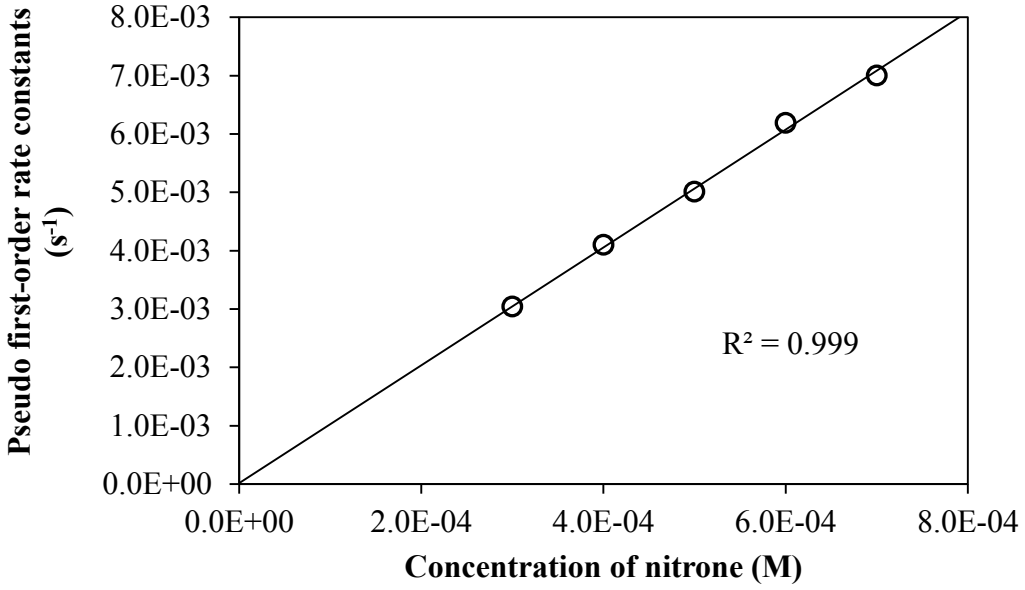

Figure A.9. Pseudo first-order rate constants of the cycloadditions of **2.7** with BARAC (**2.1**) plotted against the various concentrations of the nitrone. The slope represents the second order rate constant and equals to 10.1 $M^{-1}s^{-1}$ All reactions were done in aqueous (0.1% water) acetonitrile at 25 ± 0.1ºC

Table A.10. Observed rate constants for the kinetic studies of cycloadditions of BARAC (**2.1**) with **2.8** correlated to the various concentrations of **2.7** in aqueous (0.1% water) acetonitrile at 25 ± 0.1ºC.

Nitrone	Structure	Concentration of BARAC (x 10^{-3} M)	k_{obs} (s^{-1})
2.8	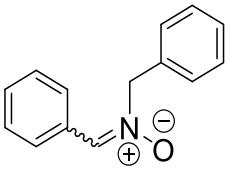	0.09	2.15 x 10^{-4}
		0.10	2.73 x 10^{-4}
		0.11	3.06 x 10^{-4}
		0.12	3.45 x 10^{-4}
		0.13	3.73 x 10^{-4}

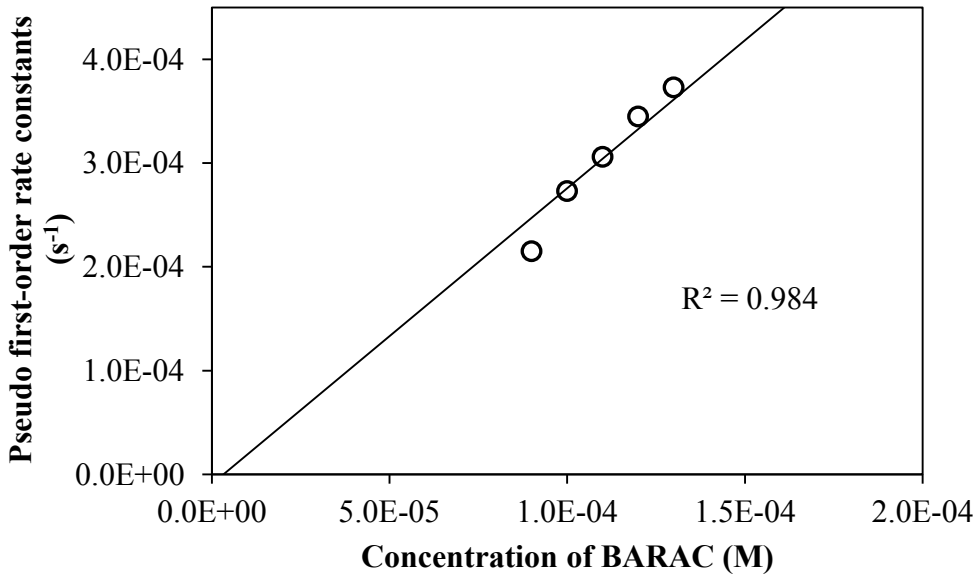

Figure A.10. Pseudo first-order rate constants of the cycloadditions of **2.8** with BARAC (**2.1**) plotted against the various concentrations of the nitrone. The slope represents the second-order rate constant and equals to 2.76 $M^{-1}s^{-1}$ All reactions were done in aqueous (0.1% water) acetonitrile at 25 ± 0.1ºC

Table A.11. Observed rate constants for the kinetic studies of cycloadditions of BARAC (**2.1**) with **2.9** correlated to the various concentrations of **2.10** in aqueous (0.1% water) acetonitrile at 25 ± 0.1ºC.

Nitrone	Structure	Concentration of BARAC (x 10^{-3} M)	k_{obs} (s^{-1})
2.9	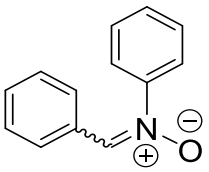	0.06	3.18 x 10^{-3}
		0.07	3.79 x 10^{-3}
		0.08	4.32 x 10^{-3}
		0.09	4.69 x 10^{-3}
		0.10	5.19 x 10^{-3}

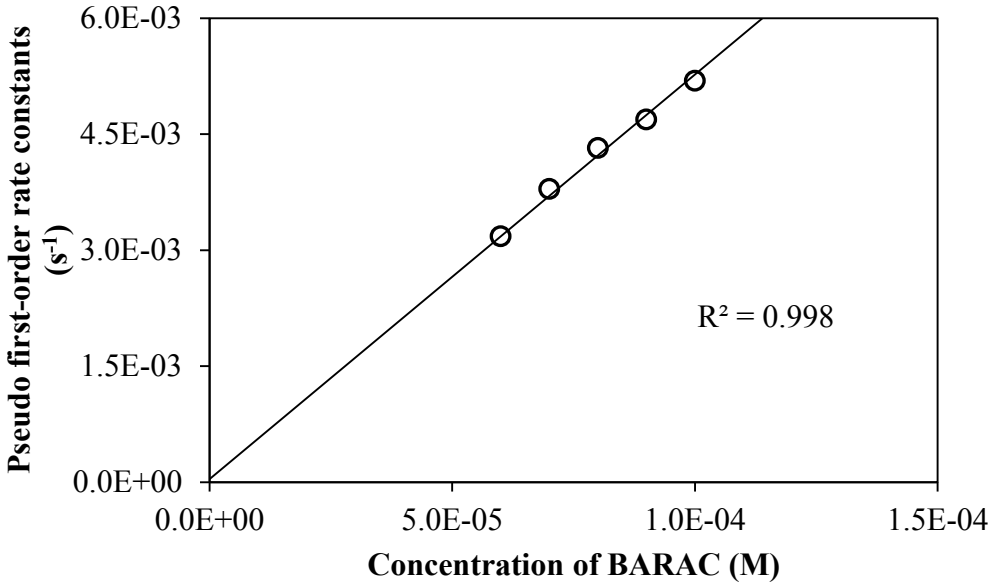

Figure A.11. Pseudo first-order rate constants of the cycloadditions of **2.9** with BARAC (**2.1**) plotted against the various concentrations of the nitrone. The slope represents the second-order rate constant and equals to 52.8 $M^{-1}s^{-1}$ All reactions were done in aqueous (0.1% water) acetonitrile at 25 ± 0.1ºC

B. Kinetic data for acid catalyzed rearrangement of BARAC analogue

Acid catalysis ([TFA] = 0.01 M)

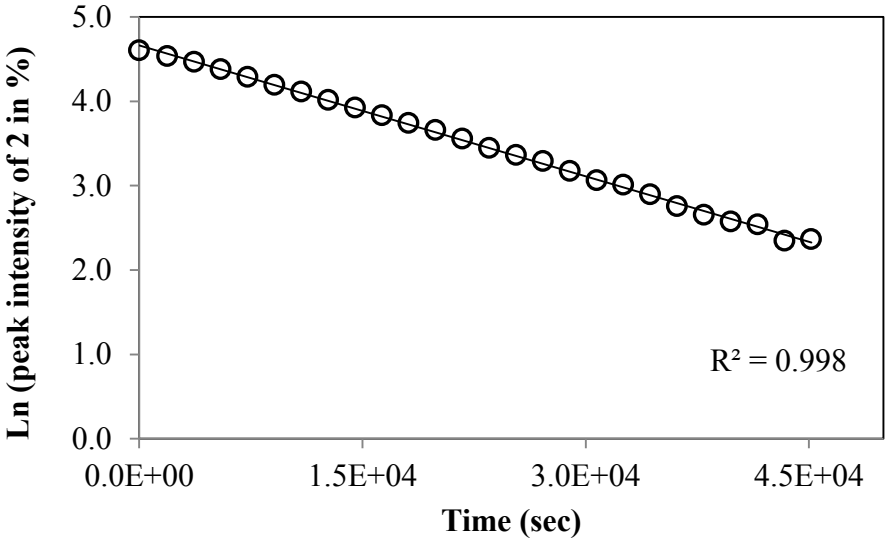

Figure B.1. Plot of Ln ([**3.2**]) vs. time for the rearrangement reaction under acidic ([TFA] = 0.01 M) conditions as monitored by ^{1}H-NMR in $CDCl_3$ at 25 ± 0.1 ºC. The slope represents the first-order rate constant of rearrangement at 0.01 M TFA and equals to value of $5.17 \bullet 10^{-5}$ s^{-1}.

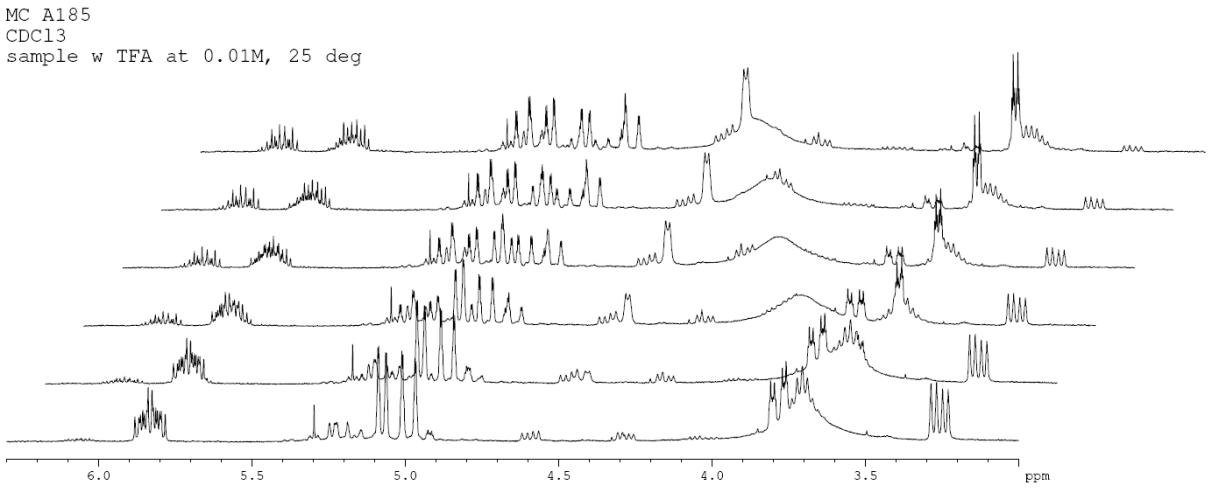

Figure B.2. Overlay of ^{1}H-NMR spectra showing the progression of the rearrangement reaction over time. Reaction was done under acidic ([TFA] = 0.01 M) conditions in $CDCl_3$ at 25 ± 0.1 ºC.

Acid catalysis ([TFA] = 0.015 M)

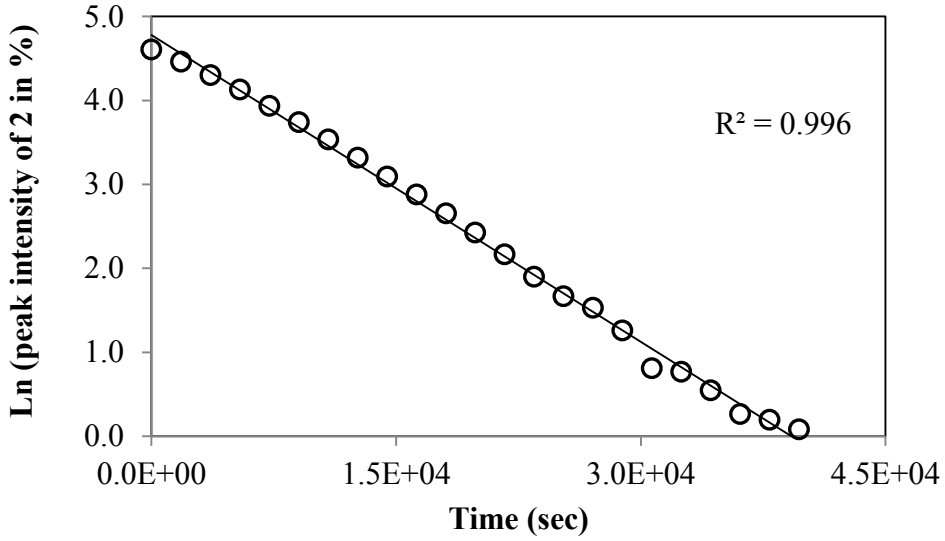

Figure B.3. Plot of Ln ([**3.2**]) vs. time for the rearrangement reaction under acidic ([TFA] = 0.015 M) conditions as monitored by ^{1}H-NMR in $CDCl_3$ at 25 ± 0.1 ºC. The slope represents the first-order rate constant of rearrangement at 0.015 M TFA and equals to value of $1.22 \bullet 10^{-4}$ s^{-1}.

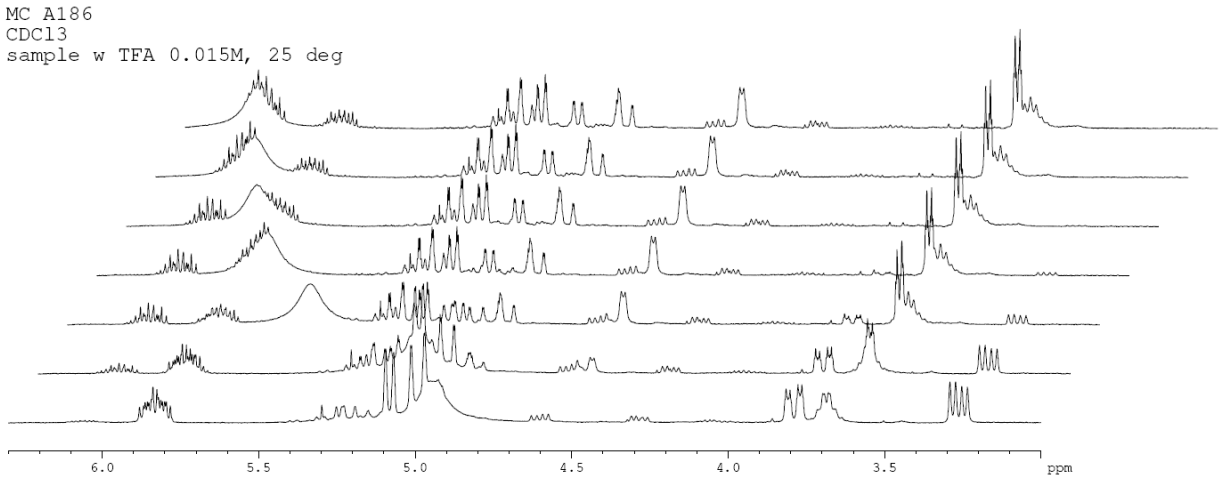

Figure B.4. Overlay of ^{1}H-NMR spectra showing the progression of the rearrangement reaction over time. Reaction was done under acidic ([TFA] = 0.015 M) conditions in $CDCl_3$ at 25 ± 0.1 ºC.

Acid catalysis ([TFA] = 0.02 M)

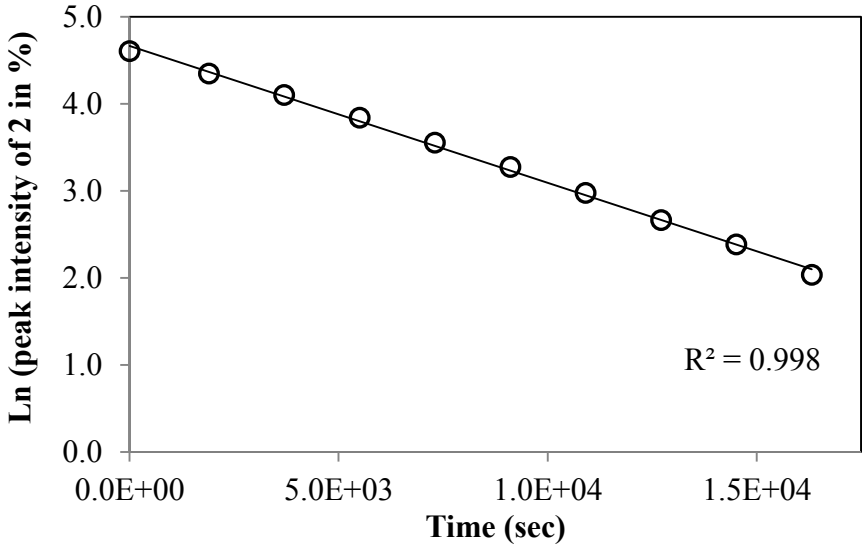

Figure B.5. Plot of Ln ([**3.2**]) vs. time for the rearrangement reaction under acidic ([TFA] = 0.02 M) conditions as monitored by ^{1}H-NMR in $CDCl_3$ at 25 ± 0.1 ºC. The slope represents the first-order rate constant of rearrangement at 0.02 M TFA and equals to value of $1.57 \bullet 10^{-4}$ s^{-1}.

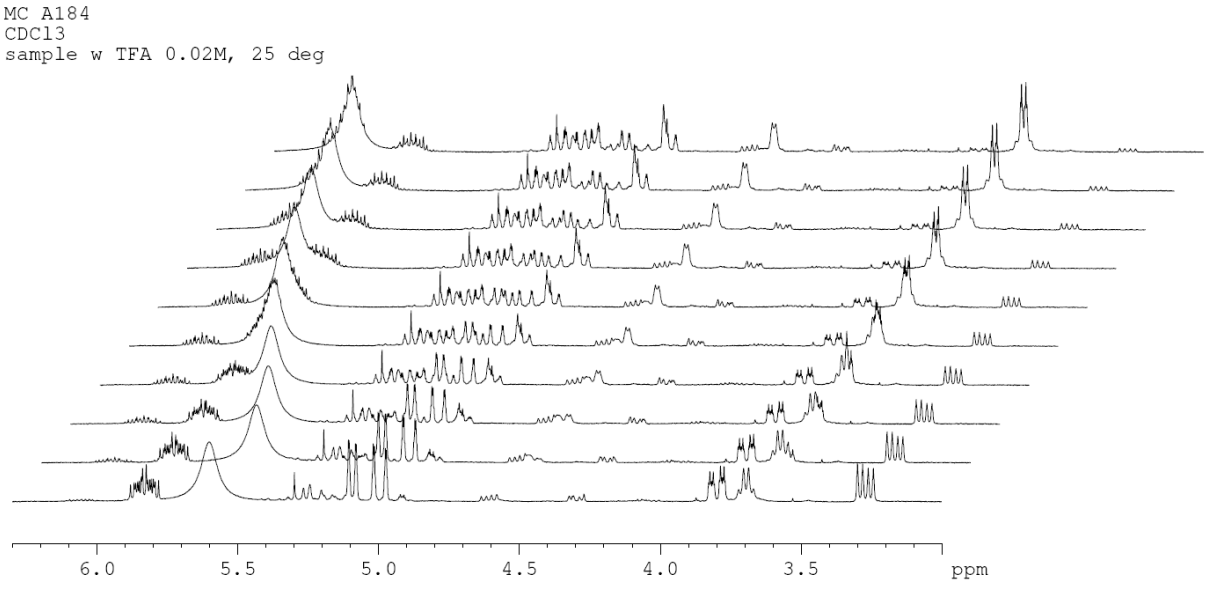

Figure B.6. Overlay of ^{1}H-NMR spectra showing the progression of the rearrangement reaction over time. Reaction was done under acidic ([TFA] = 0.02 M) conditions in $CDCl_3$ at 25 ± 0.1 ºC.

Acid catalysis ([TFA] = 0.03 M)

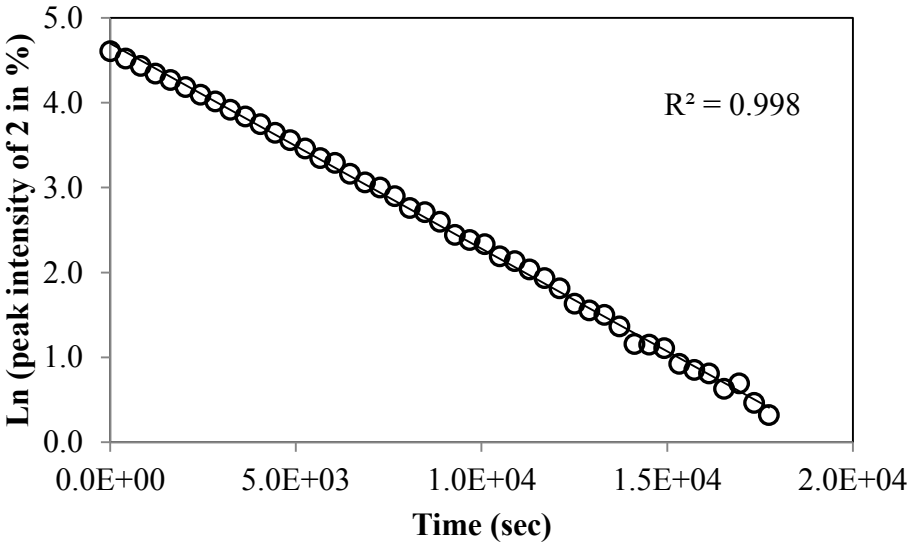

Figure B.7. Plot of Ln ([**3.2**]) vs. time for the rearrangement reaction under acidic ([TFA] = 0.03 M) conditions as monitored by ^{1}H-NMR in $CDCl_3$ at 25 ± 0.1 ºC. The slope represents the first-order rate constant of rearrangement at 0.03 M TFA and equals to value of $2.42 \bullet 10^{-4}$ s^{-1}.

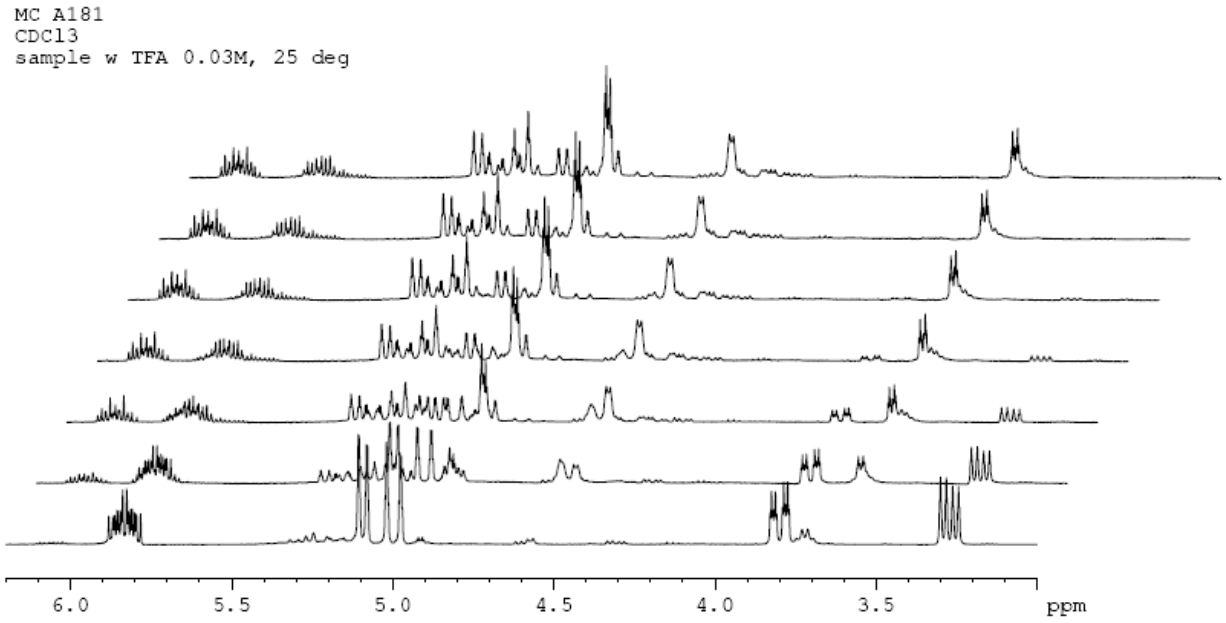

Figure B.8. Overlay of ^{1}H-NMR spectra showing the progression of the rearrangement reaction over time. Reaction was done under acidic ([TFA] = 0.03 M) conditions in $CDCl_3$ at 25 ± 0.1 ºC.

C. X-ray crystallography data

Crystal data and structural refinement of 3.3

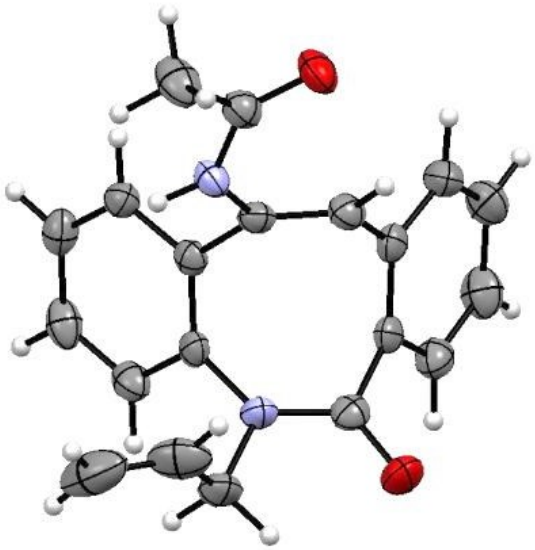

Empirical formula	C20 H18 N2 O2
Formula weight	318.36
Temperature	100.0(1) K
Wavelength	0.71070 A
Crystal system, space group	monoclinic, P21/n
Unit cell dimensions	a= 7.7470(5)A b= 26.1530(19)A c= 8.5985(6)A beta= 108.664(3)deg
Volume	1650.5(2)A^3
Z, Calculated density	4, 1.281 Mg/m^3
Absorption coefficient	0.084 mm^-1
F(000)	672
Crystal size	0.4×0.3×0.03 mm
Theta range for data collection	1.56 to 26.49 deg.
Limiting indices	-8<=h<=9, -30<=k<=32, -10<=l<=10
Reflections collected/unique	27855/ 3371
Completeness to theta 26.64	98.9%
Refinement method	Full---matrix least---squares on F^2
Data/restraints/parameters	3371/0/ 218
Goodness---of---fit on F^2	1.071
Final R indices [I>2sigma(I)]	R1= 0.0429, wR2= 0.0980
R indices (all data)	R1= 0.0644
Largest diff. peak and hole	-0.280 and 0.230 e.A^-3

Crystal data and structural refinement of 3.4

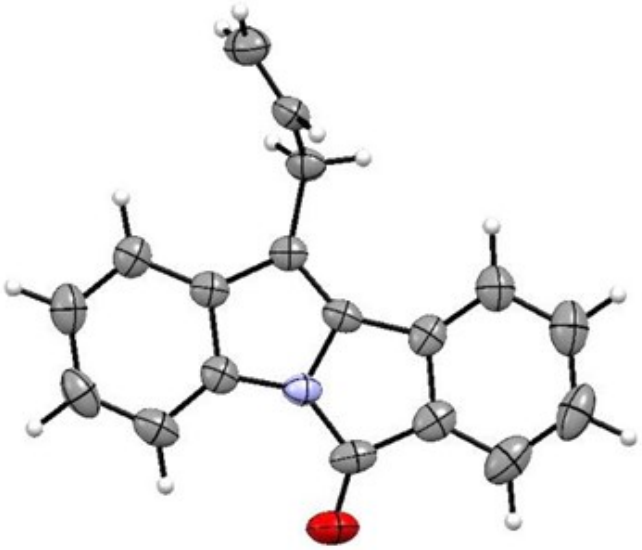

Empirical formula	C18 H13 N O
Formula weight	259.29
Temperature	100.0(1) K
Wavelength	0.71070 A
Crystal system, space group	monoclinic, P21/c
Unit cell dimensions	a= 17.1588(13)A
	b= 7.6525(7)A
	c= 20.1851(16)A
	beta= 107.382(3)deg
Volume	2529.4(4)A^3
Z, Calculated density	8, 1.362 Mg/m^3
Absorption coefficient	0.085 mm^-1
F(000)	1088
Crystal size	0.5×0.2×0.03 mm
Theta range for data collection	2.11 to 24.71 deg.
Limiting indices	-19<=h<=20, -9<=k<=8, -23<=l<=22
Reflections collected/unique	59114/ 4276
Completeness to theta 26.64	98.7%
Refinement method	Full---matrix least---squares on F^2
Data/restraints/parameters	4276/0/ 465
Goodness---of---fit on F^2	1.044
Final R indices [I>2sigma(I)]	R1= 0.0354, wR2= 0.0965
R indices (all data)	R1= 0.0487
Largest diff. peak and hole	-0.239 and 0.181 e.A^-3

Crystal data and structural refinement of 3.5

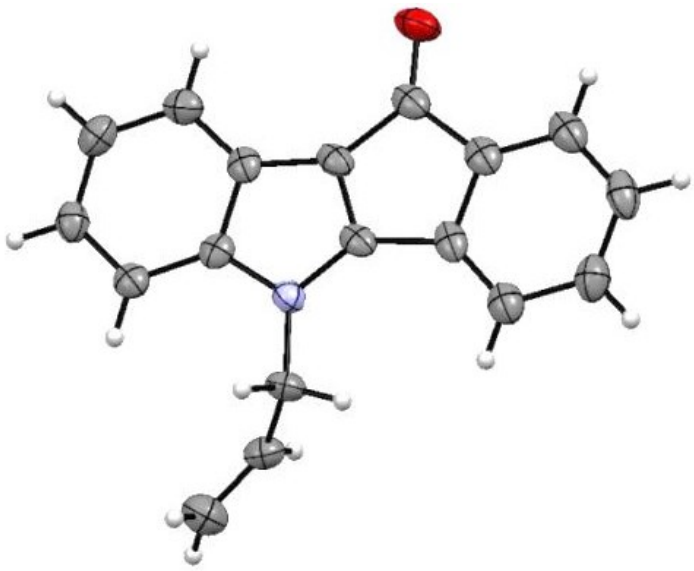

Empirical formula	C18 H13 N O
Formula weight	259.29
Temperature	100.0(1) K
Wavelength	0.71070 A
Crystal system, space group	monoclinic, P21/c
Unit cell dimensions	a=17.189(2) b=7.7634(6) c=19.771 (2) beta=107.401(4)deg
Volume	2517.6(4) A^3
Z, Calculated density	8, 1.368 Mg/m^3
Absorption coefficient	0.091 mm^-1
F(000)	1088
Crystal size	0.6×0.1×0.1 mm
Theta range for data collection	1.24 to 31.45 deg.
Limiting indices	-23<=h<=25, -9<=k<=10, -28<=l<=26
Reflections collected/unique	64552/6824
Completeness to theta 26.64	98.7%
Refinement method	Full---matrix least---squares on F^2
Data/restraints/parameters	6824/0/361
Goodness---of---fit on F^2	1.030
Final R indices [I>2sigma(I)]	R1=0.054, wR2=0.148
R indices (all data)	R1=0.090
Largest diff. peak and hole	-0.202 and 0.552 e.A^-3

Crystal data and structural refinement of 3.7

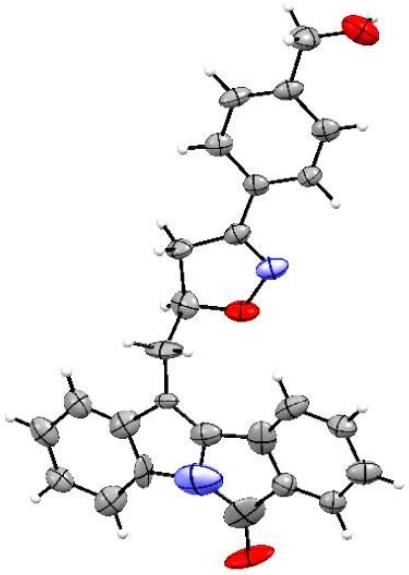

Empirical formula	C26 H20 N2 O3
Formula weight	408.44
Temperature	100.0(1) K
Wavelength	0.71070 A
Crystal system, space group	monoclinic, P21/c
Unit cell dimensions	a=5.4793(18)A
	b=20.849(7)A
	c=17.361(6)A
	beta=98.866(18) deg
Volume	1959.6(11) A^3
Z, Calculated density	4, 1.384 Mg/m^3
Absorption coefficient	0.091 mm^-1
F(000)	856
Crystal size	0.4×0.2×0.01 mm
Theta range for data collection	1.54 to 26.64 deg.
Limiting indices	-5<=h<=6, -25<=k<=25, -21<=l<=21
Reflections collected/unique	39606/15281
Completeness to theta 26.64	98.5%
Refinement method	Full---matrix least---squares on F^2
Data/restraints/parameters	39904/0/283
Goodness---of---fit on F^2	1.048
Final R indices [I>2sigma(I)]	R1=0.127, wR2=0.272
R indices (all data)	R1=0.273
Largest diff. peak and hole	-0.419 and 0.711 e.A^-3

D. ^{1}H and ^{13}C NMR spectra

^{1}H and ^{13}C NMR of **2.1**

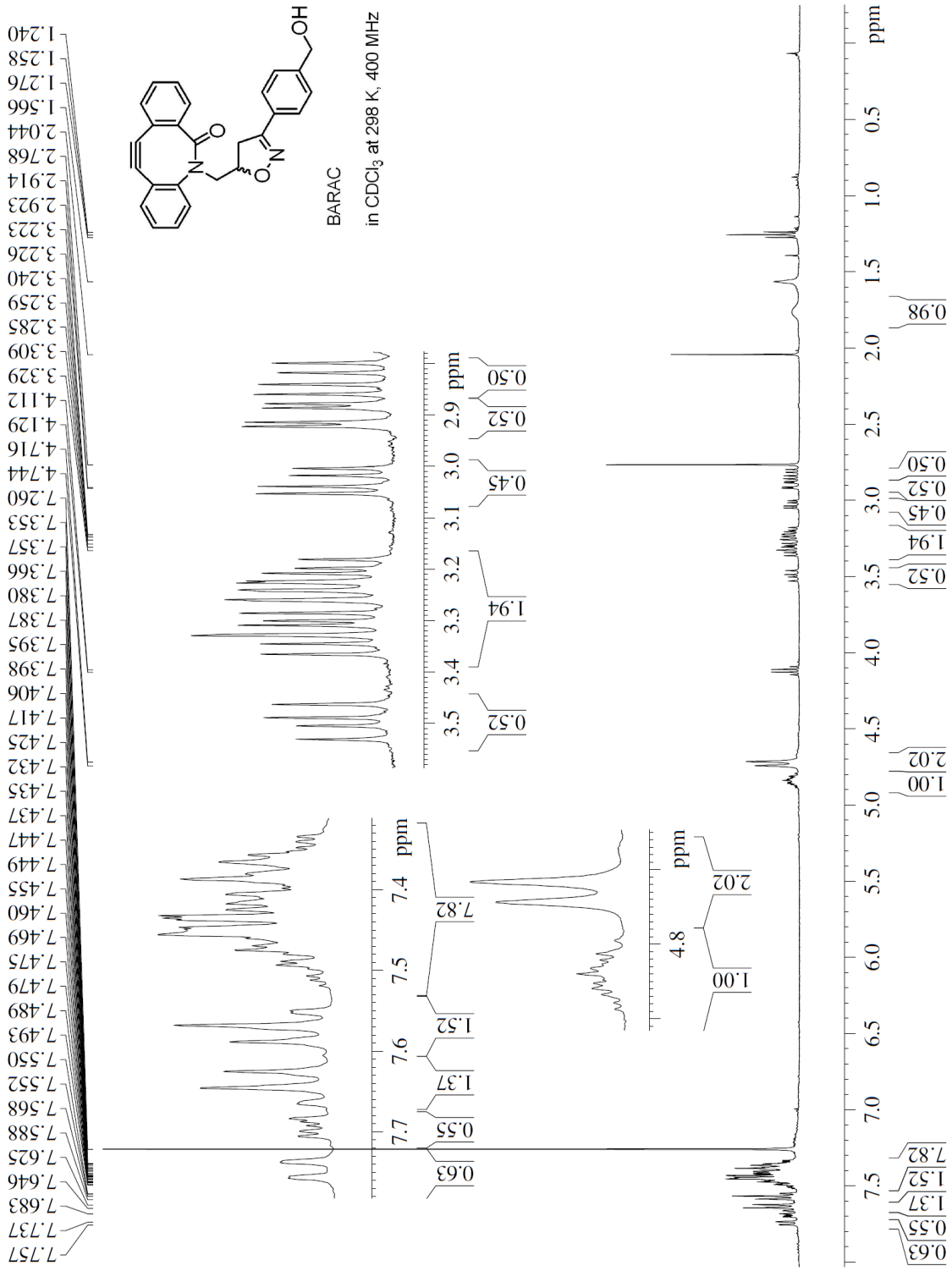

^{1}H and ^{13}C NMR of **3.2**

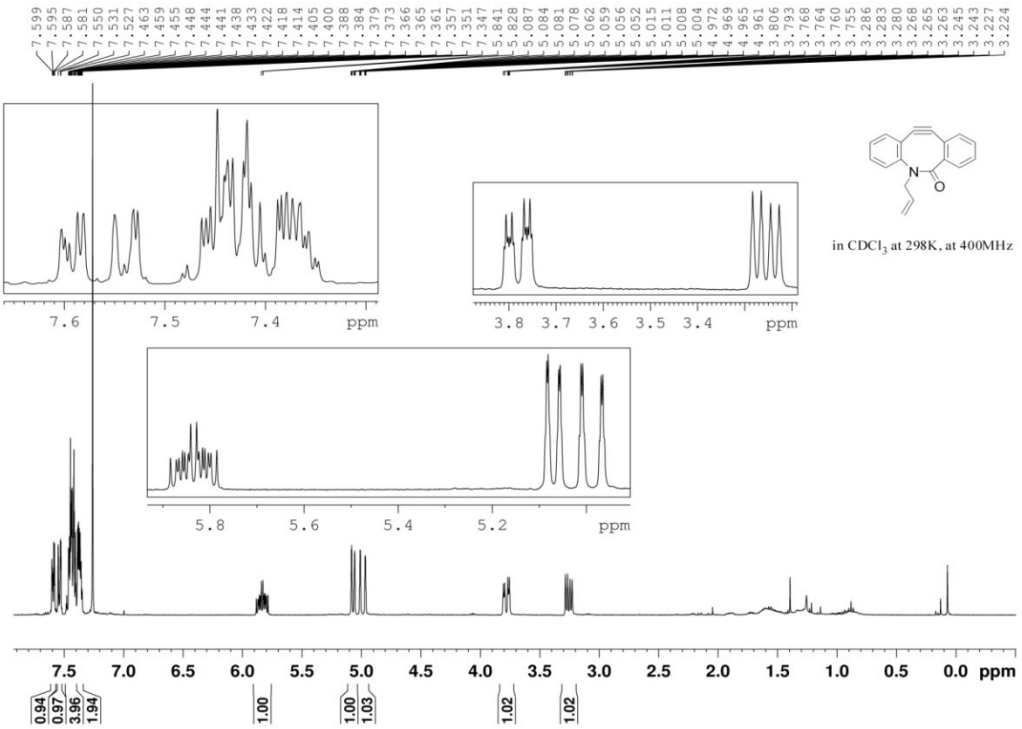

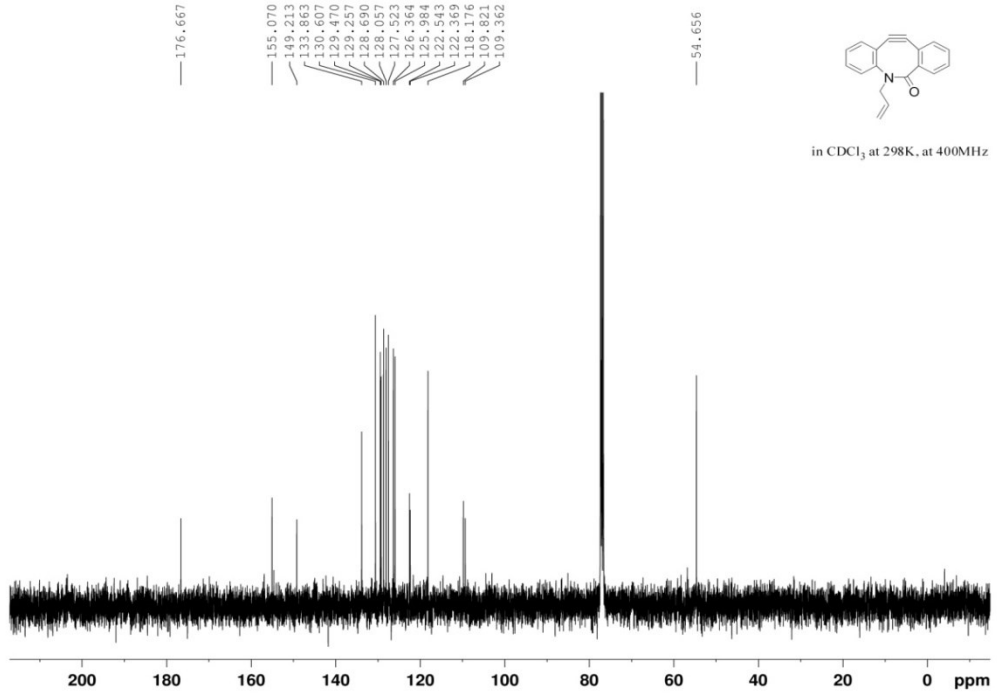

^{1}H and ^{13}C NMR of **3.3**

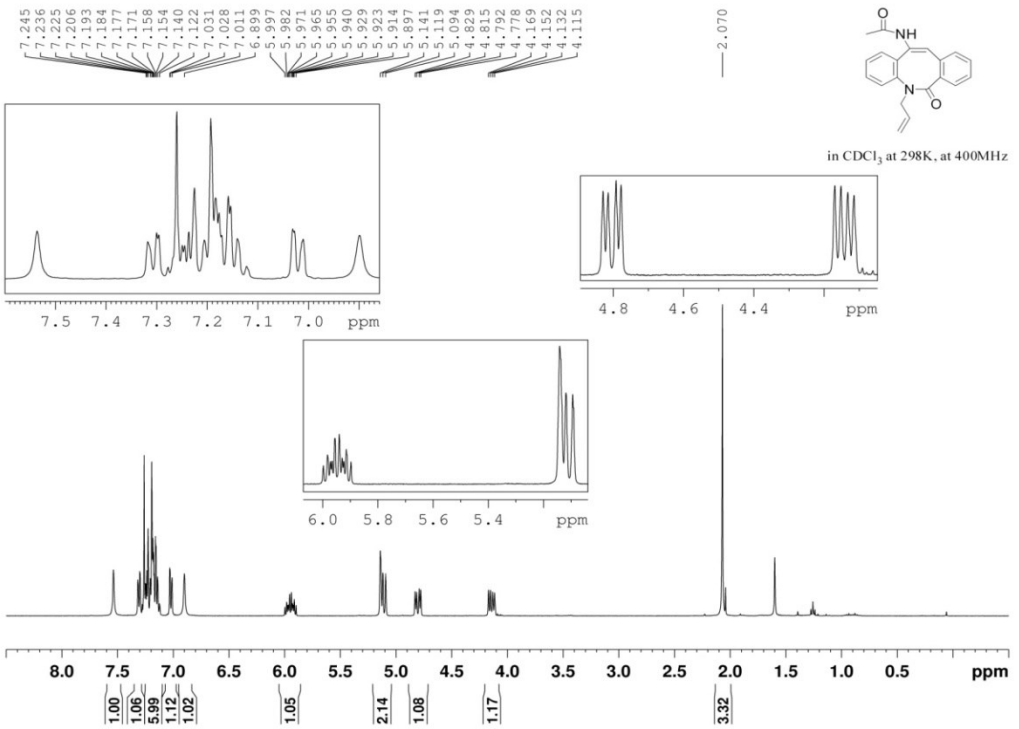

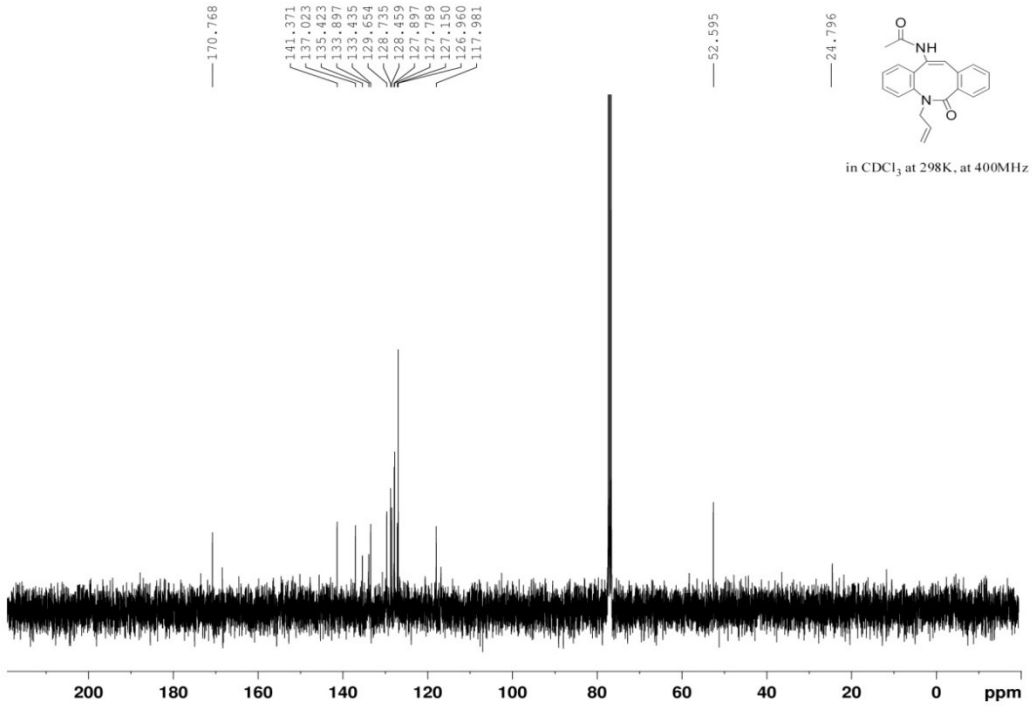

^{1}H and ^{13}C NMR of **3.4**

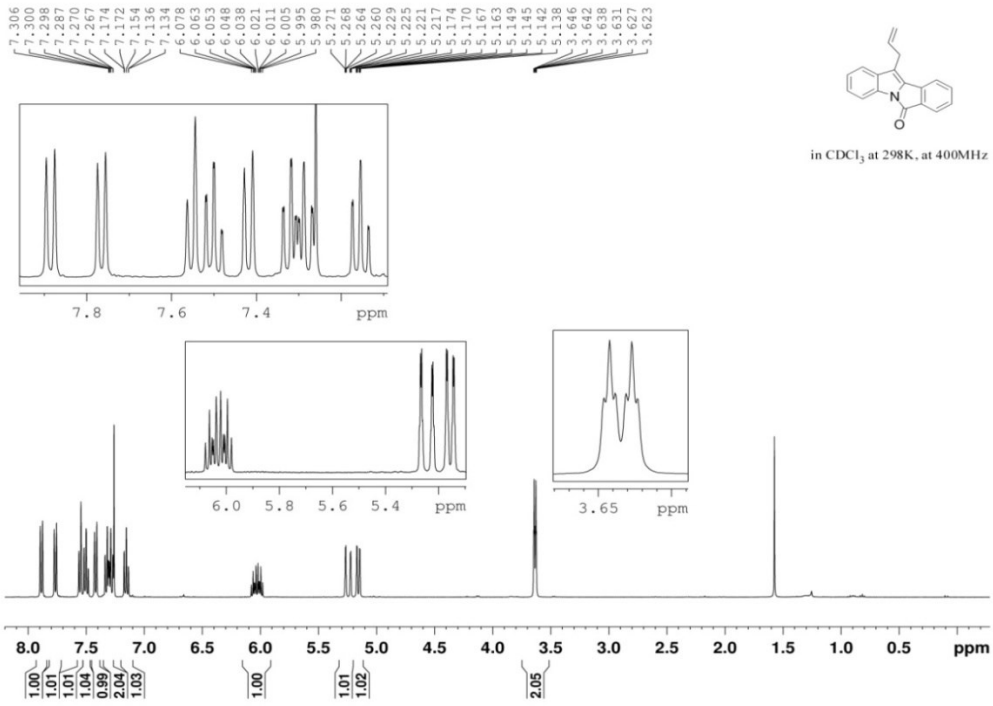

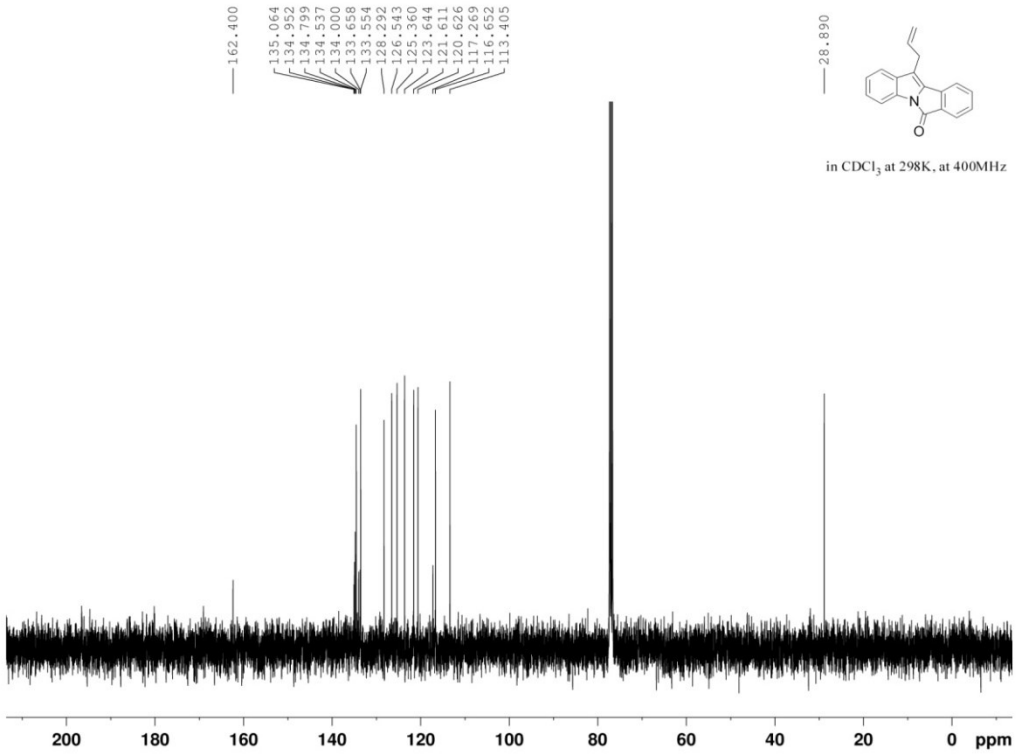

^{1}H and ^{13}C NMR of **3.5**

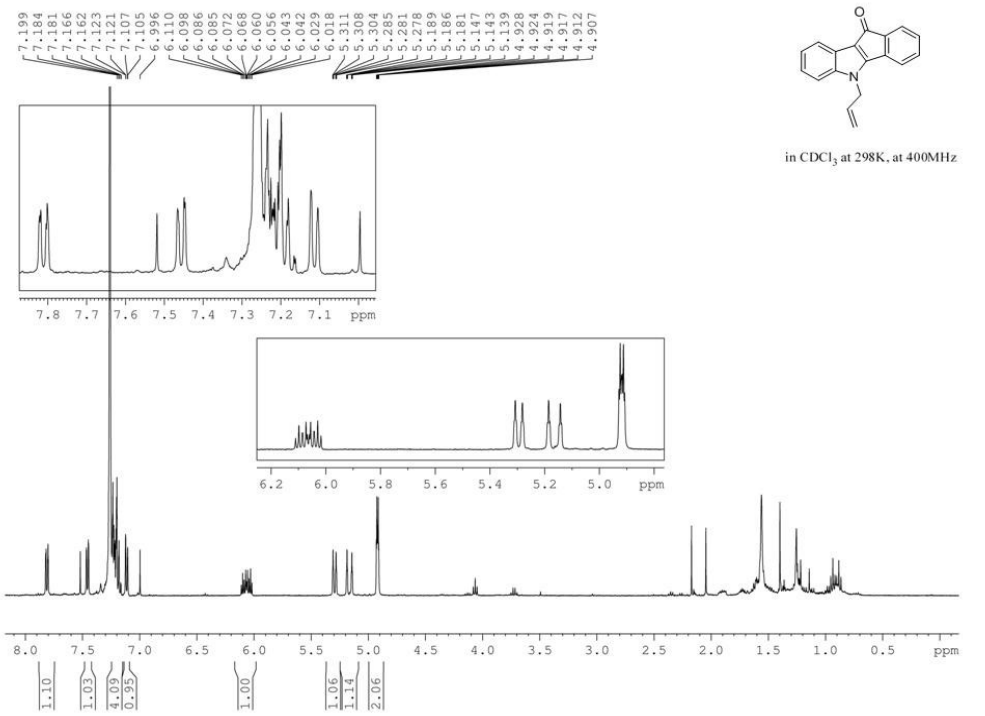

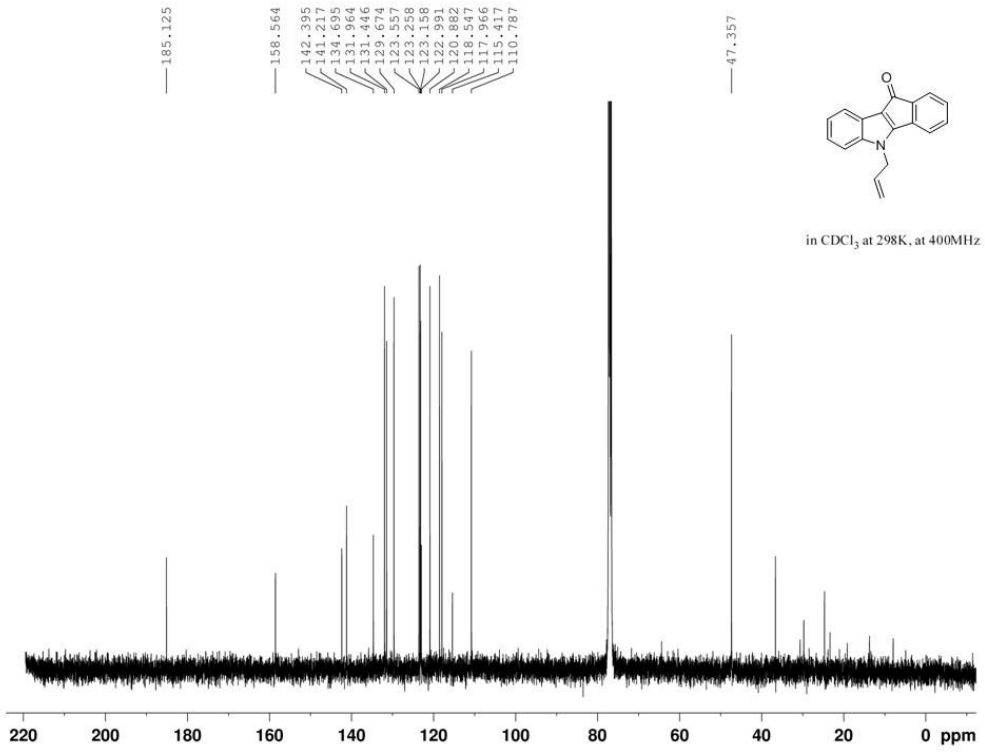

^{1}H and ^{13}C NMR of **3.7**

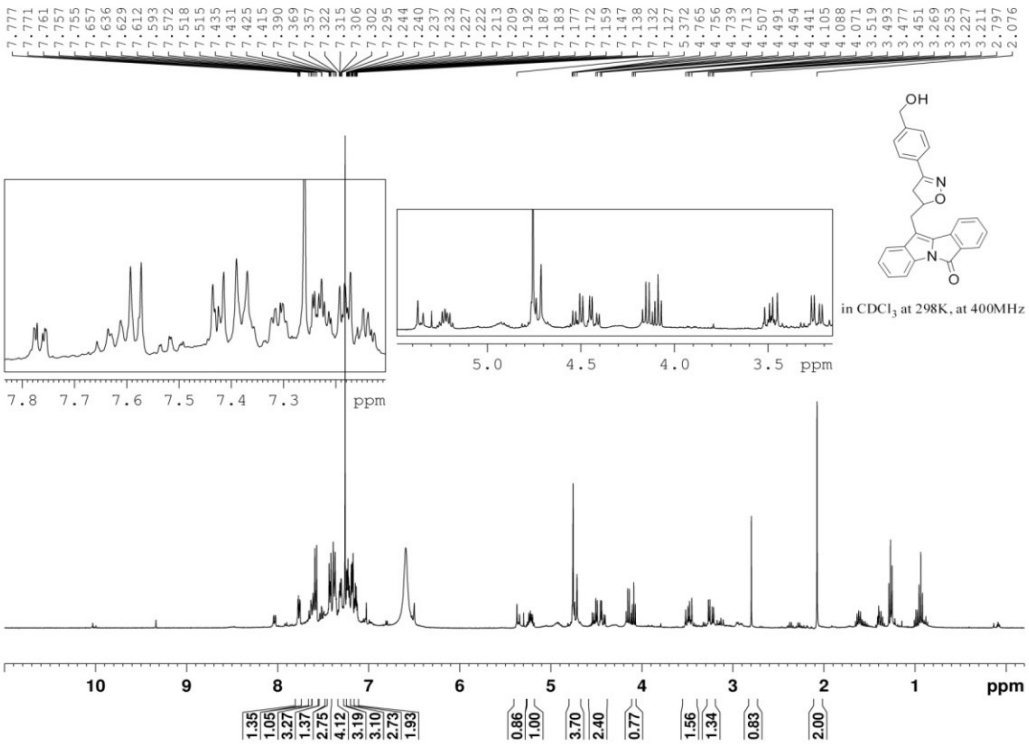

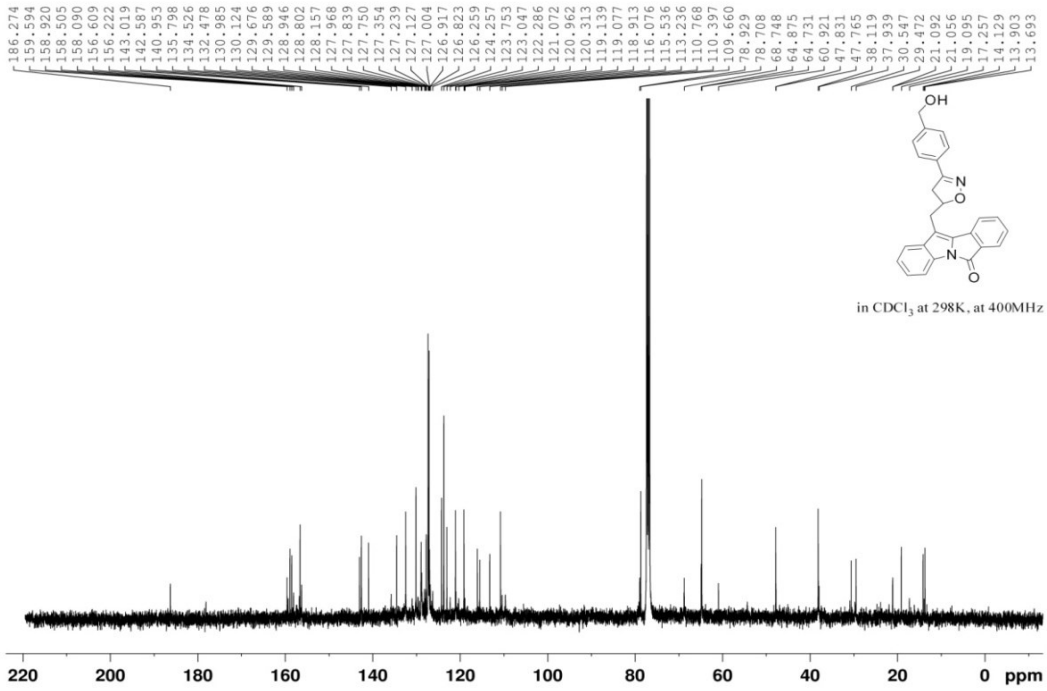

^{1}H and ^{13}C NMR of **3.8**